Ulm University Medical Center
Institute of Immunology
Head: Prof. Hassan Jumaa

Adaptive Tolerance: A Novel Mechanism for Immune Protection by Autoreactive IgM

Cumulative dissertation submitted in partial fulfillment of the requirements for the Doctoral Degree of Human Biology at the Medical Faculty of Ulm University

Timm Amendt
Worms
2022

Acting dean: Prof. Thomas Wirth

First reviewer: Prof. Hassan Jumaa, Ulm

Second reviewer: Prof. Michael Reth, Freiburg

Third reviewer: Prof. Ralf Küppers, Essen

Date of graduation: 08.07.22

Table of contents

List of abbreviations IV

1. Introduction 1
1.1 Introduction and goal of the study 1
1.2 Articles included in the thesis 5
1.3 Patents 6

2. Summary of articles included in the thesis 7
2.1 Memory IgM protects endogenous insulin from autoimmune destruction 7
2.2 Primary immune responses and affinity maturation are controlled by IgD 10
2.3 Autoreactive antibodies control blood glucose by regulating insulin homeostasis 12

3. Discussion and outlook 15

4. Abstract 19

5. References 20

6. Included publications 25
6.1 Amendt & Jumaa, 2021, *The EMBO Journal* 25
6.2 Amendt *et al.*, 2021, *Frontiers in Immunology* 43
6.3 Amendt *et al.*, 2022, *PNAS* 58

7. Acknowledgements 69

8. Curriculum vitae including publication list 70

List of abbreviations

AchR	acetyl choline receptor
ANA	anti-nuclear structure antibody
BCR	B cell antigen receptor
BLI	biolayer interferometry
CP	connecting peptide, C-peptide
CSR	class switch recombination
dsDNA	double-stranded deoxy ribonucleic acid
EIAS	exogenous insulin antibody syndrome
FACS	fluorescence activated cell sorting
GC	germinal center
HC	heavy chain
HEL	hen-egg lysozyme
IgG	immunoglobulin G
IgM	immunoglobulin M
InsA	insulin A-chain peptide
IVIg	intravenous immunoglobulin
KLH	key hole limpet hemocyanin
LC	light chain
mAb	monoclonal antibody
nIgM	natural IgM
oxLDL	oxidized low-density lipoprotein
pH	*potentia hydrogenii*
pIgM	primary IgM
PR-IgM	protective-regulatory IgM
RA	rheumatoid arthritis
SDS-PAGE	sodium dodecyl sulphate-polyacrylamide gel electrophoresis
SHM	somatic hypermutation
SLE	systemic lupus erythematosus
T1D	type 1 diabetes mellitus
V(D)J	variable, diversity, joining
WT	wild-type

1. Introduction and goal of the study

1.1 Introduction

Self-tolerance is crucial for the maintenance of physiological integrity. Therefore, immune responses against *self*-structures have to be tightly regulated in order to avoid the development of autoimmune diseases (Pieper et al., 2013; Suurmond & Diamond, 2015). Autoantibodies have been described to target an enormous variety of self-antigens including soluble autoantigens (e.g. hormones), cells (e.g. erythrocytes) or receptors (e.g. AchR) (Avrameas et al., 2007; Ludwig et al., 2017; Suurmond & Diamond, 2015; Utz et al., 2000). The hallmark of autoimmunity, which is also used as a diagnostic marker, is autoreactive IgG (Kaul et al., 2016; E. M. Tan, 1989; Zhang et al., 2015). In particular, autoreactive IgG targeting dsDNA (ANA-IgG) is associated with systemic lupus erythematosus (SLE) (E. M. Tan, 1989), whereas autoreactive IgG targeting erythrocytes is associated with autoimmune hemolytic anemia (AIHA) (Quartier et al., 2004). Thus, in severe cases, patients receive B cell-depleting therapy by Rituximab (anti-CD20-IgG) infusions valuing autoimmune disease control over immunosuppression (Wang et al., 2020). To date, autoimmune diseases are incurable chronic conditions that worsen with age showing the urgent need for a better understanding of B cell tolerance and autoantibody biology.

Under normal conditions B cell tolerance ensures physiological integrity (Pieper et al., 2013). Currently, it is assumed that self-tolerance is achieved by several mechanisms culminating in removal or functional silencing of autoreactive B cells (Noviski & Zikherman, 2018a; Pieper et al., 2013; Stebegg et al., 2018; Yarkoni et al., n.d.). During early B cell development in the bone marrow, pro- and pre- B cells randomly rearrange their variable (V), diversity (D) and joining (J) gene segments of their heavy chain (HC) and light chain (LC) gene loci to form a functional IgM-class B cell antigen receptor (BCR) (Maity et al., 2015; Tsubata & Reth, 1990). Here, a BCR repertoire consisting of virtually unlimited specificities can be generated, which harbor the risk of recognizing self-structures (Pieper et al., 2013) (**Figure 1**).

The concept of central tolerance proposes that autoreactive specificities are removed by clonal deletion via apoptosis upon recognition of self-proteins (Tan *et al*, 2019; Nemazee & Buerki, 1989a; Nemazee & Bürki, 1989b) or by sequential LC gene rearrangement, known as receptor editing, in immature B cells (Gay et al., 1993; Meffre et al., 2004; Tiegs et al., 1993). B cells that circumvent central tolerance and home to the spleen are believed to be subjected to an anergic state (functional unresponsiveness) upon autoantigen encounter (Brink et al., 1992; Goodnow et al., 1988, 1989). Here, autoreactive mature B cells downmodulate IgM-class BCR expression but maintain IgD-class BCR expression (Goodnow et al., 1988). However, recent studies showed that the anergic state is not unresponsiveness per se (Setz et al., 2019; C. Tan et al., 2019; Übelhart et al., 2015; Zikherman et al., 2012). In contrast, the responsiveness of “anergic” B cells depends on the antigen valency rather than distinguishing between self or non-self. In fact, anergic B cells respond by BCR signaling and intracellular calcium mobilization once they encounter a polyvalent antigen (Setz et al., 2019; Übelhart et al., 2015). Furthermore, single cell sequencing studies revealed that over 80 % of mature B cells are autoreactive to an extent suggesting a different tolerance mechanism compared to classical central or peripheral tolerance (Meffre et al., 2004; Wardemann et al., 2003). Interestingly, available data indicate

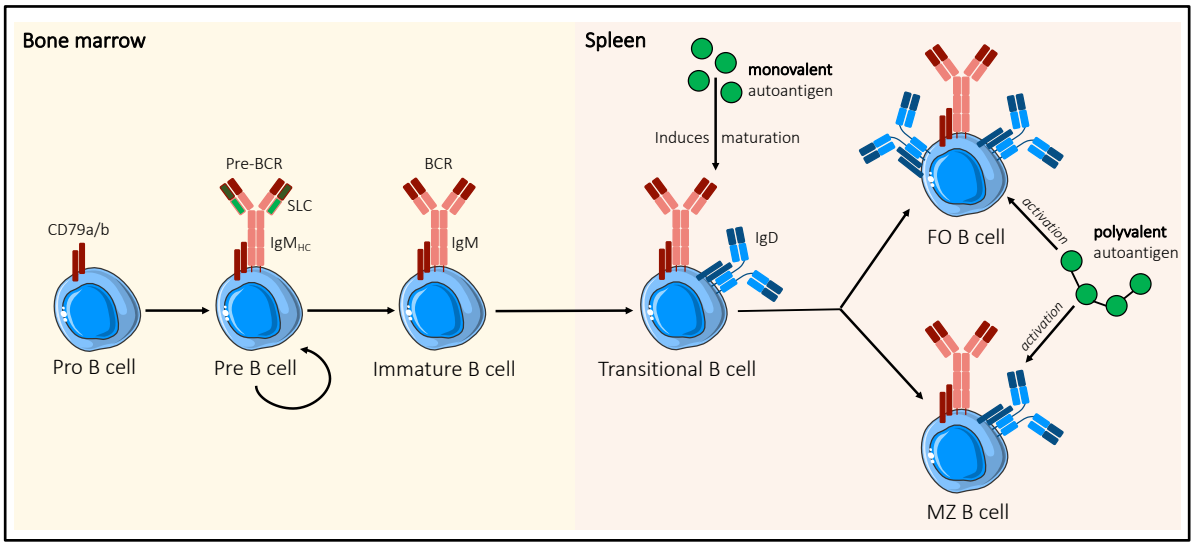


Figure 1 | B cell development and activation of mature autoreactive B cells by polyvalent antigen (Amendt & Jumaa, 2022)**.**
Early B cell progenitors arise from hematopoietic stem cells (HSC) prior to committing to the B cell lineage (Pieper et al., 2013). In the pro B cell stage variable (V), diversity (D) and joining (J) immunoglobulin gene segments of the µ-heavy chain (HC) rearrange randomly to form a functional µ-HC. Surface expression of the previously rearranged µ-HC forms a pre-B cell receptor (pre-BCR) together with surrogate light chains (SLC; VpreB and λ5) (Tsubata & Reth, 1990). Highly autoreactive B cells will get clonally deleted or undergo LC-editing in order to be less autoreactive (central tolerance) (Gay et al., 1993; D. Nemazee & Buerki, 1989; C. Tan et al., 2019). Guided by a sphingosine-1-phosphate (S1P) gradient, immature B cells home to the spleen (Pieper et al., 2013). Here, soluble autoantigen induces B cell maturation by triggering IgD-class BCR upregulation and IgM-class BCR downregulation ("anergy") (Goodnow et al., 1988; Zikherman et al., 2012). Finally, the activation of mature autoreactive B cells (follicular, FO or marginal zone, MZ) is controlled by the antigen valency encountered (Amendt et al., 2021; Amendt & Jumaa, 2021). In particular, polyvalent autoantigen is capable of activating B cells and eliciting an autoantibody response whereas monovalent autoantigen blocks B cell activation.

that the majority of mature B cells in the periphery have encountered self-antigen during development suggesting a crucial role of autoreactivity during the generation of mature naïve B cells (Zikherman et al., 2012).
Importantly, the IgD-class BCR, which is associated with the proposed anergy, possesses crucial structural differences to the IgM-class BCR despite having the same specificity on one particular B cell. First, the IgD-class BCR possesses a highly flexible Ser-Gly-rich hinge region responsible for selective responsiveness to polyvalent antigen (Übelhart et al., 2015). Second, it possesses multiple O-linked glycosylation at the HC further enhancing flexibility (Gutzeit et al., 2018). Third, IgD- and IgM-class BCR are localized inside different lipid-protein nanodomains on the surface of mature B cells (Gold & Reth, 2019). However, IgD-class BCR-specific knock out mouse models did not reveal a drastic phenotype. These mice only showed delayed germinal center formation and delayed affinity maturation (Nitschke et al., 1993; Roes & Rajewsky, 1993; Setz et al., 2019). These data reveal the limitations of the knock-out mouse models that fail to identify compensation mechanisms for the maintenance of essential regulatory circuits. Clearly, an IgD-class BCR nano cluster-specific pairing with certain co-receptors indicates a unique biological function for IgD (Becker et al., 2017; Hobeika et al., 2016; Maity et al., 2015).
The current concepts of B cell tolerance do not provide a mechanistic explanation for the vast majority of autoantibody-mediated autoimmune diseases such as rheumatoid arthritis

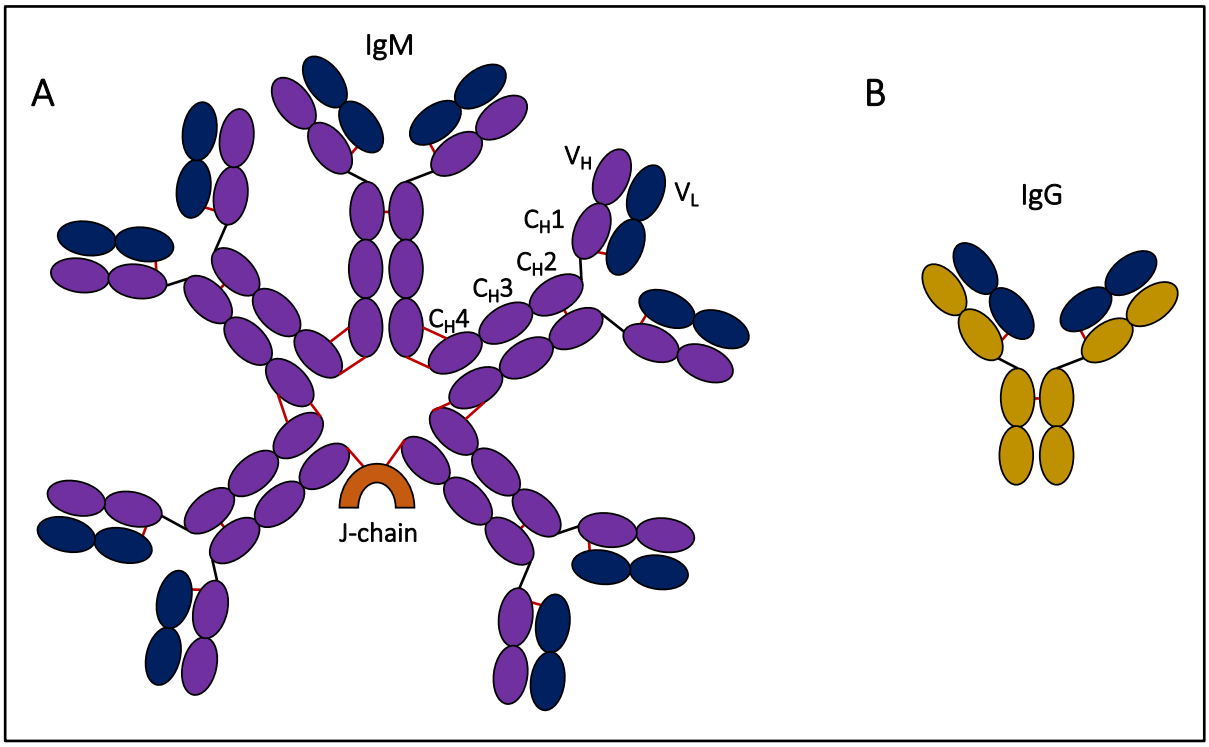


Figure 2 | Structure of IgM and IgG antibodies.
A: Pentameric IgM molecule consisting of heavy chains (purple) and light chains (dark blue). The J-chain (orange) ensures the pentameric structure providing stability. IgM antibodies are potent complement recruiters at the C_H2 and C_H3 domains. Disulfide bonds are shown in red. **B:** Monomeric IgG molecule occurring in IgG1, IgG2, IgG3 and IgG4 subclasses.

(RA) or systemic lupus erythematosus (SLE) (Suurmond & Diamond, 2015). A leakiness in central tolerance mechanisms can hardly be found in autoantibody-mediated autoimmune diseases leaving open the question as to how B cell tolerance is achieved *in vivo*.

Another observation which is not in line with strict central tolerance is the existence of so-called natural autoantibodies which are thought to fulfill crucial functions in preventing age-associated diseases such as autoinflammation and atherosclerosis (Boes, 2000; Boes et al., 1998; Tsiantoulas et al., 2012). These natural autoantibodies are represented by IgM antibodies secreted by B1 B cells (Holodick et al., 2016; Tsiantoulas et al., 2012). IgM antibodies differ from IgG antibodies in several regards (**Figure 2**). Human IgG is produced as a monomer in four subclasses (IgG1 – IgG4). The generation of IgG antibodies require T cell-dependent class-switch recombination (CSR) during germinal center (GC) reaction (McHeyzer-Williams, 2003; Ueno, 2016; Vinuesa et al., 2016). In contrast, IgM antibodies are produced T cell-independently and do not require GC reactions. However, IgM antibodies can still be modified in GCs in the course of affinity-maturation resulting in high-affinity IgM during secondary immune responses as compared to the low affinity primary IgM (Lutz et al., 2009; Shimizu et al., 2004). Further, IgM antibodies form either pentamers containing a J-chain, or very short-lived hexamers lacking the J-chain (Keyt et al., 2020). Interestingly, IgM antibodies are highly potent inflammation drivers since they are capable of recruiting complement factors very effectively (Boes, 2000; Boes et al., 1998; Cooper, 1985; Weinstein et al., 2015). The low antigen binding affinity of primary IgM is

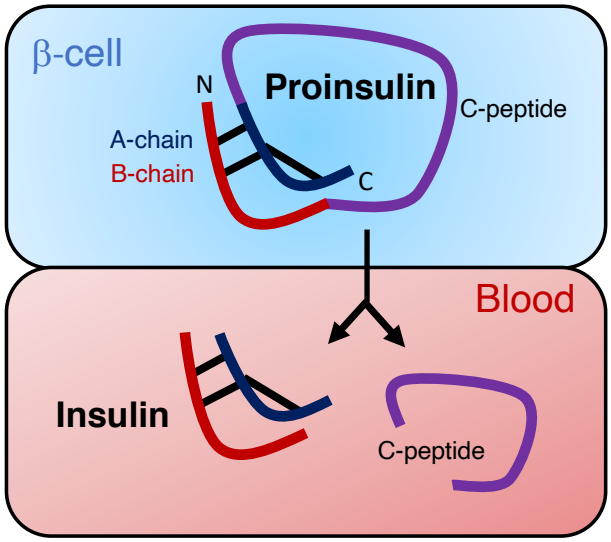


Figure 3 | Structure and secretion process of insulin.
Beta cells (blue) produce proinsulin polypeptides where a connecting peptide (C-peptide, CP) connects insulin A- and B-chains by sequence enhancing inter-chain disulfide bond formation (black lines). After proteolytic cleaving of proinsulin, both products (insulin and CP) are secreted into the blood stream. Subsequently, insulin is acting on blood glucose levels by binding to insulin receptors allowing intracellular glucose uptake. The function of CP remains still unknown and has also been reported to show a much lower half-life (Nordquist & Wahren, 2009; Zhu et al., 2016).

compensated by high avidity due to the polymeric form making IgM a crucial participant in first line defense against pathogens (Boes et al., 1998; Reyneveld et al., 2020).
Strikingly, the vast majority of serum IgM in mammalians belongs to the class of the so-called self-reactive natural IgM (nIgM) (Grönwall & Silverman, 2014). In particular, nIgM possesses low antigen affinity and shows extreme polyreactivity by binding nucleic acids and other self-molecules (Adyel et al., 1996; Haralambous et al., 1995; Tsiantoulas et al., 2012). Interestingly, the main targets of nIgM are altered self-molecules which represent a potential threat for health. For instance, nIgM clears oxidized lipoproteins (oxLDL) (Amir et al., 2012; Tsiantoulas et al., 2012) and other oxidized moieties efficiently that could induce inflammation if not removed quickly. Furthermore, nIgM removes advanced glycation end-products (AGE) associated with age-dependent inflammation (Ehrenstein et al., 2000; Holodick et al., 2016). Notably, nIgM secretion takes place in an antigen-independent manner (Hamilton et al., 1994). Moreover, the B1 B cells producing nIgM undergo self-renewal and do not participate in GC reactions, somatic-hypermutation (SHM) or class-switching (CSR) (Grönwall & Silverman, 2014).
Several studies reported nIgM as being capable of binding insulin as a representative autoantigen (Haralambous et al., 1995; Meffre et al., 2004). However, the biological function of autoantibody-mediated insulin removal remained unknown. Insulin is produced and secreted by beta cells of the pancreas as a heterodimeric polypeptide (Weiss, 2009; Wintersteiner, 1933) (**Figure 3**). The A-chains and B-chains are connected by two disulfide bonds (Cys31 > 96, Cys43 > 109) (Weiss, 2009; Wintersteiner, 1933). Further, the A-chain has an intra-chain disulfide bond. Interestingly, high insulin output by the pancreas and oxidative stress can lead to misfolding and mispairing of disulfide bonds or carbon-sulfur

bonds (sulfonylation) (Haataja et al., 2016). These processes have been reported to generate insulin complexes in a polyvalent form. Importantly, insulin is fully conserved between mouse and man making it a suitable target for studying autoimmunity.
Due to the important role in glucose metabolism and broad presence in blood, we chose insulin as a physiologically relevant autoantigen. The vast majority of other studies working on B cell tolerance used transgenic mice harboring a monospecific high-affine B cell repertoire which does not resemble physiological conditions (Eschbach et al., 2011; Goodnow et al., 1989; D. A. Nemazee & Bürki, 1989). For instance, mouse models leading to the concept of B cell "anergy" used high-affine BCR against hen-egg lysozyme (HEL) in HEL-transgenic mice which is of no relevance for human autoimmune diseases (Goodnow et al., 1988). In contrast, recent studies suggest that naïve B cells recognize their cognate antigen with a rather low to ultra-low BCR-antigen affinity (Packard et al., 2016; Shlomchik, 2008). The physiological model we used to study autoantibody responses has several advantages over conventional transgenic models:
Insulin autoantibodies are highly relevant for human pathophysiology since exogenous insulin autoimmune syndrome (EIAS) as well as type 1 diabetes (T1D) show autoantibodies targeting insulin (Hu & Chen, 2018; Lahtela et al., 1997; Taplin & Barker, 2008).
By using wildtype mice and insulin as representative autoantigen, we were able to study autoreactive B cells within a physiological B cell repertoire. In order to generate polyvalent insulin complexes we used different approaches including chemical crosslinking which also occurs under oxidative stress conditions *in vivo*. This set-up allowed us to test autoantibody responses against native insulin complexes *in vivo* and to analyze underlying molecular mechanisms.

In the presented cumulative thesis we describe a novel concept called ***adaptive tolerance***. Herein, we aimed at understanding:

(1) how autoreactive B cells are activated *in vivo*,

(2) how autoantigen valences modulate autoantibody responses,

(3) how humoral tolerance is achieved *in vivo* by focusing on (auto)antibodies.

1.2 Articles included in the thesis

This cumulative PhD thesis consists of three original articles published in international peer-reviewed journals:

(1) **Amendt T** & Jumaa H (2021) Memory IgM protects endogenous insulin from autoimmune destruction. ***The EMBO Journal***
DOI: 10.15252/embj.2020107621, 1;40(17):e107621.

(2) **Amendt T**[§], El Ayoubi O[§], Linder AT, Allies G, Young M, Setz CS, Jumaa H (2021) Primary Immune responses and affinity maturation are controlled by IgD. ***Frontiers in Immunology***
DOI: 10.3389/fimmu.2021.709240, 9;12:709240.
[§]these authors contributed equally

(3) **Amendt T**, Allies G, Nicolò A, El Ayoubi O, Young M, Röszer T, Setz CS, Warnatz K, Jumaa H (2022) Autoreactive antibodies control blood glucose by regulating insulin homeostasis. ***Proc. Natl. Acad. Sci. USA***
DOI: 10.1073/pnas.2115695119

1.3 Patents

The use of protective-regulatory IgM (PR-IgM) targeting insulin has been filed as patent applications together with Prof. Hassan Jumaa.

2. Summary of articles included in the thesis

2.1 Memory IgM protects endogenous insulin from autoimmune destruction

Amendt T & Jumaa H (2021) Memory IgM protects endogenous insulin from autoimmune destruction. *The EMBO Journal*
DOI: 10.15252/embj.2020107621, 1;40(17):e107621.

The first publication aimed at investigating how autoreactive B cells could be activated *in vivo* and what molecular features are needed to mount an autoantibody response. In particular, we wanted to understand what role antigen valences of self-molecules play in autoreactive antibody responses.
In order to examine the above-mentioned hypotheses, we chose to use wildtype mice since they resemble the most physiological conditions with a normal B cell repertoire being translatable to humans. In fact, B cell development of mouse and man is stunningly similar in terms of developmental stages and V(D)J repertoire (Pieper et al., 2013). To determine the effects of autoantigen valences, we chose a highly abundant self-molecule, namely insulin. Recent studies reported that the insulin-A-chain is the main target of autoantibodies against insulin in exogenous insulin autoimmune syndrome (EIAS) (Censi et al., 2018; Hu & Chen, 2018; Uchigata et al., 2010). For experiments testing the quality and dynamics of autoimmune responses, we used polyvalent native insulin by coupling biotinylated insulin to streptavidin (cInsulin). Strikingly, administering cInsulin into mice induced robust insulin-reactive IgG responses that bind native insulin in ELISA and biolayer interferometry (BLI). Similar to cInsulin, the injection of polyvalent C-peptide (CP) complexes also leads to anti-CP IgG supporting a general mechanism of autoantibody induction by polyvalent self-proteins. The presence of insulin-recognizing IgG should lead to insulin neutralization and increased blood glucose levels as observed in EIAS patients. As expected, mice injected with cInsulin showed highly elevated blood glucose levels as well as glucosuria in urine mimicking a diabetes-like situation. In order to show that the anti-insulin antibodies are directly causative for blood glucose dysregulation, we isolated insulin-antibodies in an autoantigen-specific manner. As expected, intravenous injections of wildtype mice with anti-insulin IgG lead to increased blood glucose levels 2 hours post injection.
However, studying the modulatory role of monovalent antigen on complex antigen by injecting precise doses of soluble to complex insulin with a certain molarity (e.g. 100:1) is impossible due to the drastic glucose regulation capacity by soluble insulin. In order to circumvent this problem, we designed peptides of the insulin-A-chain (InsA) and coupled them covalently to key hole limpet hemocyanin (KLH) to obtain polyvalent InsA complexes. Importantly, the epitope on the A-chain that we used is also the most frequent epitope occurring in EIAS patients. Here, it was possible to inject ratios of soluble to complex peptides. We could show that the generation of autoreactive IgM as well as IgG is possible in wildtype animals when injecting polyvalent insulin complexes and polyvalent InsA peptides. Furthermore, animals injected with either cInsulin or cInsA developed autoimmune diabetes symptoms by showing highly elevated blood glucose concentrations due to insulin depletion by autoantibodies. Moreover, these mice also showed glucosuria as wells as increased water consumption. Finally, FACS analyses revealed an acute pancreatitis in these mice characterized by infiltration of neutrophils and macrophages as well as highly elevated proinflammatory cytokines in the pancreas microenvironment. These

results indicate that insulin-targeting IgG autoantibodies are sufficient to establish a pancreas inflammation which could explain the link between anti-insulin IgG in early phase T1D and advanced pancreatitis together with autoreactive T cell infiltration. Interestingly however, repeated injections with cInsulin or cInsA did not lead to increasing pathology as expected, but rather led to normoglycemic mice. By day 49 post injection (boost on d42) all mice were resistant to disease induction by cInsA injections.

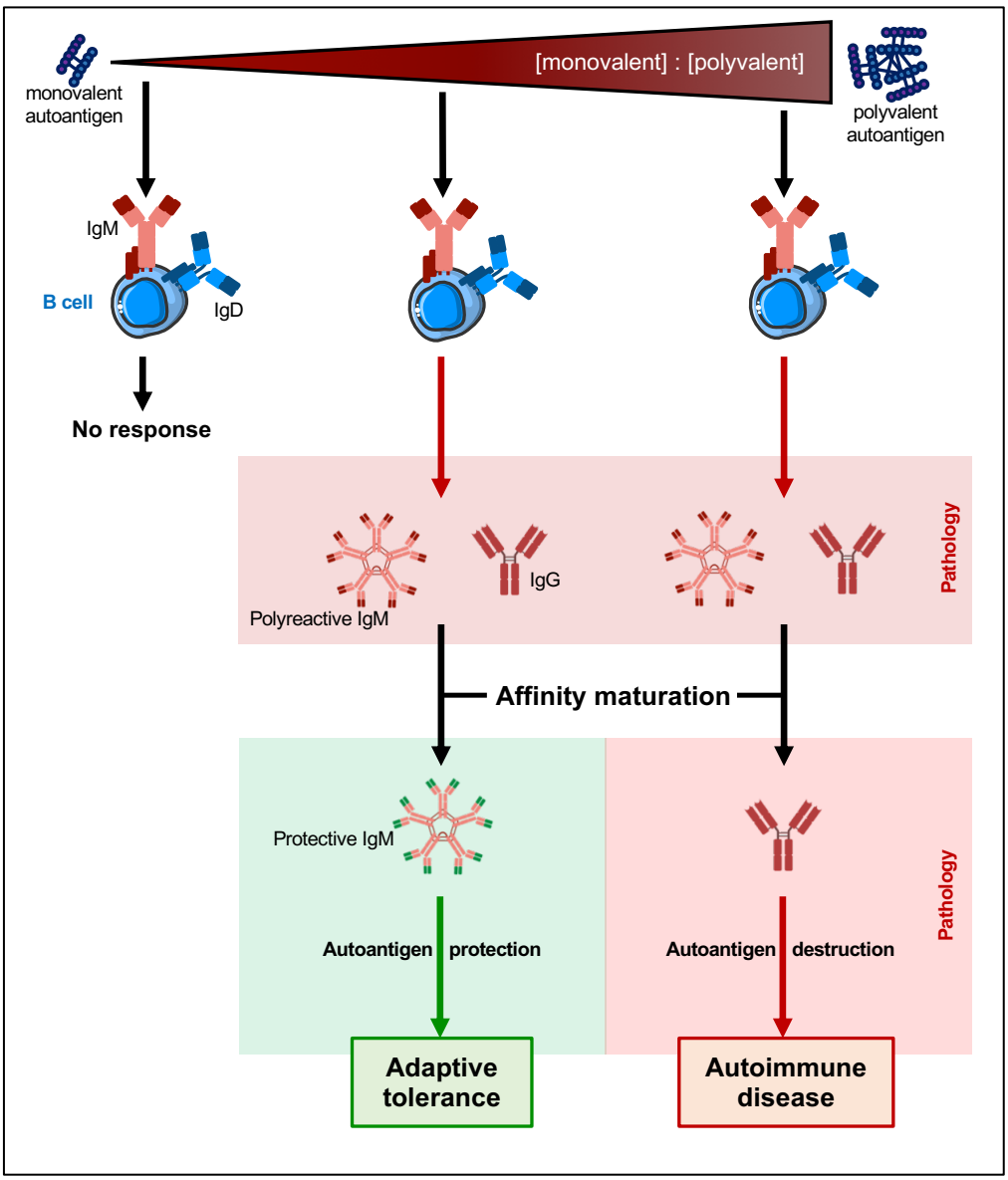


Figure 4 | The valency of autoantigens dictates the outcome of an autoantibody response (adapted from Amendt & Jumaa, 2021), CC BY 4.0, https://creativecommons.org/licenses/by/4.0/. Monovalent (soluble) autoantigen is not capable of activating autoreactive B cells. Complexation of autoantigen into a polyvalent form (here insulin) induces robust autoantibody responses. In particular, primary IgM and IgG reactive to insulin do neutralize their target inducing a pathology (red) accompanied by hyperglycemia and glucosuria. In the presence of monovalent autoantigen (insulin) insulin-reactive IgM undergoes affinity maturation. The affinity-matured insulin-reactive IgM protects its autoantigen from degradation by anti-insulin IgG and is referred to as protective-regulatory IgM (PR-IgM) (green). The adaptive generation of PR-IgM which prevents pathology and protects from autoimmune diabetes is referred to as adaptive tolerance.

Strikingly, anti-insulin-IgM titers were drastically increased and seemed to be required for the resistance of disease induction. This was in contrast to primary IgM which was collected at day 7 after immunization and which showed a vigorous capacity to neutralize insulin and cause pathologies such as hyperglycemia and subsequently pancreatitis.

Since primary IgM and secondary IgM may drastically differ in affinity, we proposed that memory IgM, which is produced during secondary immunization with insulin, possesses high affinity which is required for the observed protection from disease. We addressed that directly by performing multiple biochemical analyses. In contrast to primary IgM, we found that the anti-Insulin memory IgM has high-affinity against insulin while not binding to dsDNA suggesting a loss of polyreactivity as compared with primary IgM. We proposed that the monoreactive memory IgM binds insulin as a separate IgM pentamer, whereas polyreactive primary IgM forms high molecular weight immune complexes that can easily be phagocytosed by macrophages. In order to test this hypothesis, we isolated primary and memory IgM from cInsA injected mice and incubated the different IgM classes with insulin and dsDNA. Subsequently, we generated two fractions of low and high molecular weight by using cut off spin columns. Immune complexes consisting of multiple IgM molecules stay in the upper fraction and single IgM pentamers will migrate into the lower fraction. Coomassie-stained SDS-PAGEs revealed that, in contrast to primary IgM, the memory IgM did not form high molecular weight immune complexes in the presence of dsDNA. Next, we aimed at investigating the effects of memory IgM on insulin *in vivo*. To this end, we injected memory IgM intravenously into wildtype mice and observed a stable normoglycemic status whereas injections of anti-insulin IgG led to hyperglycemia. When injecting memory IgM in combination with IgG, the memory IgM was able to protect insulin from IgG-mediated degradation. Due to this features we refer to this antibody class as protective-regulatory IgM (PR-IgM). In addition, when injecting cInsA-immunized mice with PR-IgM intravenously, the PR-IgM was able to suppress blood glucose concentration increases by half further supporting a protective role.

Together, our data suggest the existence of a novel class of autoreactive IgM, which possesses high affinity and mono-reactivity against its autoantigen leading to stabilization *in vivo* rather than destruction. We refer to this phenomenon as adaptive tolerance. It is likely that this phenomenon is not restricted to injections with autoantigen complexes but is rather a common mechanism to protect autoantigens in the course of an immune reaction. Adaptive autoimmune IgM responses protecting autoantigens are most likely a key mechanism for the prevention of IgG-mediated autoimmunity destruction. Notably, secondary protein modifications and misfolding accumulate in aged individuals increasing the risk of forming polyvalent protein complexes suggesting that adaptive tolerance is an important mechanism for tissue homeostasis in aging (Haataja et al., 2016).

Strikingly, these data suggest that the proposed central tolerance removing autoreactive specificities has the opposite effect than expected on tolerance. Indeed, self-protection by PR-IgM requires the generation of highly autoreactive B cells which are removed by the proposed central tolerance concept.

According to our data and recent studies (du Pré et al., 2020; Setz et al., 2019; Übelhart et al., 2015) it is more likely that B cells do not discriminate between self and non-self, but rather distinguish antigen forms and valences. Once polyvalent autoantigen is present, autoreactive B cells are capable of mounting autoantibody responses with IgG autoantibodies. In particular, B cells that encounter soluble antigen will not mount antibody responses, whereas B cells encountering complex antigen will become activated and mount antibody responses attacking the target structure. If the target structure belongs to self, the

availability of soluble (monovalent) autoantigen is crucial in order to generate PR-IgM protecting the targeted self-protein (**Figure 4**).
In the next study we aimed at dissecting the underlying molecular mechanism.

2.2 Primary immune responses and affinity maturation are controlled by IgD

Amendt T[§], El Ayoubi O[§], Linder AT, Allies G, Young M, Setz CS, Jumaa H (2021) Primary Immune responses and affinity maturation are controlled by IgD. *Frontiers in Immunology* DOI: 10.3389/fimmu.2021.709240, 9;12:709240.

The second publication aimed at extending the concept of adaptive tolerance (Amendt & Jumaa, 2021) by uncovering the molecular mechanism underneath. Here, we examined the role of the two BCR classes (IgM and IgD) in adaptive tolerance and in autoimmune responses in general. Particularly, the role of the IgD-class BCR was of interest because the literature suggests a redundant function despite structural differences of IgD as compared to IgM. Furthermore, IgD-deficient mice showed only a mild phenotype supporting the view of redundant function (Nitschke et al., 1993; Roes & Rajewsky, 1993).
In order to investigate the role of the IgD-class BCR in autoimmunity, we used the immunization approach in wildtype mice as described above (Amendt & Jumaa, 2021) and combined this approach with IgD-deficient mice. We also aimed at understanding the role of the IgD-class BCR when encountering different ratios of soluble to complex (auto)antigen. Here, we used nitrophenyl (NP) coupled to KLH and in soluble form in wildtype as well as IgD-deficient mice. Since *in vitro* experiments revealed that the IgD-class BCR is sensitive for modulation by soluble antigen, we aimed at testing if this modulation is also valid *in vivo* for autoantigens. Autoantibody responses were analyzed by ELISA and ELISpot. Biochemical characterization of autoantibodies was done by autoantigen-specific isolation of IgM and IgG. Polyreactivity and antigen-affinity were assessed by HEp2 slides and biolayer interferometry, respectively.
In order to investigate if soluble autoantigen affects antibody responses by fine-tuning B cell activation and plasma cell differentiation in an IgD-class BCR-dependent manner, we injected wildtype and IgD-deficient mice with ratios of soluble to complex (monovalent to polyvalent) antigen. Injections with 100:1 (soluble:complex) insulin A-chain peptides (InsA) (Amendt & Jumaa, 2021) revealed that soluble antigen is able to suppress IgG responses significantly *in vivo*. Interestingly, this immune response modulation did not occur in IgD-deficient mice suggesting a crucial role of the IgD-class BCR in this modulation process. Next, we examined the early IgM response against insulin in wildtype and IgD-deficient mice injected with cInsA. We found that IgM secretion of wildtype mice starts around day 3 post injection, whereas IgD-deficient mice mounted strong and very rapid IgM responses already on day 1 post injection. These data suggest a role of the IgD-class BCR in the regulation of autoimmune responses because IgD-class BCR is capable of modulating the activation threshold of autoreactive B cells thereby delaying antibody secretion.
In order to further characterize this rapid antibody response, we analyzed spleens of both genotypes. Interestingly, we found that IgD-deficient mice showed a drastically increased $CD21^{-}$ $CD23^{-}$ B cell population that did not show markers for classical plasma cells or B1 B cells which are typical cells secreting antibodies. ELISpot experiments confirmed that this population is the main source of autoantibody secretion at day 1 post injection with cInsA.

In addition, we investigated if IgD-deficient mice were able to develop adaptive tolerance (Amendt & Jumaa, 2021) via PR-IgM and found that IgM affinity maturation was heavily delayed in these mice. In order to specifically discriminate between primary IgM and PR-IgM, we performed a series of biochemical analyses. Here, we show that the primary immune response always is autoreactive due to recognition of dsDNA independent of the antigen being *self* or *non-self*. Further, we could show that primary immune responses are autoreactive but nevertheless somehow antigen-specific since both primary IgM responses against insulin or NP recognized dsDNA but not the other immunogen used. This suggests dsDNA-recognition by primary IgM as a fundamental feature required for antigen clearance and potentially for immune complex formation.

Together, our data suggest that the IgD-class BCR plays a pivotal role in tolerance development, as it regulates the discrimination between monovalent and polyvalent antigen and as it controls the development of antibody secreting cells. It is conceivable that most autoantigens occur in a soluble (monovalent) form suggesting that endogenous autoantigens push the immune response towards an IgM response via an IgD-class BCR-dependent mechanism. Further, the polyreactivity of primary IgM is crucial for high molecular weight immune complex formation and is therefore fundamental for IgD-class BCR activation and further induction of effective secondary responses. In sum, the IgD-class BCR increases the B cell activation threshold, prevents rapid uncontrolled autoimmune responses and is needed in order to perform sufficient affinity maturation (**Figure 5**).

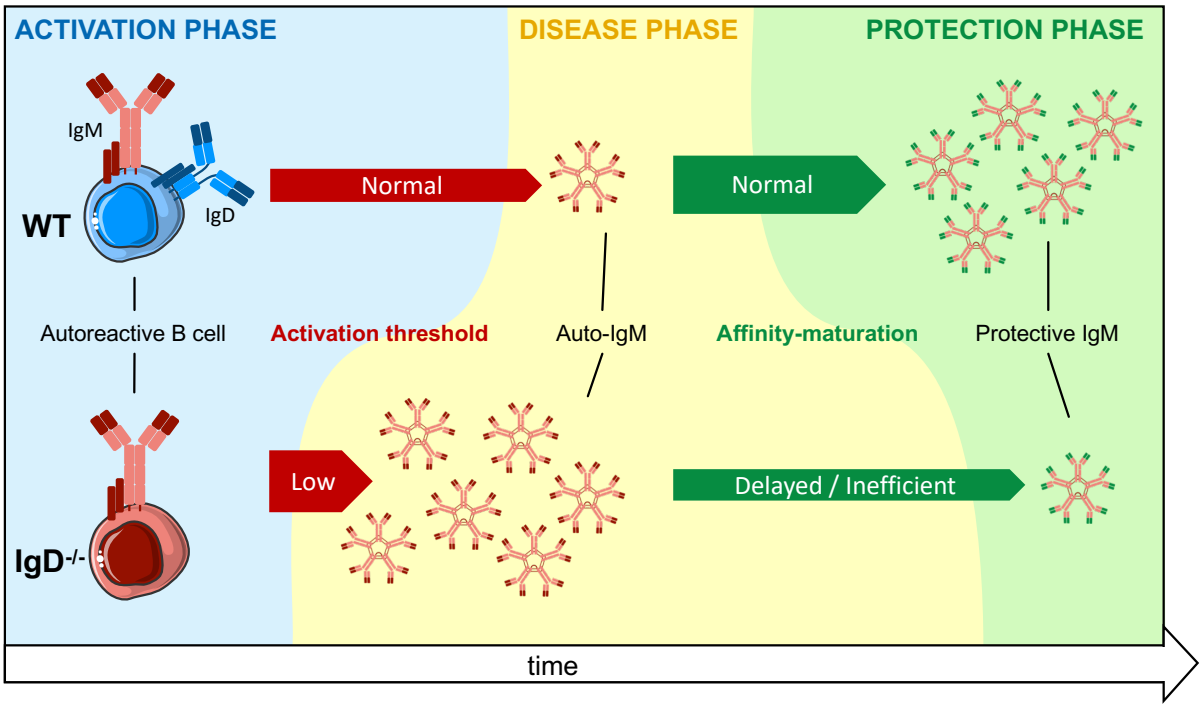


Figure 5 | The IgD-class B cell antigen receptor is required for limiting rapid autoantibody responses and controls affinity maturation (adapted from Amendt *et al*, 2021), CC BY 4.0, https://creativecommons.org/licenses/by/4.0/.

In wildtype mice insulin autoantibody responses causing hyperglycemia (yellow) are limited by later production of PR-IgM (green). B cell activation and IgM production takes 3 – 7 days post injection (blue). In contrast, B cells lacking the IgD-class B cell antigen receptor produce IgM within 24 hours post injection (blue). Further, affinity maturation and thus PR-IgM generation (green) is significantly delayed prolonging the disease phase extensively (yellow).

Thus, it will be an interesting question to examine the role of the IgD-class BCR in certain human autoimmune diseases. Previous studies reported IgD^+ $CD27^+$ memory-like B cells (Weller et al., 2004) that were highly autoreactive and suggested these cells to be involved in pathogenesis of autoimmunity.

2.3 Autoreactive antibodies control blood glucose by regulating insulin homeostasis

Amendt T, Allies G, Nicolò A, El Ayoubi O, Young M, Röszer T, Setz CS, Warnatz K, Jumaa H (2022) Autoreactive antibodies control blood glucose by regulating insulin homeostasis. *Proc. Natl. Acad. Sci. USA*
DOI: 10.1073/pnas.2115695119

After describing the initial model of adaptive tolerance in mice and showing that the IgD-class BCR is the central regulator of B cell tolerance, we aimed at investigating if our concept is also valid in humans. Briefly, the concept of adaptive tolerance proposes that autoreactivity is ubiquitously found in form of autoantibodies capable of regulating homeostasis. We proposed that a certain mix of insulin neutralizing (IgG, pIgM) and insulin protecting (PR-IgM) autoantibodies controls blood glucose levels. This scenario would allow to immediately prevent overshooting insulin output by the pancreas via insulin neutralization as well as ensuring a baseline level of insulin by depot function of PR-IgM.
Fundamental to this study was autoantibody isolation in fractions of high- and low-affine immunoglobulins. Therefore, we used bait columns and different pH shifts by applying elution buffers with pH 5 (low-affinity fraction) and pH 2.8 (high-affinity fraction). These autoantibodies were further characterized by specificity, reactivity and affinity. Finally, isolated autoantibodies were injected into wildtype and B cell-deficient mice to determine the effector function of each autoantibody fraction. Antibody isolation was performed antigen-specific (here insulin) and grouped into low and high affinity fractions. Subsequently, the insulin-affinity of the isolated antibodies was determined by using biolayer interferometry (BLI) to compare antigen affinities of different fractions and different autoantibody isotypes. In order to investigate if the isolated anti-insulin antibodies are of mono- or poly-reactivity, we performed HEp2 slide experiments. A positive signal on HEp2 slides would indicate the recognition of nuclear structures (ANA), cytoplasmic structures or phospholipids depending on the pattern. We defined HEp2-negative autoantibodies as mono-reactive autoantibodies. Polyreactive, mostly ANA-positive, autoantibodies were confirmed by dsDNA-ELISA or anti-dsDNA-BLI. As described above, we defined primary IgM (pIgM) as polyreactive but antigen-specific, while PR-IgM was defined as mono-reactive and antigen-specific.
In order to investigate the concept of adaptive tolerance in humans, we used human serum samples to isolate antibodies in combination with mouse experiments (Amendt et al., 2021; Amendt & Jumaa, 2021). First, we showed that insulin-targeting antibodies (IgM and IgG) are present in healthy individuals and are also found in common IgG preparations (IVIg) used to treat immunodeficient patients. Here, we proposed that human individuals not capable of producing any antibodies, namely CVID patients (common variable immunodeficiency), might show blood glucose dysregulation. Experiments using CVID sera were done in collaboration with Prof. Klaus Warnatz of the Albert-Ludwigs-Universität

Freiburg. As expected, CVID patients showed hypoglycemia prior to IVIg treatments. Interestingly, IVIg infusions containing insulin-neutralizing IgG restored physiological blood glucose levels. These experiments suggest a crucial involvement of insulin-targeting IgG in the baseline (steady-state) regulation of blood glucose. Next, we tested if healthy human individuals also possess pIgM and PR-IgM capable of regulating insulin homeostasis. Therefore, we isolated low and high affinity fractions of insulin-reactive IgM of young and aged individuals. We found that the human low-affinity anti-insulin IgM is indeed polyreactive and neutralizes insulin in mice and thus can be referred to as anti-insulin pIgM. Further, we showed that the human high-affinity fraction is mono-reactive and does not alter blood glucose levels of mice and can therefore be referred to as insulin-PR-IgM. Transfer experiments of human insulin antibodies into mice are possible due to the fully conserved insulin protein. Interestingly, when comparing pIgM to PR-IgM ratios of young and aged human individuals, we recognized that the ratio shifts towards PR-IgM in the elderly. This shift might well have a drastic impact on glucose metabolism.

Since high pancreatic output and oxidative stress can lead to disulfide bond mispairing and abnormal insulin complexes (Haataja et al., 2016), we used a biochemical method to generate such complexes *in vitro*. To this end, we incubated human native insulin with 1,2-phenylen-bis-maleimide to induce carbon-sulfur as well as disulfide bonds. Subsequently, we injected wildtype mice with the polyvalent insulin complexes (cInsulin) and monitored the immune response. As expected, the mice produced insulin-reactive IgM as well as IgG and showed hyperglycemia 7 and 14 days post injection. Interestingly, the high affinity human anti-insulin PR-IgM was capable of preventing hyperglycemia in injected mice when administered intravenously. These experiments suggest a superiority of anti-insulin PR-IgM over anti-insulin IgG. Further, human anti-insulin PR-IgM also decreased pancreas infiltration by macrophages significantly showing protection from pancreatitis.

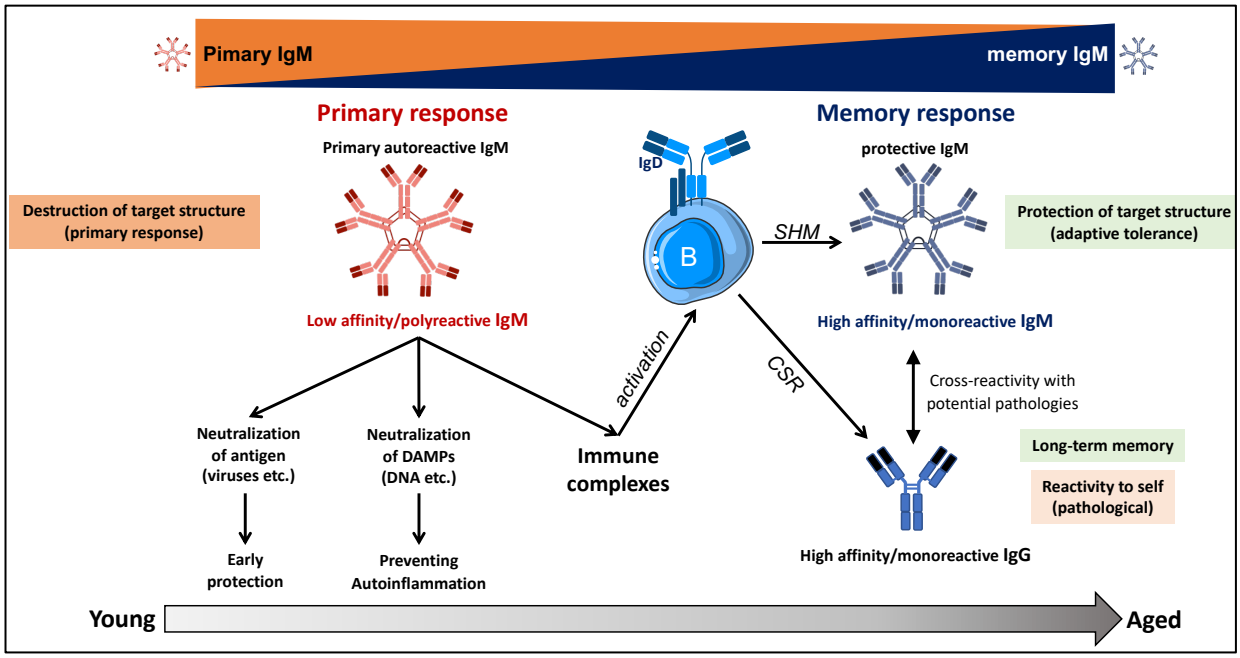


Figure 6 | Human insulin-reactive autoantibodies are capable of controlling blood glucose homeostasis (model based on Amendt & Jumaa, 2021).

The major autoantibody of young human individuals is represented by autoreactive primary IgM (pIgM) which is able to neutralize self-targets. During aging, the ratio of pIgM to self-protecting PR-IgM shifts towards PR-IgM. This imbalance might cause dysregulation of metabolism and inflammation status depending on the self-molecule recognized by these autoantibodies. A certain ratio of pIgM to PR-IgM could improve healthy aging and prevent age-associated inflammation processes known as inflamm-aging.

In order to examine the molecular mechanism of how PR-IgM is stabilizing insulin and how pIgM is neutralizing insulin *in vivo* we performed macrophage phagocytosis experiments in collaboration with PD Dr. Tamás Röszer of the Institute of Neurobiology (Ulm University). We could show that macrophages encountering pIgM-insulin-dsDNA immune complexes phagocytosed significantly more IgM and insulin compared to similar PR-IgM complexes. These results suggest that degradation of insulin in immune complexes is mainly mediated by macrophage phagocytosis.

In order to investigate the insulin regulation mechanism by autoantibodies in detail and to avoid using polyclonal insulin-antibody fractions isolated from serum and potentially recognizing different insulin epitopes, we chose to clone and express a monoclonal (mAb) insulin-specific antibody as IgM and IgG. Determination of insulin affinity by BLI revealed a K_D of 10^{-9} making the anti-insulin mAbs highly antigen-affine. HEp2 slides confirmed mono-reactivity of the anti-insulin IgM mAb categorizing it biochemically as PR-IgM. In order to test if these mAbs also protect insulin from degradation when expressed as IgM and neutralize as IgG, we injected wildtype mice intravenously. As expected, anti-insulin IgG mAb lead to hyperglycemia 2 hours post injection, whereas anti-insulin IgM mAb stabilized blood glucose supporting the notion of PR-IgM. Interestingly, when injecting both anti-insulin mAbs recognizing the same epitope, the PR-IgM class was able to protect insulin from degradation by anti-insulin IgG mAb.

In summary, we showed that human insulin-specific autoantibodies are not accidently produced without a defined function, but are rather important regulators of blood glucose metabolism by controlling the availability of insulin. Moreover, the concept of PR-IgM stabilizing self-structures *in vivo* characterized in mice (Amendt & Jumaa, 2021) seems to also be valid in humans (**Figure 6**). Interestingly, the ratio of neutralizing pIgM to PR-IgM shifts with age indicating involvement in the biology of aging. It is conceivable that autoantibodies are a crucial part of homeostasis regulating apart from insulin also other hormonal systems. Finally, the ability of PR-IgM to stabilize blood glucose levels could be of great therapeutic interest for certain groups of patients with early anti-insulin IgG-mediated T1D.

3. Discussion and outlook

The underlying hypothesis of this study was that autoreactive B cells do not discriminate between self and non-self but rather distinguish antigen valences (monovalent vs. polyvalent). Since the IgD-class BCR prevent B cell activation upon encounter of monovalent antigen, we proposed that autoreactive B cells become activated by polyvalent antigen regardless whether it is polyvalent self- or foreign-molecule. Surprisingly, we discovered high-affinity autoantibodies (PR-IgM) capable of protecting autoantigens and preventing autoimmune pathology (**Figure 7**):

(1) Strikingly, we could show that B cells produce insulin-reactive autoantibodies (primary IgM and IgG) when encountering polyvalent native insulin in wildtype mice. Further, these primary IgM and secondary IgG responses actually induced diabetes symptoms by increasing blood glucose levels and pancreatitis indicated by elevated serum pancreatic lipase and pancreas immune cell infiltration. Surprisingly however, booster injections by polyvalent Insulin complexes induced enormous titers of anti-insulin-IgM while the mice became resistant to disease development. We found that these anti-insulin memory IgM possesses high-affinity to insulin and do not neutralize it *in vivo*. Moreover, these antibodies protected insulin from degradation (protective-regulatory IgM; PR-IgM). Due to the characteristics of adapting autoimmunity leading to disease protection, we refer to this phenomenon as adaptive tolerance. We think that this concept is crucial in preventing autoimmunity against soluble self-structures such as hormones and proteins. This concept of autoantibodies being capable of protecting self-proteins might explain the spontaneous episodes of hypoglycemia reported in EIAS patients. Here, PR-IgM might function as an insulin repertoire (repertoire effect) releasing insulin depending on antigen-binding affinity, availability of antigen in solution (soluble) and avidity. Further, a network of self-protein stabilizing (PR-IgM) and self-protein degrading IgM (pIgM) might regulate the availability of self-proteins such as peptide hormones. The insight that autoantigen valences control the activation of autoreactive B cells together with the requirement of monovalent autoantigen in order to generate PR-IgM raises the question of how autoantigen-valences are altered *in vivo*. Here, several scenarios are conceivable. For instance, in the case of insulin, oxidative stress and high insulin output by the pancreas create abnormal insulin complexes (polyvalent) by disulfide or carbon-sulfur-mispairing leading to a shift in antigen-valency. Further, cells that undergo apoptosis within an inflammatory environment upregulate transglutaminases. Subsequently, these enzymes catalyze crosslinking of self-proteins by forming $\varepsilon(\gamma$-glutamyl) lysine cross-links as well as N,N-bis-(γ-glutamyl) polyamine bonds. Several autoantigens such as histones, tubulin or keratins have been reported to be highly susceptible for transglutamination-mediated crosslinking (Ballestar et al., 1996; Utz et al., 2000).

Central to the phenomenon observed in wildtype mice is the aspect of how autoreactive B cells are able to discriminate between mono- and polyvalent self-molecules *in vivo*. In particular, our second hypothesis (see 1.1) claimed that the IgD-class BCR is the element of autoantigen sensing and discrimination.

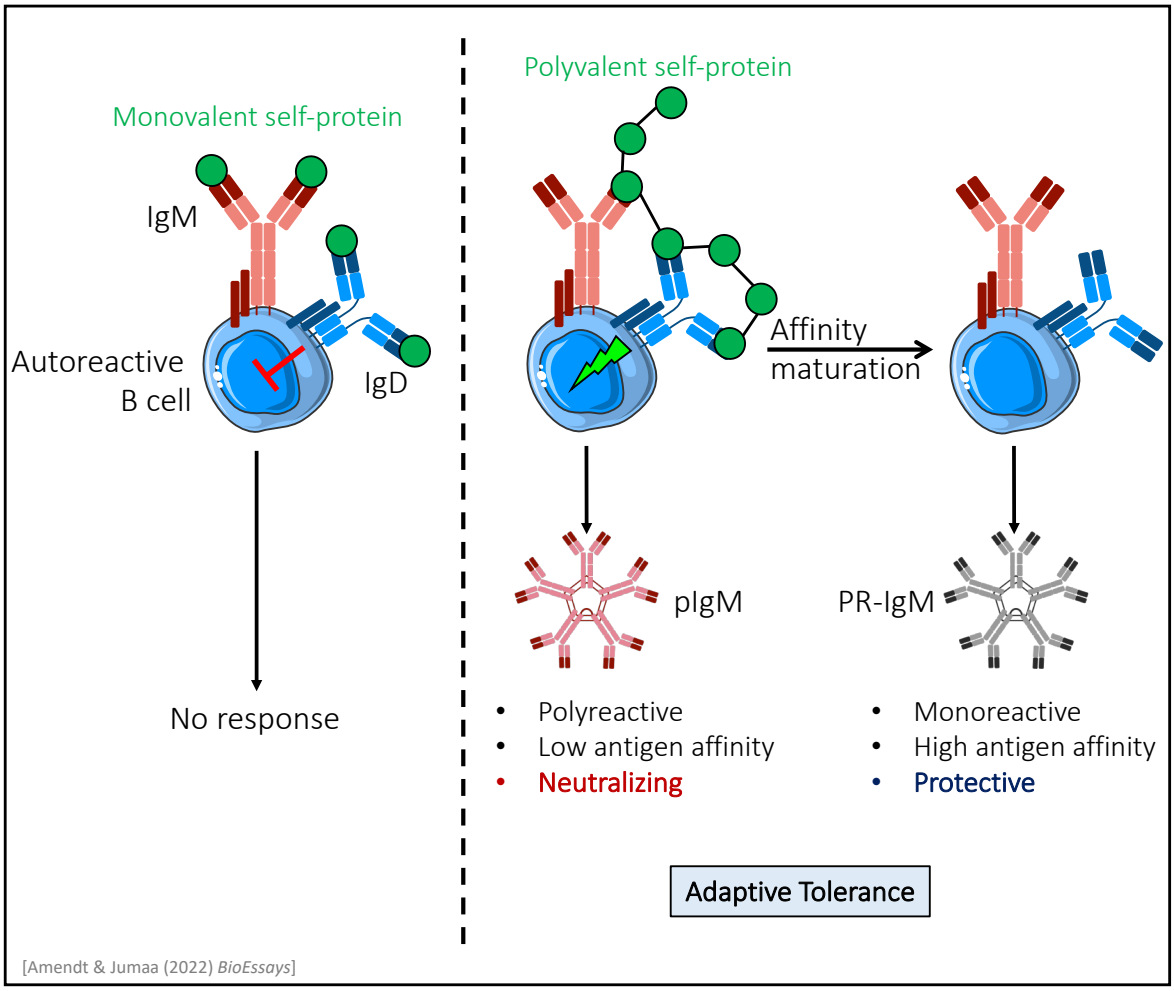


Figure 7 | Model of the mechanism of adaptive tolerance (Amendt & Jumaa 2022, *BioEssays*)**.** Low-affinity IgM possesses the ability of self-target neutralization, whereas high-affinity IgM (PR-IgM) protects its self-target *in vivo*. Here, biochemical properties define the class of autoreactive IgM. For instance, pIgM is defined by low antigen-affinity together with high polyreactivity, whereas PR-IgM shows high antigen-affinity. Certain ratios of primary IgM to PR-IgM determine the homeostasis of autoantigens. We propose that these ratios shift with age making the organism prone to inflamm-aging.

(2) Next, we tested the hypothesis that the IgD-class BCR is the main regulator of adaptive tolerance by mediating selective responsiveness to polyvalent antigen. In order to do so, we immunized IgD-deficient mice and wildtype mice with polyvalent insulin complexes and found that IgD-deficient mice fail to switch to PR-IgM efficiently. Further, we found that the IgD-class BCR is a negative regulator of B cell activation and antibody secretion *in vivo*. In fact, B cells lacking the IgD-class BCR were already activated 1 day post injection, whereas wildtype B cells were activated only 3 days post injection. Together, these data suggest that the IgD-class BCR is important for preventing polyreactive primary IgM responses by sensing monovalent antigen while being able to activate sufficient secondary responses by sensing polyvalent antigen possibly in the form of immune complexes. The notion that the IgD-class BCR is a negative regulator is also supported by the fact that IgM^+ malignant B cells have downregulated IgD-class BCR expression (Kläsener et al., 2021).

(3) To examine if the concept of adaptive tolerance is also valid in humans, we investigated human autoantibodies. We found, that human autoreactive IgM can be classified into low- and high-affinity fractions and that the high-affinity fraction is also able to protect autoantigens in mice. Our data suggest that certain ratios of neutralizing to protective autoantibodies are crucial for the homeostasis of self-molecules.

The results presented in this work drastically shift the current view of B cell tolerance from a static model including deletion of autoreactive B cells and functional silencing towards a highly dynamic model. Several recent publications showing that mature autoreactive B cells are present in the periphery (Noviski & Zikherman, 2018b; C. Tan et al., 2019; Zikherman et al., 2012) support our concept of adaptive tolerance.

Discrimination of antigen-valences (mono- vs. polyvalent) is enabled by the IgD-class BCR suggesting that the IgD-class BCR plays an important role in B cell tolerance (Amendt et al., 2021; Setz et al., 2019; Übelhart et al., 2015). This role was identified by using wildtype mice together with insulin as physiological autoantigen involved in diseases. In particular, oxidative stress (Karimi et al., 2016), sterile inflammation (Franceschi et al., 2017; Roh & Sohn, 2018) and aging (Frasca et al., 2010) may increase the likelihood of covalent autoantigen-complex formation and thus deregulation of physiological homeostasis (Utz et al., 2000).

Recurrent activation of autoreactive B cells by polyvalent autoantigen in the presence of sufficient monovalent autoantigen leads to the generation of PR-IgM. Interestingly, as a result of high antigen-affinity to the cognate self-protein and the inability to form large immune complexes, PR-IgM protects self-targets from degradation thus prolonging its half-lives *in vivo*. Thus, the ratio of pIgM to PR-IgM is most likely involved in physiological homeostasis by controlling the baseline availability of most hormones. For instance, insulin neutralizing pIgM or IgG could prevent postprandial pancreatic overshooting by limiting the maximum levels of soluble insulin or even remove insulin from insulin receptors. Further, PR-IgM which is providing an insulin repertoire could control the threshold of minimal insulin molecules available in the blood thus preventing hyperglycemia.

It is therefore conceivable that certain ratios of neutralizing to protecting autoantibodies are able to regulate hormone base-line levels and thus the sensitivity of its receptors. Since self-target neutralizing pIgM is inducible in contrast to nIgM which is produced antigen-encounter-independent, it is conceivable that autoreactive B cells might respond to changes in physiology immediately by rapid plasma cell differentiation. Thus, the secreted autoreactive pIgM is capable of controlling the availability of self-proteins in an adaptive manner. Moreover, autoreactive pIgM could use two different structural forms in order to provide ultra-low (hours) or low half-life (days) autoantibodies. In particular, pentameric pIgM with a half-life of few days might have a lasting neutralization effect, whereas hexameric pIgM could be utilized to neutralize a certain number of molecules without affecting a possible next wave of self-proteins (e.g. insulin wave) one day after autoantibody secretion.

Proposing that these ratios shift with age towards protective autoantibodies adds another dimension to the emerging role of autoantibodies in regulating hemostasis. Interestingly, this shift might also protect disease promoting factors such as inflammatory cytokines.

In particular,

Finally, several open questions are interesting to be investigated. First, determination of the exact ratios of monovalent to polyvalent autoantigen regulating GC entry and plasma cell

formation. Second, examining the role of autoreactive pIgM and PR-IgM in homeostasis of self-proteins. Third, how the ratio of pIgM to PR-IgM and autoreactive IgG shifts with age. Together, it is likely that understanding these unexpected dynamic interactions between autoreactive pIgM, IgG and PR-IgM will improve the therapeutic intervention in autoimmune diseases and autoinflammatory disorders.

4. Abstract

The enormous diversity of antibody specificities, which is generated by random rearrangement of immunoglobulin gene segments, harbors the risk of producing self-reactive antibodies. It is assumed that autoreactive B cell specificities are removed during early B cell development by clonal deletion or receptor editing creating a mature repertoire devoid of autoreactive B cells. However, the vast majority of autoantibody-mediated autoimmune diseases such as systemic lupus erythematosus (SLE) or rheumatoid arthritis (RA) question the view of strict central tolerance mechanisms. Further, encounter of peripheral autoantigen is thought to induce peripheral tolerance defined by downregulation of IgM-class BCR and functional unresponsiveness which is also known as *anergy*. The remaining IgD-class BCR is thought to be unresponsive to antigen stimulation and therefore the respective cells are referred to as anergic B cells. However, our results demonstrated that IgD-class BCR is selectively responsive to polyvalent antigen and that IgD-class BCR responsiveness is modulated by monovalent antigen. Thus, antigen form and configuration regulate immune tolerance rather than a mechanism based on absolute distinguishing *self* from *non-self*.

Here, we used a broad repertoire of methods including mouse immunizations, flow cytometric analysis and biochemical characterizations of autoantibodies to investigate immune tolerance of B cells. We show that **(1)** autoreactive B cells can easily be activated *in vivo* when encountering polyvalent autoantigen complexes. Consequently, polyvalent autoantigen complexes were able to induce autoreactive IgM as well as IgG responses in wildtype mice. These results suggest that neither central tolerance nor anergy removed autoreactive B cells from the mature B cell pool. Further, we observed that **(2)** soluble autoantigen is able to repress IgG responses and to enhance IgM responses when outnumbering the molarity of complex autoantigen in an IgD-class BCR-dependent manner. Strikingly, we discovered **(3)** a novel class of autoreactive IgM antibodies possessing high-affinity and mono-specificity. This IgM protected its cognate autoantigen from degradation by autoreactive IgG and therefore we refer to this IgM form as protective-regulatory IgM (PR-IgM). Finally, we show that **(4)** human individuals harbor autoantigen-specific protective-regulatory IgM that is able to stabilize the cognate autoantigen *in vivo*.

We propose that PR-IgM is a central player in preventing harmful autoimmunity and refer to that phenomenon as ***adaptive tolerance***. Furthermore, we propose that adaptive tolerance plays important roles beyond immune tolerance, as it might control the levels of self-proteins including important hormones thereby regulating physiological homeostasis.

5. References

Adyel, F. Z., Hentati, B., Boulila, A., Hachicha, J., Ternynck, T., Avrameas, S., & Ayadi, H. (1996). Characterization of autoantibody activities in sera anti-DNA antibody and circulating immune complexes from 12 systemic lupus erythematosus patients. *Journal of Clinical Laboratory Analysis*, *10*(6), 451–457. https://doi.org/10.1002/(SICI)1098-2825(1996)10:6<451::AID-JCLA24>3.0.CO;2-V

Amendt, T., El Ayoubi, O., Linder, A. T., Allies, G., Young, M., Setz, C. S., & Jumaa, H. (2021). Primary Immune Responses and Affinity Maturation are Controlled by IgD. *Frontiers in Immunology*, *12:709240*. https://doi.org/10.3389/fimmu.2021.709240

Amendt, T., & Jumaa, H. (2021). Memory IgM protects endogenous Insulin from autoimmune destruction. *The EMBO Journal*.

Amendt, T., & Jumaa, H. (2022). Adaptive tolerance: Protection through self-recognition. *BioEssays*, *December 2021*, 1–12. https://doi.org/10.1002/bies.202100236

Amir, S., Hartvigsen, K., Gonen, A., Leibundgut, G., Que, X., Jensen-Jarolim, E., Wagner, O., Tsimikas, S., Witztum, J. L., & Binder, C. J. (2012). Peptide mimotopes of malondialdehyde epitopes for clinical applications in cardiovascular disease. *Journal of Lipid Research*, *53*(7), 1316–1326. https://doi.org/10.1194/jlr.M025445

Avrameas, S., Ternynck, T., Tsonis, I. A., & Lymberi, P. (2007). Naturally occurring B-cell autoreactivity: A critical overview. In *Journal of Autoimmunity* (Vol. 29, Issue 4, pp. 213–218). J Autoimmun. https://doi.org/10.1016/j.jaut.2007.07.010

Ballestar, E., Abad, C., & Franco, L. (1996). Core histones are glutaminyl substrates for tissue transglutaminase. *Journal of Biological Chemistry*, *271*(31), 18817–18824. https://doi.org/10.1074/jbc.271.31.18817

Becker, M., Hobeika, E., Jumaa, H., Reth, M., & Maity, P. C. (2017). CXCR4 signaling and function require the expression of the IgD-class B-cell antigen receptor. *Proceedings of the National Academy of Sciences of the United States of America*, *114*(20), 5231–5236. https://doi.org/10.1073/pnas.1621512114

Boes, M. (2000). Role of natural and immune IgM antibodies in immune responses. *Molecular Immunology*, *37*(18), 1141–1149. https://doi.org/10.1016/S0161-5890(01)00025-6

Boes, M., Prodeus, A. P., Schmidt, T., Carroll, M. C., & Chen, J. (1998). A critical role of natural immunoglobulin M in immediate defense against systemic bacterial infection. *Journal of Experimental Medicine*, *188*(12), 2381–2386. https://doi.org/10.1084/jem.188.12.2381

Brink, R., Goodnow, C. C., Crosbie, J., Adams, E., Eris, J., Mason, D. Y., Hartley, S. B., & Basten, A. (1992). Immunoglobulin M and D Antigen Receptors are Both Capable of Mediating B Lymphocyte Activation, Deletion, or Anergy After Interaction with Specific Antigen. *Journal of Experimental Medicine*, *176*(4), 991–1005. https://doi.org/10.1084/jem.176.4.991

Censi, S., Mian, C., & Betterle, C. (2018). Insulin autoimmune syndrome: from diagnosis to clinical management. *Annals of Translational Medicine*, *6*(17), 335–335. https://doi.org/10.21037/atm.2018.07.32

Cooper, N. R. (1985). The Classical Complement Pathway: Activation and Regulation of the First Complement Component. *Advances in Immunology*, *37*(C), 151–216. https://doi.org/10.1016/S0065-2776(08)60340-5

du Pré, M. F., Blazevski, J., Dewan, A. E., Stamnaes, J., Kanduri, C., Sandve, G. K., Johannesen, M. K., Lindstad, C. B., Hnida, K., Fugger, L., Melino, G., Qiao, S.-W., & Sollid, L. M. (2020). B cell tolerance and antibody production to the celiac disease autoantigen transglutaminase 2. *Journal of Experimental Medicine*, *217*(2). https://doi.org/10.1084/jem.20190860

Ehrenstein, M. R., Cook, H. T., & Neuberger, M. S. (2000). Deficiency in serum immunoglobulin (Ig)M predisposes to development of IgG autoantibodies. *Journal of Experimental Medicine*, *191*(7), 1253–1257. https://doi.org/10.1084/jem.191.7.1253

Eschbach, C., Bach, M. P., Fidler, I., Pelanda, R., Köhler, F., Rajewsky, K., & Jumaa, H. (2011). Efficient generation of B lymphocytes by recognition of self-antigens. *European Journal of Immunology*, *41*(8), 2397–2403. https://doi.org/10.1002/eji.201041344

Franceschi, C., Garagnani, P., Vitale, G., Capri, M., & Salvioli, S. (2017). Inflammaging and 'Garb-aging.' In *Trends in Endocrinology and Metabolism* (Vol. 28, Issue 3, pp. 199–212). Elsevier Inc. https://doi.org/10.1016/j.tem.2016.09.005

Frasca, D., Diaz, A., Romero, M., Landin, A. M., & Blomberg, B. B. (2010). *Age effects on B cells and humoral immunity in humans*. https://doi.org/10.1016/j.arr.2010.08.004

Gay, D., Saunders, T., Camper, S., & Weigert, M. (1993). Receptor editing: An approach by autoreactive B cells to escape tolerance. *Journal of Experimental Medicine*, *177*(4), 999–1008. https://doi.org/10.1084/jem.177.4.999

Gold, M. R., & Reth, M. G. (2019). Antigen Receptor Function in the Context of the Nanoscale Organization of the B Cell Membrane. *Annual Review of Immunology*, *37*(1), 97–123. https://doi.org/10.1146/annurev-immunol-042718-041704

Goodnow, C. C., Crosbie, J., Adelstein, S., Lavoie, T. B., Smith-Gill, S. J., Brink, R. A., Pritchard-Briscoe, H., Wotherspoon, J. S., Loblay, R. H., Raphael, K., Trent, R. J., & Basten, A. (1988). Altered immunoglobulin expression and functional silencing of self-reactive B lymphocytes in transgenic mice. *Nature*, *334*(6184), 676–682. https://doi.org/10.1038/334676a0

Goodnow, C. C., Crosbie, J., Jorgensen, H., Brink, R. A., & Basten, A. (1989). Induction of self-tolerance in mature peripheral B lymphocytes. *Nature*, *342*(6248), 385–391. https://doi.org/10.1038/342385a0

Grönwall, C., & Silverman, G. J. (2014). Natural IgM: Beneficial autoantibodies for the control of inflammatory and autoimmune disease. In *Journal of Clinical Immunology* (Vol. 34, Issue SUPPL. 1). Springer New York LLC. https://doi.org/10.1007/s10875-014-0025-4

Gutzeit, C., Chen, K., & Cerutti, A. (2018). The enigmatic function of IgD: some answers at last. In *European Journal of Immunology* (Vol. 48, Issue 7, pp. 1101–1113). Wiley-VCH Verlag. https://doi.org/10.1002/eji.201646547

Haataja, L., Manickam, N., Soliman, A., Tsai, B., Liu, M., & Arvan, P. (2016). Disulfide mispairing during proinsulin folding in the endoplasmic reticulum. *Diabetes*, *65*(4), 1050–1060. https://doi.org/10.2337/db15-1345

Hamilton, A. M., Lehuen, A., & Kearney, J. F. (1994). Immunofluorescence analysis of B-1 cell ontogeny in the mouse. *International Immunology*, *6*(3), 355–361. https://doi.org/10.1093/intimm/6.3.355

Haralambous, S., Blackwell, C., Mappouras, D. G., Weir, D. M., Kemmett, D., & Lymberi, P. (1995). Increased natural autoantibody activity to cytoskeleton proteins in sera from patients with necrobiosis lipoidica, with or without insulin-dependent diabetes mellitus. *Autoimmunity*, *20*(4), 267–275. https://doi.org/10.3109/08916939508995704

Hobeika, E., Maity, P. C., & Jumaa, H. (2016). Control of B Cell Responsiveness by Isotype and Structural Elements of the Antigen Receptor. In *Trends in Immunology* (Vol. 37, Issue 5, pp. 310–320). Elsevier Ltd. https://doi.org/10.1016/j.it.2016.03.004

Holodick, N. E., Vizconde, T., Hopkins, T. J., & Rothstein, T. L. (2016). Age-Related Decline in Natural IgM Function: Diversification and Selection of the B-1a Cell Pool with Age. *The Journal of Immunology*, *196*(10), 4348–4357. https://doi.org/10.4049/jimmunol.1600073

Hu, X., & Chen, F. (2018). Exogenous insulin antibody syndrome (EIAS): A clinical syndrome associated with insulin antibodies induced by exogenous insulin in diabetic patients. *Endocrine Connections*, *7*(1), R47–R55. https://doi.org/10.1530/EC-17-0309

Karimi, M., Ignasiak, M. T., Chan, B., Croft, A. K., Radom, L., Schiesser, C. H., Pattison, D. I., & Davies, M. J. (2016). Reactivity of disulfide bonds is markedly affected by structure and environment: Implications for protein modification and stability. *Scientific Reports*, *6*(1), 1–12. https://doi.org/10.1038/srep38572

Kaul, A., Gordon, C., Crow, M. K., Touma, Z., Urowitz, M. B., Van Vollenhoven, R., Ruiz-Irastorza, G., & Hughes, G. (2016). Systemic lupus erythematosus. *Nature Reviews Disease Primers*, *2*(1), 16039. https://doi.org/10.1038/nrdp.2016.39

Keyt, B. A., Baliga, R., Sinclair, A. M., Carroll, S. F., & Peterson, M. S. (2020). Structure, Function, and Therapeutic Use of IgM Antibodies. *Antibodies*, *9*(4), 53. https://doi.org/10.3390/antib9040053

Kläsener, K., Jellusova, J., Andrieux, G., Salzer, U., Böhler, C., Steiner, S. N., Albinus, J. B., Cavallari, M., Süß, B., Voll, R. E., Boerries, M., Wollscheid, B., & Reth, M. (2021). CD20 as a gatekeeper of the resting state of human B cells. *Proceedings of the National Academy of Sciences of the United States of America*, *118*(7), 2021342118. https://doi.org/10.1073/pnas.2021342118

Lahtela, J. T., Knip, M., Paul, R., Antonen, J., & Salmi, J. (1997). Severe antibody-mediated human insulin resistance: Successful treatment with the insulin analog lispro: A case report. *Diabetes Care*, *20*(1), 71–73. https://doi.org/10.2337/diacare.20.1.71

Ludwig, R. J., Vanhoorelbeke, K., Leypoldt, F., Kaya, Z., Bieber, K., McLachlan, S. M., Komorowski, L., Luo, J., Cabral-Marques, O., Hammers, C. M., Lindstrom, J. M., Lamprecht, P., Fischer, A., Riemekasten, G., Tersteeg, C., Sondermann, P., Rapoport, B., Wandinger, K. P., Probst, C., … Nimmerjahn, F. (2017). Mechanisms of autoantibody-induced pathology. In *Frontiers in Immunology* (Vol. 8, Issue MAY). Frontiers Media S.A. https://doi.org/10.3389/fimmu.2017.00603

Lutz, H. U., Binder, C. J., & Kaveri, S. (2009). Naturally occurring auto-antibodies in homeostasis and disease. In *Trends in Immunology* (Vol. 30, Issue 1, pp. 43–51). Trends Immunol. https://doi.org/10.1016/j.it.2008.10.002

Maity, P. C., Blount, A., Jumaa, H., Ronneberger, O., Lillemeier, B. F., & Reth, M. (2015). B cell antigen receptors of the IgM and IgD classes are clustered in different protein islands that are altered during B cell activation. *Science Signaling*, *8*(394). https://doi.org/10.1126/scisignal.2005887

McHeyzer-Williams, M. G. (2003). B cells as effectors. In *Current Opinion in Immunology* (Vol. 15, Issue 3, pp. 354–361). Elsevier Ltd. https://doi.org/10.1016/S0952-7915(03)00046-3

Meffre, E., Schaefer, A., Wardemann, H., Wilson, P., Davis, E., & Nussenzweig, M. C. (2004). Surrogate Light Chain Expressing Human Peripheral B Cells Produce Self-reactive Antibodies. *Journal of Experimental Medicine*, *199*(1), 145–150. https://doi.org/10.1084/jem.20031550

Nemazee, D. A., & Bürki, K. (1989). Clonal deletion of B lymphocytes in a transgenic mouse bearing anti-MHC class I antibody genes. *Nature*, *337*(6207), 562–566. https://doi.org/10.1038/337562a0

Nemazee, D., & Buerki, K. (1989). Clonal deletion of autoreactive B lymphocytes in bone marrow chimeras. *Proceedings of the National Academy of Sciences of the United States of America*, *86*(20), 8039–8043. https://doi.org/10.1073/pnas.86.20.8039

Nitschke, L., Kosco, M. H., Kohler, G., & Lamers, M. C. (1993). Immunoglobulin D-deficient mice can mount normal immune responses to thymus-independent and -dependent antigens. *Proceedings of the National Academy of Sciences of the United States of America*, *90*(5), 1887–1891. https://doi.org/10.1073/pnas.90.5.1887

Nordquist, L., & Wahren, J. (2009). C-peptide: The missing link in diabetic nephropathy? *Review of Diabetic Studies*, *6*(3), 203–210. https://doi.org/10.1900/RDS.2009.6.203

Noviski, M., & Zikherman, J. (2018a). Control of autoreactive B cells by IgM and IgD B cell receptors: maintaining a fine balance. *Current Opinion in Immunology*, *55*, 67–74. https://doi.org/10.1016/j.coi.2018.09.015

Noviski, M., & Zikherman, J. (2018b). *IgM and IgD B cell receptors differentially respond to endogenous antigens and control B cell fate | eLife*. https://elifesciences.org/articles/35074

Packard, T., Smith, M., Conrad, F., Johnson, S., Getahun, A., Lindsay, R., Hinman, R., Friedman, R., Thomas, J., & Cambier, J. (2016). B Cell Receptor Affinity for Insulin Dictates Autoantigen Acquisition and B Cell Functionality in Autoimmune Diabetes. *Journal of Clinical Medicine*, *5*(11), 98. https://doi.org/10.3390/jcm5110098

Pieper, K., Grimbacher, B., & Eibel, H. (2013). B-cell biology and development. In *Journal of Allergy and Clinical Immunology* (Vol. 131, Issue 4, pp. 959–971). J Allergy Clin Immunol. https://doi.org/10.1016/j.jaci.2013.01.046

Quartier, P., Bustamante, J., Sanal, O., Plebani, A., Debré, M., Deville, A., Litzman, J., Levy, J., Fermand, J. P., Lane, P., Horneff, G., Aksu, G., Yalçin, I., Davies, G., Tezcan, I., Ersoy, F., Catalan, N., Imai, K., Fischer, A., & Durandy, A. (2004). Clinical, immunologic and genetic analysis of 29 patients with autosomal recessive hyper-IgM syndrome due to Activation-Induced Cytidine Deaminase deficiency. *Clinical Immunology*, *110*(1), 22–29. https://doi.org/10.1016/j.clim.2003.10.007

Reyneveld, G. Ij., Savelkoul, H. F. J., & Parmentier, H. K. (2020). Current Understanding of Natural Antibodies and Exploring the Possibilities of Modulation Using Veterinary Models. A Review. *Frontiers in Immunology*, *11*(September), 1–19. https://doi.org/10.3389/fimmu.2020.02139

Roes, J., & Rajewsky, K. (1993). Immunoglobulin D (IgD)-deficient mice reveal an auxiliary receptor function for IgD in antigen-mediated recruitment of B cells. *Journal of Experimental Medicine*, *177*(1), 45–55. https://doi.org/10.1084/jem.177.1.45

Roh, J. S., & Sohn, D. H. (2018). Damage-associated molecular patterns in inflammatory diseases. In *Immune Network* (Vol. 18, Issue 4). Korean Association of Immunologists. https://doi.org/10.4110/in.2018.18.e27

Setz, C. S., Khadour, A., Renna, V., Iype, J., Gentner, E., He, X., Datta, M., Young, M., Nitschke, L., Wienands, J., Maity, P. C., Reth, M., & Jumaa, H. (2019). Pten controls B-cell responsiveness and germinal center reaction by regulating the expression of IgD BCR . *The EMBO Journal*, *38*(11). https://doi.org/10.15252/embj.2018100249

Shimizu, T., Kozono, Y., Kozono, H., Oda, M., & Azuma, T. (2004). Affinity maturation of secreted IgM pentamers on B cells. *International Immunology*, *16*(5), 675–684. https://doi.org/10.1093/intimm/dxh069

Shlomchik, M. J. (2008). Sites and Stages of Autoreactive B Cell Activation and Regulation. In *Immunity* (Vol. 28, Issue 1, pp. 18–28). Elsevier. https://doi.org/10.1016/j.immuni.2007.12.004

Stebegg, M., Kumar, S. D., Silva-Cayetano, A., Fonseca, V. R., Linterman, M. A., & Graca, L. (2018). Regulation of the germinal center response. *Frontiers in Immunology*, *9*(OCT), 1–13. https://doi.org/10.3389/fimmu.2018.02469

Suurmond, J., & Diamond, B. (2015). Autoantibodies in systemic autoimmune diseases: Specificity

and pathogenicity. *Journal of Clinical Investigation*, *125*(6), 2194–2202. https://doi.org/10.1172/JCI78084
Tan, C., Noviski, M., Huizar, J., & Zikherman, J. (2019). Self-reactivity on a spectrum: A sliding scale of peripheral B cell tolerance. *Immunological Reviews*, *292*(1), 37–60. https://doi.org/10.1111/imr.12818
Tan, E. M. (1989). Antinuclear Antibodies: Diagnostic Markers for Autoimmune Diseases and Probes for Cell Biology. *Advances in Immunology*, *44*(C), 93–151. https://doi.org/10.1016/S0065-2776(08)60641-0
Taplin, C., & Barker, J. (2008). Autoantibodies in type 1 diabetes. *Autoimmunity*, *41*(1), 11–18. https://doi.org/10.1080/08916930701619169
Tiegs, S. L., Russell, D. M., & Nemazee, D. (1993). Receptor editing in self-reactive bone marrow B cells. *Journal of Experimental Medicine*, *177*(4), 1009–1020. https://doi.org/10.1084/jem.177.4.1009
Tsiantoulas, D., Gruber, S., & Binder, C. J. (2012). B-1 cell immunoglobulin directed against oxidation-specific epitopes. *Frontiers in Immunology*, *3*(JAN), 1–6. https://doi.org/10.3389/fimmu.2012.00415
Tsubata, T., & Reth, M. (1990). The products of pre-B cell-specific genes (λ5 and VpreB) and the immunoglobulin μ chain form a complex that is transported onto the cell surface. *Journal of Experimental Medicine*, *172*(3), 973–976. https://doi.org/10.1084/jem.172.3.973
Übelhart, R., Hug, E., Bach, M. P., Wossning, T., Dühren-Von Minden, M., Horn, A. H. C., Tsiantoulas, D., Kometani, K., Kurosaki, T., Binder, C. J., Sticht, H., Nitschke, L., Reth, M., & Jumaa, H. (2015). Responsiveness of B cells is regulated by the hinge region of IgD. *Nature Immunology*, *16*(5), 534–543. https://doi.org/10.1038/ni.3141
Uchigata, Y., Hirata, Y., & Iwamoto, Y. (2010). Insulin autoimmune syndrome (Hirata disease): Epidemiology in Asia, including Japan. *Diabetology International*, *1*(1), 21–25. https://doi.org/10.1007/s13340-010-0001-z
Ueno, H. (2016). T follicular helper cells in human autoimmunity. In *Current Opinion in Immunology* (Vol. 43, pp. 24–31). Elsevier Ltd. https://doi.org/10.1016/j.coi.2016.08.003
Utz, P. J., Gensler, T. J., & Anderson, P. (2000). Death, autoantigen modifications, and tolerance. *Arthritis Research*, *2*(2), 101–114. https://doi.org/10.1186/ar75
Vinuesa, C. G., Linterman, M. A., Yu, D., & Maclennan, I. C. M. (2016). Follicular Helper T Cells. *Annual Review of Immunology*, *34*, 335–368. https://doi.org/10.1146/annurev-immunol-041015-055605
Wang, L., Li, L. rong, & Young, K. H. (2020). New agents and regimens for diffuse large B cell lymphoma. *Journal of Hematology and Oncology*, *13*(1), 1–23. https://doi.org/10.1186/s13045-020-01011-z
Wardemann, H., Yurasov, S., Schaefer, A., Young, J. W., Meffre, E., & Nussenzweig, M. C. (2003). Predominant autoantibody production by early human B cell precursors. *Science*, *301*(5638), 1374–1377. https://doi.org/10.1126/science.1086907
Weinstein, J. R., Quan, Y., Hanson, J. F., Colonna, L., Iorga, M., Honda, S. -i., Shibuya, K., Shibuya, A., Elkon, K. B., & Moller, T. (2015). IgM-Dependent Phagocytosis in Microglia Is Mediated by Complement Receptor 3, Not Fc / Receptor. *The Journal of Immunology*, *195*(11), 5309–5317. https://doi.org/10.4049/jimmunol.1401195
Weiss, M. A. (2009). Chapter 2 The Structure and Function of Insulin. Decoding the TR Transition. In *Vitamins and Hormones* (Vol. 80, Issue C, pp. 33–49). Vitam Horm. https://doi.org/10.1016/S0083-6729(08)00602-X
Weller, S., Braun, M. C., Tan, B. K., Rosenwald, A., Cordier, C., Conley, M. E., Plebani, A., Kumararatne, D. S., Bonnet, D., Tournilhac, O., Tchernia, G., Steiniger, B., Staudt, L. M., Casanova, J. L., Reynaud, C. A., & Weill, J. C. (2004). Human blood IgM "memory" B cells are circulating splenic marginal zone B cells harboring a prediversified immunoglobulin repertoire. *Blood*, *104*(12), 3647–3654. https://doi.org/10.1182/blood-2004-01-0346
Wintersteiner. (1933). *Isoelectric Point of Insulin*. 473–478.
Yarkoni, Y., Getahun, A., & Cambier, J. C. (n.d.). *Molecular underpinning of B-cell anergy Modes of B-cell tolerance*. https://doi.org/10.1111/j.1600-065X.2010.00936.x
Zhang, H., Li, P., Wu, D., Xu, D., Hou, Y., Wang, Q., Li, M., Li, Y., Zeng, X., Zhang, F., & Shi, Q. (2015). Serum IgG subclasses in autoimmune diseases. *Medicine (United States)*, *94*(2), e387. https://doi.org/10.1097/MD.0000000000000387
Zhu, S., Larkin, D., Lu, S., Inouye, C., Haataja, L., Anjum, A., Kennedy, R., Castle, D., & Arvan, P. (2016). Monitoring C-Peptide Storage and Secretion in Islet b-Cells In Vitro and In Vivo. *Diabetes*, *65*, 699–709. https://doi.org/10.2337/db15-1264
Zikherman, J., Parameswaran, R., & Weiss, A. (2012). Endogenous antigen tunes the responsiveness of naive B cells but not T cells. *Nature*, *489*(7414), 160–164.

https://doi.org/10.1038/nature11311

6. Included publications

6.1 Amendt & Jumaa, 2021, *The EMBO Journal*

Amendt T & Jumaa H (2021) Memory IgM protects endogenous insulin from autoimmune destruction. *The EMBO Journal*
DOI: 10.15252/embj.2020107621, 1;40(17):e107621.

Copy right:

This publication was published as an open access article by the Wiley publishing house and falls under the terms of the CC BY NC ND 4.0 license.
https://creativecommons.org/licenses/by-nc-nd/4.0/

Author contribution:

Conceptualization and performance of all experiments. Interpretation of data and generation of the figures used in the publication. Contribution to writing of the article as well as performance of the peer-review process.

6.2 Amendt *et al*, 2021, *Frontiers in Immunology*

Amendt T[§], El Ayoubi O[§], Linder AT, Allies G, Young M, Setz CS, Jumaa H (2021) Primary Immune responses and affinity maturation are controlled by IgD. ***Frontiers in Immunology*** DOI: 10.3389/fimmu.2021.709240, 9;12:709240.
[§]these authors contributed equally

Copy right:

This publication was published as an open access article by the Frontiers Media publishing house and falls under the terms of the CC BY 4.0 license.
https://creativecommons.org/licenses/by/4.0/

Author contribution:

Conceptualization and performance of experiments (especially performance of biochemical characterization of autoantibodies and animal experiments). Preparation of the figures and interpretation of data. Contribution to the writing of the article and performance of the peer-review process.

6.3 Amendt *et al*, 2022, *PNAS*

Amendt T, Allies G, Nicolò A, El Ayoubi O, Young M, Röszer T, Setz CS, Warnatz K, Jumaa H (2022) Autoreactive antibodies control blood glucose by regulating insulin homeostasis. ***Proc. Natl. Acad. Sci. USA***
DOI: 10.1073/pnas.2115695119

Copy right:

This publication was published as an open access article by the proceedings of the national academy of sciences of the USA (PNAS USA) publishing house and falls under the terms of the CC BY NC ND 4.0 license.
https://creativecommons.org/licenses/by-nc-nd/4.0/

Author contribution:

Conceptualization and performance of experiments (especially performance of biochemical characterization of autoantibodies and animal experiments). Preparation of the figures and interpretation of data. Contribution to the writing of the article and performance of the peer-review process.

7. Acknowledgements

8. Curriculum vitae including publication list

LIST OF PUBLICATIONS

1. Amendt T, Allies G, Nicolò A, El Ayoubi O, Young M, Röszer T, Setz CS, Warnatz K, Jumaa H. Autoreactive antibodies control blood glucose by regulating insulin homeostasis. (2022) *PNAS*

2. Amendt T, Jumaa H. Adaptive Tolerance: Protection through self-recognition. (2022) *BioEssays*

3. Renna V, Surova E, Khadour A, Datta M, Amendt T, Hobeika E, Jumaa H. Defective allelic exclusion by IgD in the absence of autoantigen. (2022) *The Journal of Immunology*

4. Amendt T, Jumaa H. Memory IgM protects endogenous insulin from autoimmune destruction. (2021) *The EMBO Journal*

5. Amendt T, El Ayoubi O, Linder A, Allies G, Young M, Setz CS, Jumaa H. Primary immune responses and affinity maturation are controlled by IgD. (2021) *Frontiers in Immunology*

Article

SOURCE DATA | TRANSPARENT PROCESS | OPEN ACCESS

THE EMBO JOURNAL

Memory IgM protects endogenous insulin from autoimmune destruction

Timm Amendt & Hassan Jumaa*

Abstract

The enormous diversity of antibody specificities is generated by random rearrangement of immunoglobulin gene segments and is important for general protection against pathogens. Since random rearrangement harbors the risk of producing self-destructive antibodies, it is assumed that autoreactive antibody specificities are removed during early B-cell development leading to a peripheral compartment devoid of autoreactivity. Here, we immunized wild-type mice with insulin as a common self-antigen and monitored diabetes symptoms as a measure for autoimmune disease. Our results show that autoreactive anti-insulin IgM and IgG antibodies associated with autoimmune diabetes can readily be generated in wild-type animals. Surprisingly, recall immunizations induced increased titers of high-affinity insulin-specific IgM, which prevented autoimmune diabetes. We refer to this phenomenon as adaptive tolerance, in which high-affinity memory IgM prevents autoimmune destruction by competing with self-destructive antibodies. Together, this study suggests that B-cell tolerance is not defined by the absolute elimination of autoreactive specificities, as harmful autoantibody responses can be generated in wild-type animals. In contrast, inducible generation of autoantigen-specific affinity-matured IgM acts as a protective mechanism preventing self-destruction.

Keywords B-cell selection; central tolerance; diabetes; autoimmune diseases
Subject Categories Immunology; Molecular Biology of Disease
DOI 10.15252/embj.2020107621 | Received 29 December 2020 | Revised 21 May 2021 | Accepted 28 May 2021
The EMBO Journal (2021) e107621

Introduction

Self-tolerance is crucial for maintaining physiological integrity by avoiding autoimmune reactions. Currently, central and peripheral tolerance mechanisms are believed to control the B-cell antigen receptor (BCR) repertoire during B-cell development thereby preventing the generation or survival of self-reactive B cells (Goodnow *et al*, 1988; Nemazee & Buerki, 1989; Benschop *et al*, 2001).

It is assumed that autoreactive B cells are subjected to receptor editing by secondary immunoglobulin (Ig) gene rearrangement that removes the autoreactive specificity and enables the expression of non-autoreactive BCR (Gay *et al*, 1993; Tiegs *et al*, 1993; Zhang *et al*, 2003). B cells that fail to remove their autoreactivity are subjected to clonal deletion by central tolerance mechanisms during early B-cell development in the bone marrow (Nossal & Pike, 1978; Nemazee & Buerki, 1989; Hartley *et al*, 1991; Wardemann *et al*, 2003). Self-reactive B cells that circumvent central tolerance and migrate to the periphery are thought to undergo clonal anergy (peripheral tolerance) which is characterized by downmodulation of IgM-BCR expression and supposed functional unresponsiveness of the respective cells (Nossal & Pike, 1980; Goodnow *et al*, 1988; Brink *et al*, 1992; Cyster *et al*, 1994; O'Neill *et al*, 2011).

However, the high expression level of IgD-BCR on the supposedly anergic cells and the differences in responsiveness between IgM and IgD-BCR suggest that IgD marks maturation and selective B-cell responsiveness rather than anergy (Übelhart *et al*, 2015; Setz *et al*, 2019). In addition, the finding that the vast majority of normal serum IgM is autoreactive is not in agreement with the concept of general elimination of autoreactive B cells by strict tolerance mechanisms (Lobo, 2016). In fact, natural serum IgM plays important roles in homeostasis but is polyreactive and thus possesses a self-destructive potential (Grönwall *et al*, 2012). Conventionally, transgenic mouse models expressing a defined autoreactive BCR specificity were used in the presence or absence of cognate antigen to investigate B-cell tolerance and the prevention of self-destructive antibody responses (Goodnow *et al*, 1988, 1989; Nemazee & Buerki, 1989; Nemazee & Bürki, 1989; Hartley *et al*, 1991). However, replacement of the germline configuration of the Ig genes by expression cassettes for high-affinity mutated autoreactive BCR creates an abnormal situation for early B-cell development and results in an unphysiologically monospecific repertoire (Goodnow *et al*, 1988; Nemazee & Bürki, 1989; Hartley *et al*, 1991). Moreover, the studied model autoantigens have no relevance to known autoimmune diseases (Cooper & Stroehla, 2003; Suurmond & Diamond, 2015). Therefore, there is urgent need for the development of physiologically relevant experimental models to study the mechanisms of immune tolerance and autoimmune diseases.

Epidemiological studies show that up to 5% of the population in industrialized countries suffers from autoimmune diseases such as rheumatoid arthritis (RA), systemic lupus erythematosus (SLE), or diabetes type 1 (T1D) (Cooper & Stroehla, 2003). Notably, autoantibodies are present in the vast majority of autoimmune diseases and

Institute of Immunology, University Hospital Ulm, Ulm, Germany
*Corresponding author. Tel: +49 731 500 65200; E-mail: hassan.jumaa@uni-ulm.de

© 2021 The Authors. Published under the terms of the CC BY NC ND 4.0 license

often are the driving force for pathogenesis (Suurmond & Diamond, 2015).

We recently described that mature B cells are responsive to polyvalent antigen, while monovalent antigen modulates this responsiveness (Übelhart *et al*, 2015; Setz *et al*, 2019) suggesting alternative mechanisms for the control of self-reactive B cells and how autoantibody responses are resolved. To investigate these mechanisms, we selected a disease-related autoantigen (insulin) and established a novel experimental system in wild-type mice. The results uncover an unexpected mechanism of adaptive tolerance in which autoantigen-specific high-affinity protective memory IgM (PR-IgM) plays a pivotal role counteracting self-destructive antibody responses.

Results

Polyvalent autoantigen induces autoreactive IgG

To avoid the usage of transgenic mice that artificially harbor monospecific antigen-reactive B cells, we used wild-type mice with a physiological BCR repertoire. Here, we selected native insulin and insulin-related autoantigens as a physiologically relevant system for autoimmune diseases. During biosynthesis in the pancreas, proinsulin is cleaved into the well-studied hormone insulin and the so-called C-peptide (CP), which are both secreted into the bloodstream (Fig 1A). In contrast to insulin, CP is less conserved between mouse and man (Fig 1B). In addition, insulin is found in nanomolar concentrations in the blood and plays pivotal roles in regulating blood glucose levels and diabetes. In contrast, CP is barely detectable in the blood (picomolar concentrations) and has no clearly reported physiological function (Zhu *et al*, 2016). Using full-length CP or native insulin, we aimed at investigating autoreactive antibody responses toward an abundant, functionally important, and highly regulated autoantigen (i.e., insulin) compared to a barely detectable autoantigen lacking obvious physiological function (CP).

To this end, we used biotinylated full-length CP to generate polyvalent antigen complexes (cCP) by incubation with streptavidin (SAV). The non-complexed, soluble form of the CP (sCP) was used as monovalent antigen. We injected wild-type mice with sCP, cCP to test their potential to induce autoreactive antibody responses (Fig 1C). Similar to control immunization (CI), sCP induced no detectable IgG immune responses, whereas the polyvalent form cCP induced IgG as measured at d14 and d28, respectively (Fig 1D). In addition to ELISA experiments, a Western blot analysis was performed to determine the specificity of the generated antibody responses. The serum of mice immunized with cCP contained IgG antibodies recognizing pancreatic Proinsulin (Appendix Fig S1). To confirm the memory response against CP, we performed another recall immunization at d42 using cCP again without adjuvant and detected at d49 a robust IgG response against CP (Fig 1D). To confirm these findings, we performed ELISpot analysis to determine the number of anti-CP-IgG secreting cells. In agreement with the serum Ig results, the ELISpot experiments showed that mice immunized with cCP possess increased numbers of IgG secreting cells (Fig 1E).

Together, these data show that antibody responses can be directed against an autoantigen, that is, CP, suggesting that the respective autoreactive B cells were neither clonally deleted by central tolerance nor functionally silenced by anergy.

Native insulin induces autoreactive IgG responses

To test our hypothesis that autoreactive anti-insulin B cells are naturally present in the periphery and are not deleted by central tolerance nor turned unresponsive by anergy, we generated polyvalent insulin complexes (cInsulin) by incubating biotinylated native insulin with streptavidin (Fig 1F). Importantly, the biotinylated insulin used for the reported experiments is biologically active when injected in monovalent form into mice as determined in our own previous experiments.

Wild-type mice were injected with 10 μg of cInsulin and monitored over time for the presence of anti-insulin antibodies in serum. In parallel, we tested whether the immunized mice developed a diabetes-like dysregulation of glucose metabolism by monitoring glucose levels in blood and urine as well as signs of acute pancreatitis. We detected considerable amounts of anti-insulin IgG at d14 and after booster immunization at d27 (Fig 1G). In order to exclude any drastic effects of CpG that we used in initial injections, we performed immunization experiments by injecting InsA-KLH on day 0 without CpG. The mice immunized without CpG showed a robust anti-insulin IgM response (Appendix Fig S2A and B). To confirm the ELISA results, we performed ELISpot analysis and detected increased numbers of anti-insulin IgG secreting B cells in the spleen of cInsulin-immunized mice (Fig 1H). Furthermore, we analyzed spleens of mice immunized with cInsulin on day 5 after boost (d26). We observed a drastic increase in the germinal center (GC) B-cell

Figure 1. Polyvalent native self-molecules induce robust autoreactive IgG responses *in vivo*.

A Schematic illustration of proinsulin-derived full-length C-peptide and insulin.

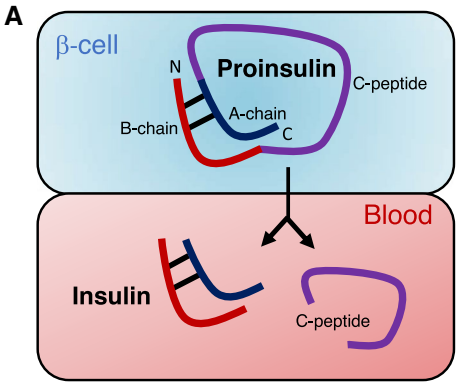
B Table comparing human to murine C-peptide amino acid sequences. Underlined: sequence used as peptide for immunization.

C Schematic immunization schedule.

D–H (D) Serum anti-C-peptide-immunoglobulins (coating: C-peptide) titers of mice immunized with cCP ($n = 9$ for d14 and d28; $n = 5$ for d49) and (G) anti-insulin-immunoglobulins (coating: insulin) titers of mice immunized with complex native insulin (cInsulin, $n = 5$) and control-immunized (CI: CpG only, $n = 3$) measured by ELISA at indicated days. Dots represent individual mice. Mean ± SD, statistical significance was calculated by using Mann–Whitney U-test. (E, H) ELISpot assays showing CP-specific IgG ($n = 4$ mice/group) (E) and insulin-specific IgG ($n = 3$ mice/group) (H) producing splenocytes at day 14. Top lane showing representative images of wells. Mean ± SD, statistical significance was calculated by using Mann–Whitney U-test, $*P < 0.05$, $**P < 0.01$. (F) Schematic illustration of native insulin (cInsulin) and full-length C-peptide (cCP) tetrameric polyvalent complexes.

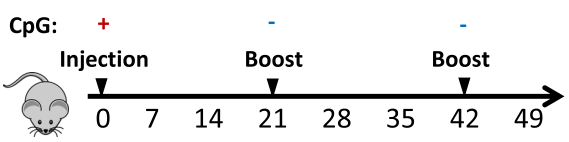
I Flow cytometric analysis of splenocytes of mice immunized with cInsulin or control immunization on day 26. Left and middle panel showing germinal center (GC) B cells (GL-7$^+$) pre-gated on B cells (CD19$^+$ B220$^+$). Right panel showing insulin-reactive GC B cells pre-gated on GL-7$^+$ cells in a histogram. Data are representative of two independent experiments with $n = 4$/group.

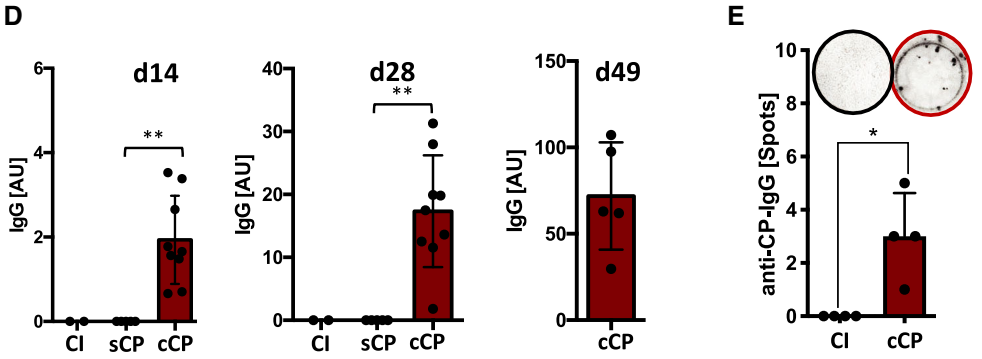
© 2021 The Authors

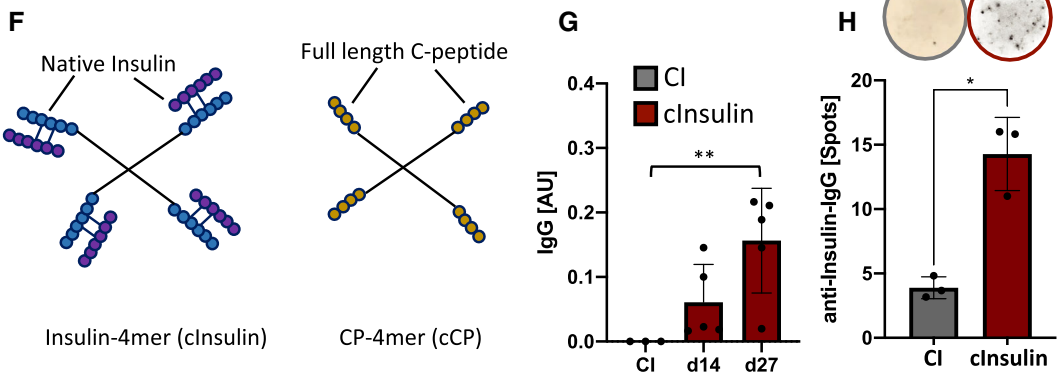


B

Species	Proinsulin domain	Amino acid sequence	UniProtID
Human	C-peptide	EAEDLQVGQVELGGGPGAGSLQPLALEGSLQ	P01308
Mouse	C-peptide	EVEDPQVEQLELGGSPGDLQTLALEVARQ	P01325







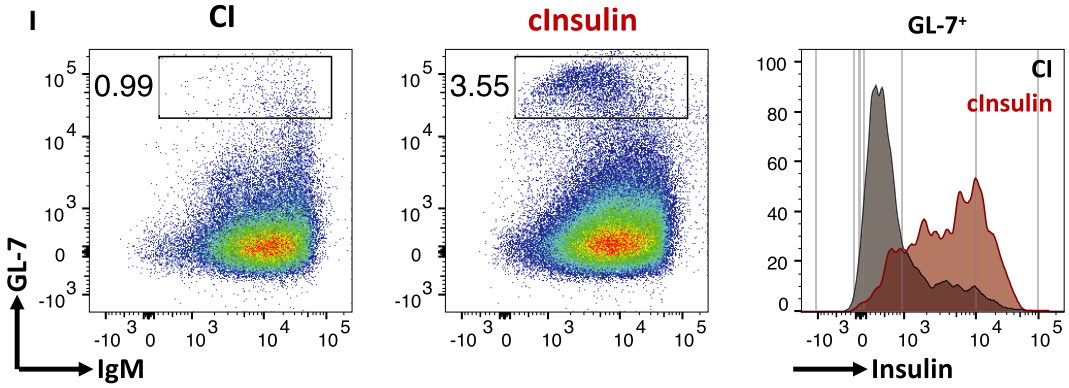


Figure 1.

population (GL-7$^+$) in cInsulin-immunized mice as compared to the control mice (Fig 1I). Interestingly, GC B cells of cInsulin-immunized mice showed clear binding to native insulin (Fig 1I). In contrast to polyvalent streptavidin, immunization with insulin coupled to a monovalent streptavidin failed to induce antibody responses suggesting that the foreign carrier is not required to induce autoantibody responses and that the antigen valency is essential for eliciting the autoimmune response (Appendix Fig S3A and B).

Mice immunized with cInsulin showed substantial signs of diabetes as measured by increased concentrations of blood glucose, starting at d7 and continuing through d14 to d26 after booster immunization (see below).

Together, these data show that regardless of concentration, antibody responses can easily be directed against autoantigens suggesting that the respective autoreactive B cells are present in the periphery and capable of generating autoimmune responses.

B cells are required for autoimmune diabetes induced by polyvalent insulin

To test whether antibody production and thus B cells and autoantibodies induce the elevated blood glucose levels, we injected 10 μg cInsulin into B-cell-deficient, mb1-knockout mice (Hobeika *et al*, 2006) lacking the BCR component Igα, also known as CD79A (Fig 2A). In contrast to wild-type animals, no increase in blood glucose levels was observed in the B-cell-deficient mice suggesting that the presence of B cells and autoantibody secretion are crucial for the development of diabetes symptoms observed in wild-type mice (Fig 2B). Moreover, the increase in blood glucose was accompanied by detectable glucose in the urine of wild-type mice injected with cInsulin (Fig 2C). In agreement with diabetes development, water consumption of wild-type mice injected with cInsulin dramatically increased (Fig 2D). Due to the severity of diabetes symptoms, we sacrificed the mice at day 26 and analyzed the pancreas and spleen.

In contrast to control immunization, cInsulin-immunized mice showed highly increased recruitment of macrophages (CD11b$^+$), neutrophils (Ly6G$^+$), and B cells (CD19$^+$) to the pancreas (Fig 2E). Interestingly, increased recruitment of neutrophils has previously been shown to be associated with severe pancreatitis (Yang *et al*, 2015). Moreover, IgG$^+$ macrophages of mice immunized with cInsulin showed augmented binding to native insulin (Fig 2E) which supports autoantibody-mediated acute inflammatory processes at the pancreas (Yang *et al*, 2015). In addition, characterization of inflammatory cytokines by bead arrays using pancreas supernatants showed elevated levels of TNF-α and IL-12 in mice immunized with cInsulin supporting the notion of acute pancreatitis (Appendix Fig S4A and B). Consequently, the observed acute pancreatitis triggered organ damage indicated by highly elevated serum pancreatic lipase levels (Smith *et al*, 2005; Gomez *et al*, 2012) (Fig 2F). FACS analysis of the spleen showed no difference of B cells between control immunization mice and those immunized with cInsulin (Appendix Fig S5).

To show that the secreted insulin-specific IgG was responsible for the diabetes symptoms, we performed IgG pulldown experiments using serum from mice immunized with cInsulin or control immunization (Fig 2G and H). Since the IgG purification may result in dissociation of endogenous insulin from insulin-specific serum IgG, we determined the anti-insulin binding capacity. Here, we compared insulin binding of total IgG before and after purification by pulldown. We found that a considerable amount of the IgG isolated from cInsulin mice was reactive to insulin, which may suggest that direct serum IgG measurements may not detect the entire insulin-specific IgG due to masking of the antibody binding sites by endogenous insulin (Fig 2G). To test the pathogenicity of purified anti-insulin IgG, we injected equal amounts of IgG from control immunization or mice immunized with cInsulin

Figure 2. Polyvalent native insulin induces autoreactive IgG responses and autoimmune diabetes in wild-type mice.

A Flow cytometric analysis of peripheral blood showing B cells (CD19$^+$ Thy1.2$^-$) and T cells (Thy1.2$^+$ CD19$^-$) of wild-type (left) and B-cell-deficient (right) mice. Cells were pre-gated on lymphocytes. Representative of three independent experiments (n = 5/group).

B Blood glucose levels of cInsulin-immunized (red: WT, n = 5; yellow: B-cell-deficient, n = 5) and CI mice (gray, n = 8) were assessed at indicated days post-immunization. Dots represent individual mice, mean ± SD. Statistical significance was calculated by using repeated measure ANOVA test, ***P < 0.001, ****P < 0.0001.

C Urine glucose levels of cInsulin-immunized (red, n = 3 for d0, d26; n = 5 for d14) and CI mice (gray, n = 3) were monitored at indicated days post-immunization. Upper panel showing visualization of glucose standard (top lane) and representative images of tested animals (middle and bottom lanes), respectively. Dots represent individual mice, mean ± SD. Statistical significance was calculated by using repeated measure ANOVA test, *P < 0.05.

D Water intake of cInsulin-immunized (n = 5) and CI mice (gray, n = 5) monitored from d21 to d26, mean ± SD.

E Flow cytometric analysis of the pancreas of cInsulin-immunized (red) and CI mice (gray) at day 26. Upper panel showing pancreatic macrophages (CD11b$^+$ Ly6G$^-$), neutrophils (Ly6G$^+$ CD11b+), and B cells (CD19$^+$) pre-gated on living cells (FVD$^-$). Lower panel showing histograms for insulin binding (left) and streptavidin (SAV)-binding (right). Representative of two independent experiments with n = 5/group. F: Serum pancreatic lipase titers of mice immunized with cInsulin (n = 5) or control immunization (n = 4) measured by ELISA. Dots represent individual mice. Mean ± SD, statistical significance was calculated by using Mann–Whitney U-test, **P < 0.01.

F Serum pancreatic lipase titers of mice immunized with cInsulin (n = 5) or control immunization (n = 4) measured by ELISA. Dots represent individual mice. Mean ± SD, statistical significance was calculated by using Mann–Whitney U-test, **P < 0.01.

G Quantification of total (red) and insulin-specific (salmon) IgG after serum IgG purification of cInsulin-immunized mice via ELISA with n = 3/group (coating: anti-IgG). Mean ± SD, statistical significance was calculated by using Mann–Whitney U-test, *P < 0.05.

H Coomassie-stained SDS–PAGE showing purified serum IgG of cInsulin-immunized (red) and CI mice (gray) under reducing (+β-ME), and non-reducing conditions. Representative of two independent experiments.

I Blood glucose levels of intravenously (i.v.) injected wild-type mice at indicated hours post-injection. 20 μg of purified serum IgG from cInsulin-immunized mice (red, n = 6) or CI mice (gray, n = 5) was used for injection. Dots represent individual mice. Mean ± SD, statistical significance was calculated by using repeated measure ANOVA test, ***P < 0.001, ****P < 0.0001.

Source data are available online for this figure.

© 2021 The Authors

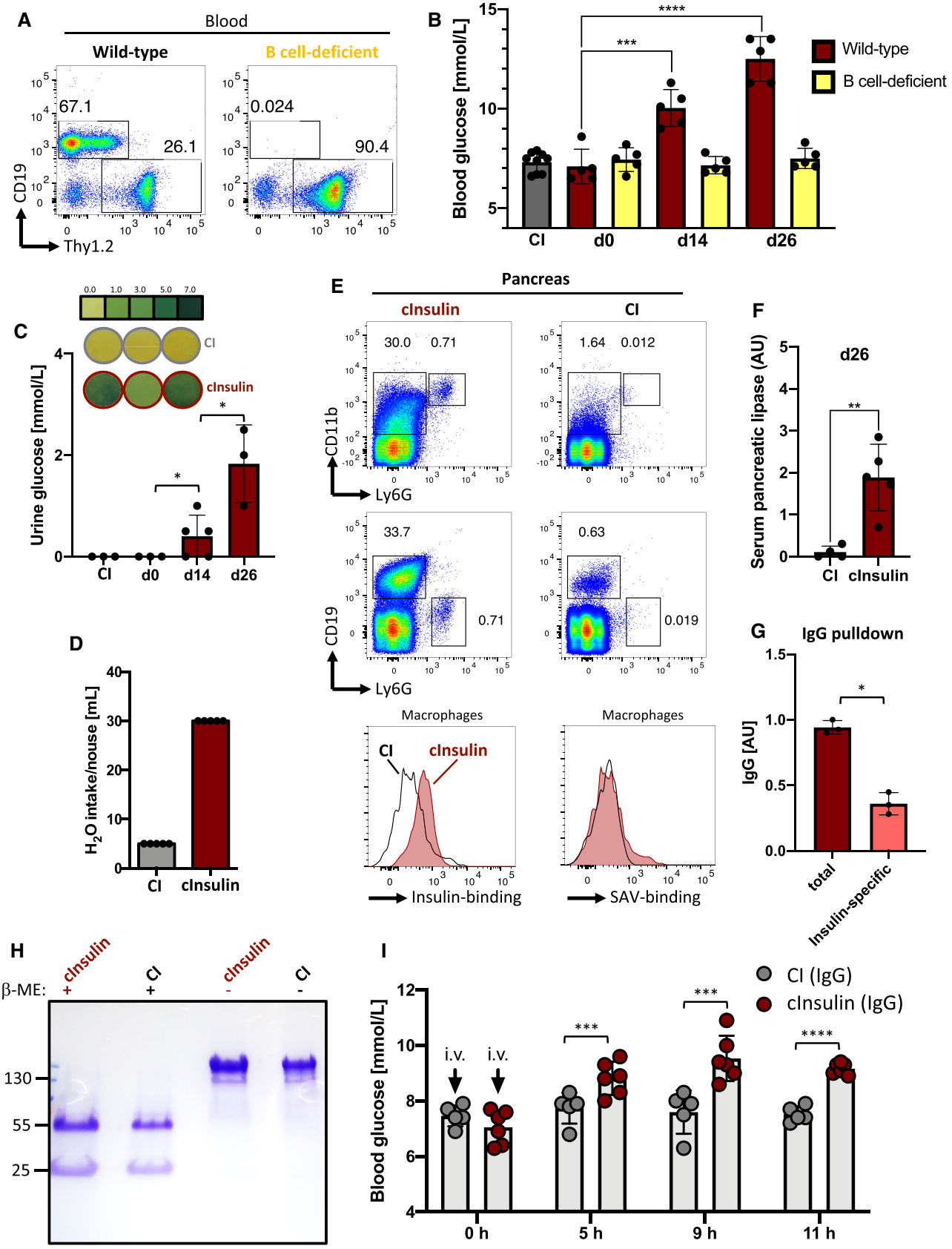

A
Blood
Wild-type
B cell-deficient
67.1
26.1
0.024
90.4
CD19
Thy1.2
B
Blood glucose [mmol/L]
Wild-type
B cell-deficient
Cl
d0
d14
d26
C
Urine glucose [mmol/L]
Cl
cInsulin
D
H2O intake/nouse [mL]
E
Pancreas
cInsulin
Cl
30.0
0.71
1.64
0.012
33.7
0.71
0.63
0.019
CD11b
CD19
Ly6G
Macrophages
Insulin-binding
SAV-binding
F
Serum pancreatic lipase (AU)
d26
G
IgG pulldown
IgG [AU]
total
Insulin-specific
H
β-ME:
130
55
25
I
Blood glucose [mmol/L]
Cl (IgG)
cInsulin (IgG)
i.v.
0 h
5 h
9 h
11 h

Figure 2.

intravenously into wild-type animals and monitored blood glucose. We found that injecting total IgG containing 2 μg anti-insulin IgG was sufficient to induce hyperglycemia in recipient mice suggesting that anti-insulin-IgG neutralizes insulin thereby causing diabetes symptoms (Fig 2I).

These data demonstrate that autoreactive B cells recognizing a metabolism-regulating hormone are neither deleted nor functionally silenced and can induce severe autoimmunity when the autoantigen valency is shifted toward polyvalency.

Presence of monovalent autoantigen suppresses IgG antibody responses

It is conceivable that the immune response toward polyvalent CP or polyvalent cInsulin used in this study was affected by the presence of endogenous monovalent counterparts. Therefore, we tested the effect of combining the monovalent and polyvalent antigen forms in immunization experiments.

To this end, we injected wild-type mice with sCP alone, cCP alone, or combinations of both and monitored the generation of autoreactive antibody responses over time. While the monovalent sCP alone induced no detectable IgM or IgG responses, it modulated the immune responses elicited by the polyvalent CP (cCP). In fact, the IgG response at d14 was significantly reduced in mice immunized with sCP:cCP ratio of 20:1 as compared to mice immunized with only cCP (0:1) (Fig 3A). In contrast to IgG, CP-specific IgM was slightly increased in mice immunized with sCP:cCP combination at 20:1 ratio (Fig 3A). Importantly, no difference was detected in the IgG response against streptavidin (SAV) which was used to generate polyvalent CP complexes (Appendix Fig S6).

These data suggest that soluble monovalent antigen modulates the immune response and determines the IgG:IgM ratio of antibody-secreting cells during immune responses. To confirm this conclusion, we performed ELISpot analysis to determine the number of IgG or IgM secreting cells in the spleens of the different groups of mice. In agreement with the serum Ig results, the ELISpot

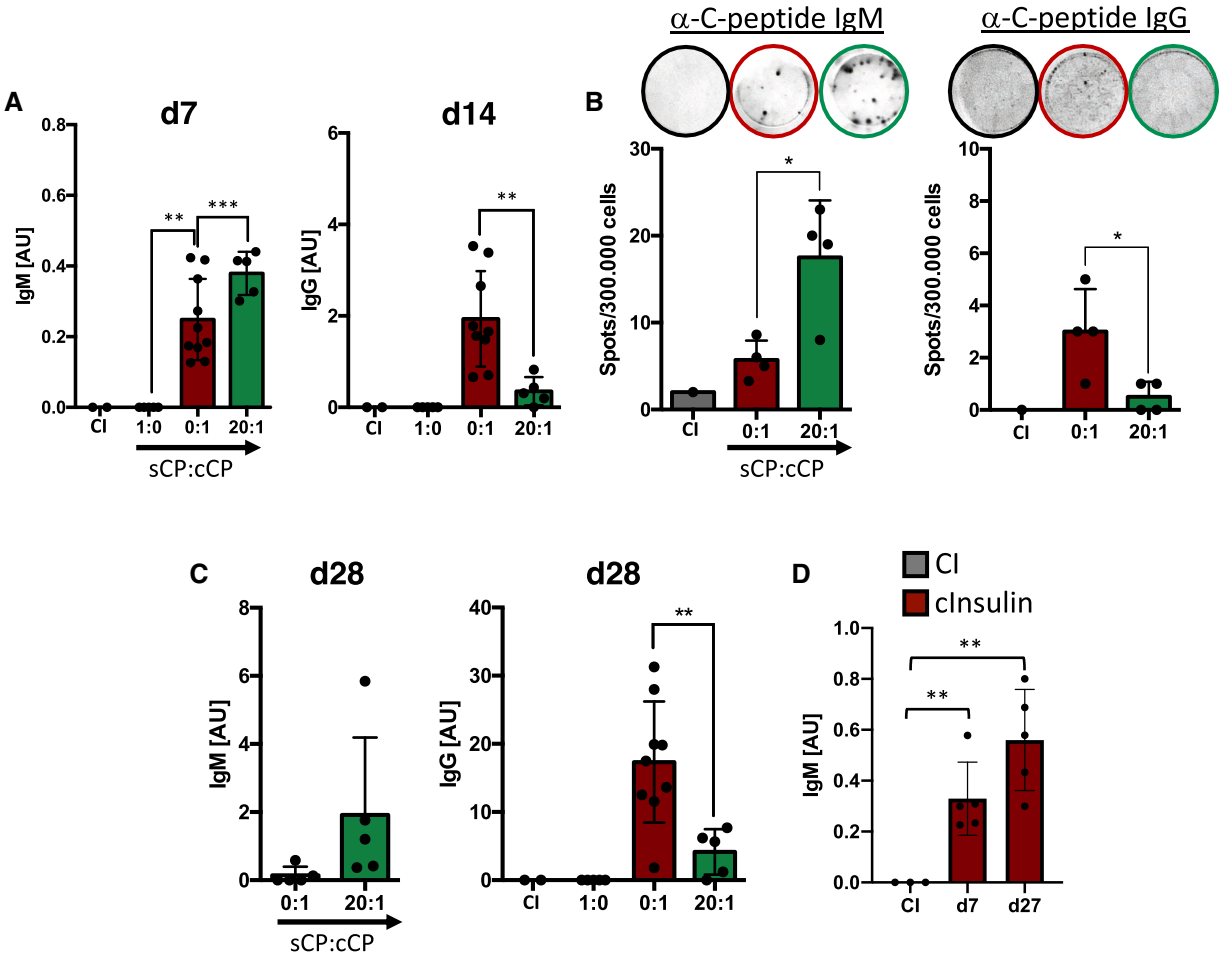


Figure 3. Ratios of monovalent to polyvalent autoantigen control the isotype composition of secreted antibodies.

A–D (A, C) Serum anti-C-peptide-immunoglobulins titers of mice immunized with CP (0:1 $n = 10$; 20:1 $n = 5$) (coating: C-peptide) and (D) anti-insulin-IgM titers of mice immunized with complex insulin (cInsulin, $n = 5$) (coating: insulin) and control immunization (Cl: CpG only, $n = 3$) measured by ELISA at indicated days. Dots represent individual mice. Mean ± SD, statistical significance was calculated by using Kruskal–Wallis test. (B) ELISpot assay showing CP-specific immunoglobulin producing splenocytes at day 7 (left panel) and day 14 (right panel). Top lane showing representative images of wells. Dots represent individual mice ($n = 4$/group) Mean ± SD, statistical significance was calculated by using Kruskal–Wallis test, $^*P < 0.05$, $^{**}P < 0.01$, $^{***}P < 0.001$.

© 2021 The Authors

experiments showed that mice immunized with a ratio of 20:1 of sCP:cCP possess increased numbers of IgM secreting cells while the numbers of IgG secreting cells were decreased as compared to mice immunized with cCP (stated as sCP:cCP = 0:1) (Fig 3B).

Later challenge with the same antigen at d21 resulted in further increase of CP-specific IgM at d28 in mice immunized with sCP:cCP ratio of 20:1 while the IgG response was reduced in these mice as compared with mice immunized with only with cCP, sCP:cCP ratio of 0:1 (Fig 3C).

To further support the notion that the presence of endogenous monovalent antigen augments antigen-specific IgM antibody responses, we measured the IgM responses against polyvalent cInsulin and observed an increased anti-insulin IgM response at d7 and d27 (Fig 3D).

In summary, the results show that B-cell responses are induced by polyvalent antigen and modulated by monovalent counterparts thereby regulating B-cell responsiveness and the isotype composition of generated antibody. This leads to a dynamic and pivotal B-cell function that differs from the conventional view.

Insulin-derived epitope induces harmful IgG response

Since monovalent native insulin has a drastic effect on blood glucose levels, we were not able to test combinations of polyvalent and monovalent native insulin in immunization experiments. However, to further confirm the presented findings we performed immunization experiments using an insulin-A-chain-derived peptide, referred to as InsA, which is a frequently reported epitope targeted by human autoantibody responses (Padoa *et al*, 2005). We coupled the selected peptide to the protein-carrier KLH to generate a polyvalent antigen complex (cInsA) which was used in further experiments either alone or in combination with the monovalent peptide (sInsA). We found that InsA induced IgM and IgG autoantibody responses binding native insulin (Fig 4A). However, the polyvalent cInsA alone (sInsA:cInsA ratio of 0:1) readily induced the production of anti-insulin-IgG, whereas addition of soluble peptide (sInsA:cInsA ratio of 100:1) resulted in significant reduction of autoreactive IgG at d14 and, one week after boost, at d28 (Fig 4A). Most likely, the amount of autoreactive anti-insulin IgG is higher than detected in direct serum ELISA as anti-insulin-IgG bound to endogenous insulin escapes detection as described above.

Notably, comparable IgM and IgG responses were observed against the carrier protein KLH underlining the autoantigen-specific effect of the monovalent InsA antigen on the suppression of IgG responses induced by cInsA in the KLH-InsA complexes (Appendix Fig S7A and B).

Moreover, the presence of soluble InsA resulted in robust insulin-specific IgM production at d7 and d28, which was slightly higher than in mice immunized with polyvalent cInsA alone (sInsA:cInsA ratio of 0:1) (Fig 4A). Since insulin is present in high amounts in the circulatory system, we conclude that the presence of endogenous monovalent insulin modulates the immune response elicited by cInsA, thereby leading to increased autoreactive IgM responses as compared to IgG. Taken together, our data indicate that the ratio of polyvalent to monovalent antigen is mirrored by the ratio of antigen-specific IgG to IgM (γ/μ ratio) during memory responses (Fig 4B).

Serum IgG of mice immunized with polyvalent peptide only (sInsA:cInsA ratio of 0:1) readily detected native insulin in Western blot analysis (Fig 4C), while serum IgG of mice immunized in the presence of soluble peptide (sInsA:cInsA ratio of 100:1) was insufficient to clearly detect insulin (Fig 4C). In addition, ELISpot analysis using splenic B cells from mice immunized with cInsA confirmed the increased presence of anti-insulin IgG secreting cells in respective mice (Fig 4D).

To confirm that the increased anti-insulin IgG is associated with harmful autoimmune responses, we tested whether mice immunized with cInsA show signs of diabetes. One week after immunization at d7, we found that both groups of mice immunized with cInsA only (sInsA:cInsA ratio of 0:1), or combination of monovalent and polyvalent cInsA (sInsA:cInsA ratio of 100:1) show increased blood glucose as compared to control immunization (Fig 4E).

One week after booster immunization, however, increased blood glucose was observed only in mice immunized with polyvalent InsA (0:1 ratio of sInsA:cInsA) (Fig 4F). In addition, we tested whether the glucose concentration was also increased in the urine. Indeed, the increased autoreactive anti-insulin IgG led to detectable glucose in the urine (Fig 4G). In contrast to IgG, no detectable signs of

Figure 4. Soluble insulin-A peptides modulate autoimmune responses.

A Serum anti-insulin-immunoglobulin titers of mice immunized with InsA peptide (red: 0:1, $n = 10$ and green: 100:1, $n = 5$) and control immunization (CI: CpG only, gray, $n = 3$) measured by ELISA at indicated days (coating: insulin). Dots represent individual mice. Mean ± SD, statistical significance was calculated by using Kruskal–Wallis test, $^{*}P < 0.05$, $^{***}P < 0.001$.

B Ratios of IgG to IgM derived from ELISA values plotted against molar ratios of antigens for $n = 5$/group. Mean ± SD, statistical significance was calculated by using Kruskal–Wallis test, $^{*}P < 0.05$, $^{***}P < 0.001$.

C Western blot analysis of insulin-specific serum IgG derived from InsA peptide-immunized mice. Top panel (green): 100:1 serum, lower panel (red): 0:1 serum (sInsA:cInsA). Serum of mice was used as primary antibody and detection was done with anti-mouse-IgG-HRP. Black filled arrow: Proinsulin (12 kD), Black non-filled arrow: insulin (6 kD), β-actin (42 kD, loading control). Representative of two independent experiments.

D ELISpot of InsA peptide-immunized (red, $n = 11$) and CI mice (gray, $n = 8$) showing insulin-specific IgG-producing splenocytes on day 14. Representative wells are shown (top lane). Mean ± SD, statistical significance was calculated by using Mann–Whitney U-test, $^{****}P < 0.0001$.

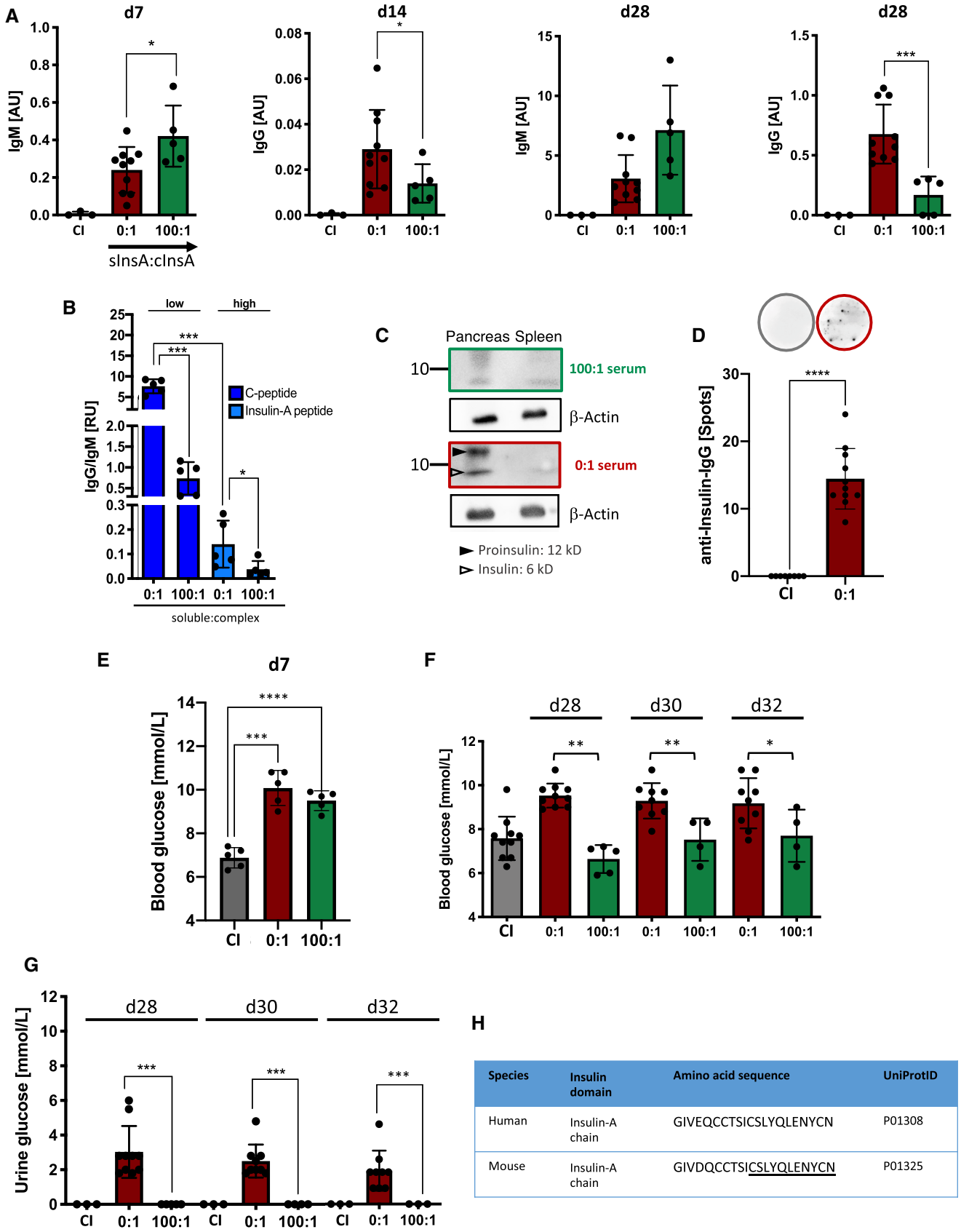
E, F Blood glucose levels of InsA peptide-immunized (red: 0:1, $n = 5$ for E and $n = 10$ for F; green: 100:1, $n = 5$ and $n = 4$ for F, d30, d32) and CI (gray, $n = 5$ for E and $n = 10$ for F) mice were assessed at indicated days. Dots represent individual mice. Mean ± SD, statistical significance was calculated by using Kruskal–Wallis test (E) and repeated measure ANOVA test (F), $^{*}P < 0.05$, $^{**}P < 0.01$, $^{***}P < 0.001$, $^{****}P < 0.0001$.

G Urine glucose levels of InsA-peptide-immunized (red: $n = 10$ for d28, d32 and $n = 8$ for d30; green: $n = 5$ for d28, $n = 4$ for d30, $n = 3$ for d32) and CI (gray, $n = 3$) mice were monitored at indicated days post-immunization. Dots represent individual mice. For 100:1: representative data are shown for two independent experiments with total $n = 10$. Mean ± SD, statistical significance was calculated by using repeated measure ANOVA test, $^{***}P < 0.001$.

H Table comparing human to murine insulin-A-chain amino acid sequences. Underlined: sequence used as peptide.

Source data are available online for this figure.

© 2021 The Authors



Species	Insulin domain	Amino acid sequence	UniProtID
Human	Insulin-A chain	GIVEQCCTSICSLYQLENYCN	P01308
Mouse	Insulin-A chain	GIVDQCCTSICSLYQLENYCN	P01325

Figure 4.

© 2021 The Authors

autoimmune diabetes were observed in mice immunized with 100:1 ratio and possessing increased amounts of autoreactive anti-insulin IgM after booster immunization (Fig 4F, for IgM amount compare Fig 4A).

FACS analysis of splenic B cells at d28 after immunization suggests that InsA immunization resulted in an increase of B cells with elevated amount of IgM (Appendix Fig S8A and B). Moreover, mice immunized with cInsA only (sInsA:cInsA = 0:1) showed increased number of macrophages in the pancreas which bound autoreactive IgG as determined by the increased InsA peptide binding (Appendix Fig S8C). Similar results were observed in the spleen (Appendix Fig S9).

Interestingly, InsA is highly conserved between mouse and man (Fig 4H) and anti-InsA antibodies bind native insulin and are often involved in human autoimmune diabetes (Padoa *et al*, 2005). Therefore, this model might be of great use for investigating the molecular mechanisms underlying autoantibody-driven diabetes development and pancreatitis.

Together, our data suggest that increased ratio of complex polyvalent autoantigen leads to increased amount of autoreactive IgG and subsequent self-destructive autoimmune responses in wild-type animals. In contrast, an increase in monovalent antigen results in increased autoreactive memory IgM which seems to prevent self-destructive immune responses.

Adaptive immune tolerance by autoreactive memory IgM

The data presented above suggest that high titers of memory anti-insulin-IgM during secondary immune responses protect from dysregulation of glucose metabolism and autoimmune diabetes in mice immunized with InsA.

To test whether increased ratios of secondary autoreactive anti-insulin-IgM counter the pathological effects on glucose metabolism induced by autoreactive anti-insulin-IgG, we challenged the mice initially immunized in the presence of monovalent InsA peptide (sInsA:cInsA ratio 100:1) with polyvalent antigen cInsA at d51 (Fig 5A). This treatment usually induces autoimmune diabetes from d7 to 28 (Appendix Fig S10A–C, d7 vs. d14). However, mice pre-immunized in the presence of monovalent InsA peptide (sInsA: cInsA ratio 100:1) showed no dysregulation of glucose metabolism at d51 to 59 (Fig 5B and C). These mice produced autoreactive anti-insulin-IgM but no anti-insulin IgG (Fig 5D and E). Our data suggest that primary immunization in the presence of monovalent InsA peptide (sInsA:cInsA ratio 100:1) induced adaptive tolerance against the pathogenic immunization with polyvalent cInsA. Moreover, these findings indicate that this unique tolerance mechanism creates a novel class of memory responses by eliciting and maintaining the production of protective regulatory IgM (PR-IgM).

We tested whether mice immunized with only cInsA (sInsA: cInsA ratio 0:1) also developed adaptive tolerance by PR-IgM. While mice immunized with 100:1 ratio were protected against diabetes already at the first booster immunization by d21, mice immunized with 0:1 ratio showed diabetes signs until d32 (Fig 4G). When these mice were subjected to a second booster immunization at d42, they showed weaker diabetes signs and reduced duration as compared to the first booster immunization (Fig 5F, compare Fig 4G). In agreement with the role of PR-IgM in preventing diabetes, we observed elevated amounts of anti-insulin IgM and no detectable anti-insulin IgG at d49, one week after booster immunization (Fig 5F). Moreover, the increased levels of PR-IgM also correlated with a decrease in serum pancreatic lipase levels (Appendix Fig S11).

These data show that PR-IgM protects from destructive autoimmune responses and that the presence of monovalent autoantigen accelerates the development of PR-IgM as compared with only complex autoantigen.

Higher antigen affinity for memory anti-insulin-IgM

Our data suggest that an increased amount of insulin-reactive PR-IgM as compared to insulin-reactive IgG is key for protection from diabetes after booster immunization with InsA. To determine the autoreactive IgG to IgM ratio required for protection, we plotted the ratios of insulin-reactive IgG to IgM obtained from ELISA measurements on a two-dimensional graph against blood glucose levels or urine glucose levels. According to this analysis, the ratio of insulin-reactive IgG to IgM must be below 0.1 ($\gamma/\mu < 0.1$) to avoid the development of diabetes symptoms (Fig 6A).

Next, we addressed the question whether PR-IgM responses resemble memory responses by providing long-term tolerance. To this end, we monitored the decline of anti-insulin IgM levels over time followed by anti-insulin recall responses (Fig 6B). We found that anti-insulin IgM persists for weeks and that booster immunization with cInsA at day 71 induces only IgM, but neither IgG nor signs of dysregulated glucose metabolism in blood or urine (Fig 6B and C, and Appendix Fig S10B and C). IgM memory responses are associated with increase of antibody-affinity toward antigen which can be monitored by determining the antibody binding capacity to low-valence antigen as compared to high-valence counterpart (Shimizu *et al*, 2004). Therefore, we performed ELISA experiments using monovalent InsA (1) or polyvalent InsA (4) as antigen for coating of ELISA plates. Increased binding to monovalent InsA indicates increased affinity of the insulin-specific antibodies. Interestingly, IgM generated after booster InsA immunization shows higher anti-insulin affinity compared to the primary IgM collected on day 7 (Fig 6D). To further examine the role of autoreactive memory PR-IgM generated during immune responses, we purified total IgM from control immunization or InsA-immunized mice (Fig 6E). To confirm that PR-IgM (d85) has an increased affinity to insulin, we performed interferometric assays for affinity characterization (Kumaraswamy & Tobias, 2015). We found that purified PR-IgM shows a highly increased binding affinity to insulin compared to the primary IgM or isotype control (Fig 6F).

When administered intravenously into naïve wild-type mice, insulin-reactive memory PR-IgM from InsA-boosted mice, collected at d85, showed no effect on blood glucose levels and behaved similar to control IgM suggesting that PR-IgM binds insulin without inducing insulin depletion (Fig 6G). However, primary insulin-reactive IgM, collected at d7, led to increased blood glucose levels by 5 h after intravenous injection (Fig 6G).

Together, autoreactive memory PR-IgM does not induce dysregulation in blood glucose levels despite its increased anti-insulin affinity.

Protective memory anti-insulin-IgM is monospecific

The results presented above point toward an unexpected fundamental difference between autoreactive primary IgM and PR-IgM. In fact,

© 2021 The Authors

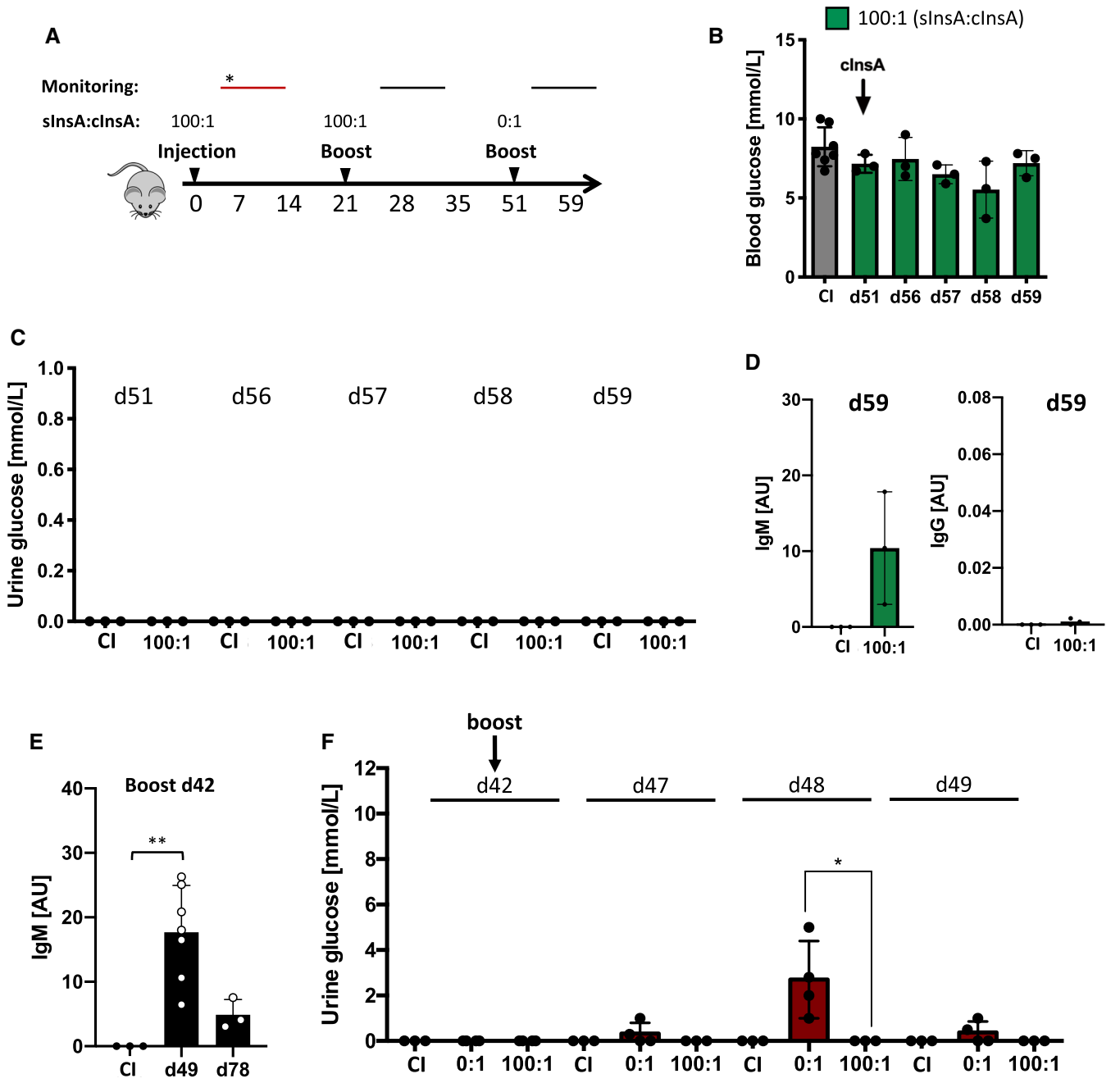


Figure 5. Monovalent insulin-A peptides induce immune tolerance via autoreactive memory IgM.

A Immunization scheme. *monitoring: diabetes symptoms observed (red bar).

B Blood glucose levels of InsA-peptide-immunized mice ($n = 3$) and CI ($n = 7$) mice were assessed at indicated days post-immunization. Dots represent individual mice. Mean ± SD, statistical significance was calculated by using repeated measure ANOVA test, all comparisons were not significant.

C–F (C, F) Urine glucose levels of InsA-peptide-immunized ($n = 3$) and CI ($n = 3$) mice were monitored at indicated days post-immunization. Dots represent individual mice. Mean ± SD, statistical significance was calculated by using repeated measure ANOVA test, *$P < 0.05$. (D, E) Serum anti-insulin-immunoglobulin titers of mice immunized with InsA peptide (day 59, day 78: $n = 3$, day 49: $n = 7$) and control immunization (CI: CpG only, $n = 3$) measured by ELISA at indicated days (coating: insulin). Dots represent individual mice. Mean ± SD, statistical significance was calculated by using Mann–Whitney U-test (D) and repeated measure ANOVA test (E). *$P < 0.05$, **$P < 0.01$.

primary anti-insulin-IgM induced diabetes symptoms although produced at much lower quantity as compared to memory PR-IgM which possesses a higher insulin affinity but did not induce pathology. To directly test the protective function of autoreactive memory PR-IgM against destructive autoimmunity, mice were immunized with cInsA alone or cInsA together with intravenous

© 2021 The Authors

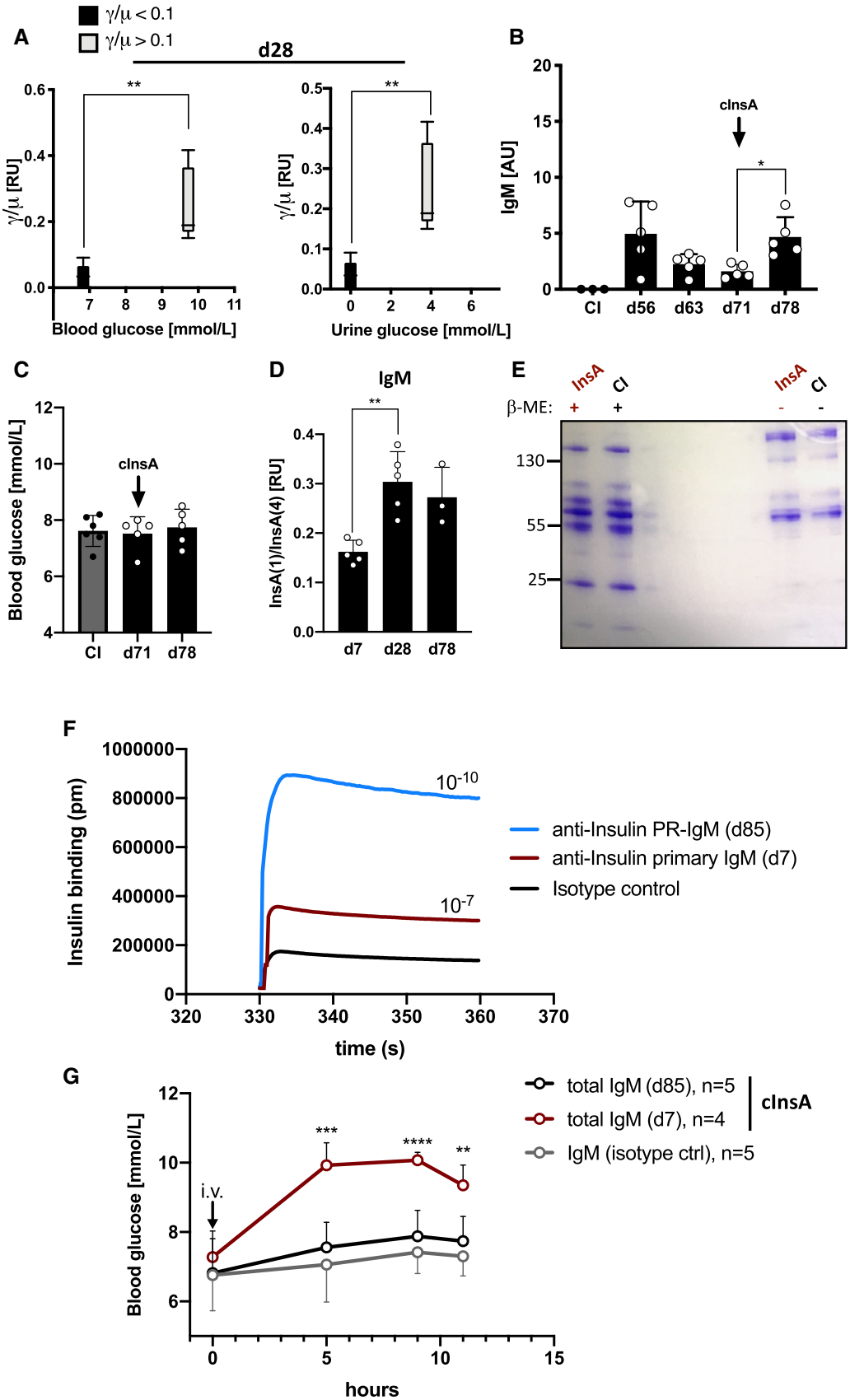

A
γ/μ < 0.1
γ/μ > 0.1
d28
γ/μ [RU]
Blood glucose [mmol/L]
Urine glucose [mmol/L]
B
IgM [AU]
clnsA
Cl
d56
d63
d71
d78
C
Blood glucose [mmol/L]
clnsA
Cl
d71
d78
D
IgM
InsA(1)/InsA(4) [RU]
d7
d28
d78
E
InsA
Cl
β-ME:
130
55
25
F
Insulin binding (pm)
time (s)
10-10
10-7
anti-Insulin PR-IgM (d85)
anti-Insulin primary IgM (d7)
Isotype control
G
Blood glucose [mmol/L]
hours
i.v.
total IgM (d85), n=5
total IgM (d7), n=4
IgM (isotype ctrl), n=5
clnsA

Figure 6.

Figure 6. High-affinity memory IgM counteracts IgG-mediated self-destructive autoimmune responses *in vivo*.

A Ratios of IgG to IgM derived from ELISA values plotted on a two-dimensional graph against blood glucose levels (left panel) and urine glucose levels (right panel) for $n = 5$/group. Central bands: median, boxes: interquartile range, whiskers: max./min., statistical significance was calculated by using Mann–Whitney U-test, $^{**}P < 0.01$.

B Serum anti-insulin-IgM titers of mice immunized with InsA peptide with a γ/μ ratio < 0.1 (black, $n = 5$) and CI (gray, $n = 3$) mice measured by ELISA at indicated days (coating: insulin). Dots represent individual mice. Mean ± SD, statistical significance was calculated by using repeated measure ANOVA test, $^{*}P < 0.05$.

C Blood glucose levels of InsA-peptide-immunized mice (γ/μ < 0.1, black, $n = 5$) and CI (gray, $n = 6$) mice were assessed at indicated days post-immunization with a commercial blood glucose monitor device. Dots represent individual mice. Mean ± SD, statistical significance was calculated by using Kruskal–Wallis test, all comparisons were not significant.

D Insulin-specific IgM affinity maturation of InsA-peptide-immunized mice at indicated days was measured by ELISA. Ratios of IgM binding to InsA(1) and InsA(4) (referring to molar antigen density) were calculated and plotted as relative units ($n = 5$ for d7, d28; $n = 3$ for d78). Dots represent individual mice. Mean ± SD, statistical significance was calculated by using repeated measure ANOVA test, $^{**}P < 0.01$. Serum dilutions: 1:25.

E Coomassie-stained SDS–PAGE showing purified serum IgM of complex InsA-peptide (cInsA)-immunized and CI mice under reducing (+β-ME), and non-reducing conditions. Representative of two independent experiments.

F Anti-insulin affinity of PR-IgM (blue), primary IgM (red), and isotype control (black) measured by bio-layer interferometry. IgM binding to insulin was acquired in pm and used to calculate the dissociation constant shown in the graph ($K_d = 1/K_a$). Graph is showing antigen-antibody association phase. Data are representative for three independent experiments.

G Blood glucose levels of intravenously injected mice with purified IgM from control immunization (CI, $n = 5$), complex InsA peptide (cInsA) immunization day 7 (total IgM d7, $n = 4$) and day 85 (total IgM d85, $n = 5$). Mean ± SD, statistical significance was calculated by using repeated measure ANOVA test showing comparison of red to black line, $^{**}P < 0.01$, $^{***}P < 0.001$, $^{****}P < 0.0001$.

Source data are available online for this figure.

injections of 50 μg total IgM containing 5 μg of anti-insulin memory PR-IgM every 48 h starting from d0 (Fig 7A and B). Interestingly, the presence of insulin-specific PR-IgM mitigated autoimmune dysglycemia and completely prevented glycosuria on day 7 as compared to mice immunized with cInsA alone (Fig 7B). To exclude that PR-IgM injections neutralized injected cInsA, we performed anti-carrier (KLH) ELISA and found no difference in anti-KLH-IgM levels between the two groups at day 7 (Appendix Fig S12). Similarly, intravenous injections of anti-insulin PR-IgM together with total IgG pulldown from cInsA immunized mice prevented hyperglycemia induced by anti-insulin IgG in the pulldown (Fig 7C).

These data suggest that memory anti-insulin PR-IgM directly prevents the depletion of insulin by primary anti-insulin IgM as well as anti-insulin IgG thereby blocking diabetes development.

One explanation for the differences between the autoreactive primary and memory PR-IgM might be that primary IgM is polyreactive and might be produced by B1 B cells as a first line of immune protection (Benedict & Kearney, 1999; McHeyzer-Williams, 2003; Lobo, 2016; Kreslavsky *et al*, 2018). Presumably, this polyreactivity results in joint immune complexes with a high molecular weight containing multiple autoantigens allowing elimination by phagocytes thereby depleting the bound insulin. In contrast, autoreactive memory PR-IgM might be monospecific for autoantigen and may therefore release the autoantigen after binding without formation of immune complexes. To test this, we analyzed the polyreactive potential of primary IgM as compared to memory PR-IgM. Anti-DNA ELISA (Fig 7D) and indirect immune fluorescence using HEp-2 slides (Fig 7E) showed that in contrast to primary IgM, memory PR-IgM is not polyreactive but specifically binds to insulin (Fig 7D and E).

To show that anti-insulin IgM is specifically responsible for the observed effects, we performed insulin-specific pulldown assays

Figure 7. Differences in the affinity and specificity of primary versus memory IgM control autoimmune responses.

A Schematic illustration of immunization schedule with complex InsA peptides (cInsA) intraperitoneally and insulin-specific protective IgM (PR-IgM) in 48 h cycles intravenously (i.v.). *monitoring: diabetes symptoms were only observed within cInsA only group.

B Blood and urine glucose levels of mice immunized with complex InsA peptides (cInsA) (red, $n = 5$) and cInsA plus intravenously injected (i.v.) pIgM (salmon, $n = 5$) at day 7. Dots represent individual mice. Mean ± SD, statistical significance was calculated by using Mann–Whitney U-test, $^{*}P < 0.05$.

C Blood glucose levels of mice intravenously injected with total IgG pulldown of cInsA immunized mice (red, $n = 4$), or total IgG (cInsA) together with anti-insulin PR-IgM (black, $n = 4$). Measurements were done 5 h post-intravenous injection. Data were collected from two independent experiments. Mean ± SD, statistical significance was calculated by using Mann–Whitney U-test, $^{**}P < 0.01$.

D, F (D) Serum (dilution: 1:50) and (F) insulin-specific IgM (concentration: 500 ng/ml) tested for dsDNA (left panel, coating: calf thymus dsDNA) and insulin (right panel, coating: insulin) reactivity measured by ELISA. Mice were immunized with cInsA and serum was collected on day 7 (D: $n = 8$, left; $n = 5$, right; F: $n = 4$) and day 85 (D: $n = 4$, left; $n = 5$, right, F: $n = 4$) post-immunization. Dots represent individual mice. Mean ± SD, statistical significance was calculated by using Mann–Whitney U-test, $^{**}P < 0.01$, $^{****}P < 0.0001$.

E, G Anti-nuclear-IgM (ANA) of control-immunized (CI, $n = 3$) and complex InsA-peptide(cInsA)-immunized mice on day 7 ($n = 3$) and day 85 ($n = 3$) analyzed by indirect immunofluorescence. We used (E) total serum (dilutions: 1:20) or (G) insulin-specific IgM (concentration: 500 ng/ml) purified from serum at indicated days on commercial HEp-2 slides. Scale bar: 10 μm. Green fluorescence indicates IgM bound to nuclear structures. Data are representative for three independent experiments with isotype control: $n = 3$, day 7: $n = 3$, day 85: $n = 3$.

H Coomassie-stained SDS–PAGE showing primary (cInsA d7) and memory (cInsA d85) insulin-specific purified IgM pre-incubated with insulin and calf thymus dsDNA. Samples were loaded onto the gel after size exclusion with a cut-off at 10,000 kD (fractions referring to >/< 10^4 kD). IgM heavy chain (HC): 69 kD, IgM light chain (LC): 25 kD, J-chain: 15 kD. Data shown are representative of three independent experiments.

I Blood glucose levels of mice intravenously injected with either IgM isotype ctrl ($n = 6$), anti-insulin PR-IgM (d85, $n = 5$), anti-insulin primary IgM (d7, $n = 4$) after insulin-specific pulldown. Mean ± SD, statistical significance was calculated by using repeated measure ANOVA test showing comparison of red and black line, $^{***}P < 0.001$, $^{****}P < 0.0001$.

© 2021 The Authors

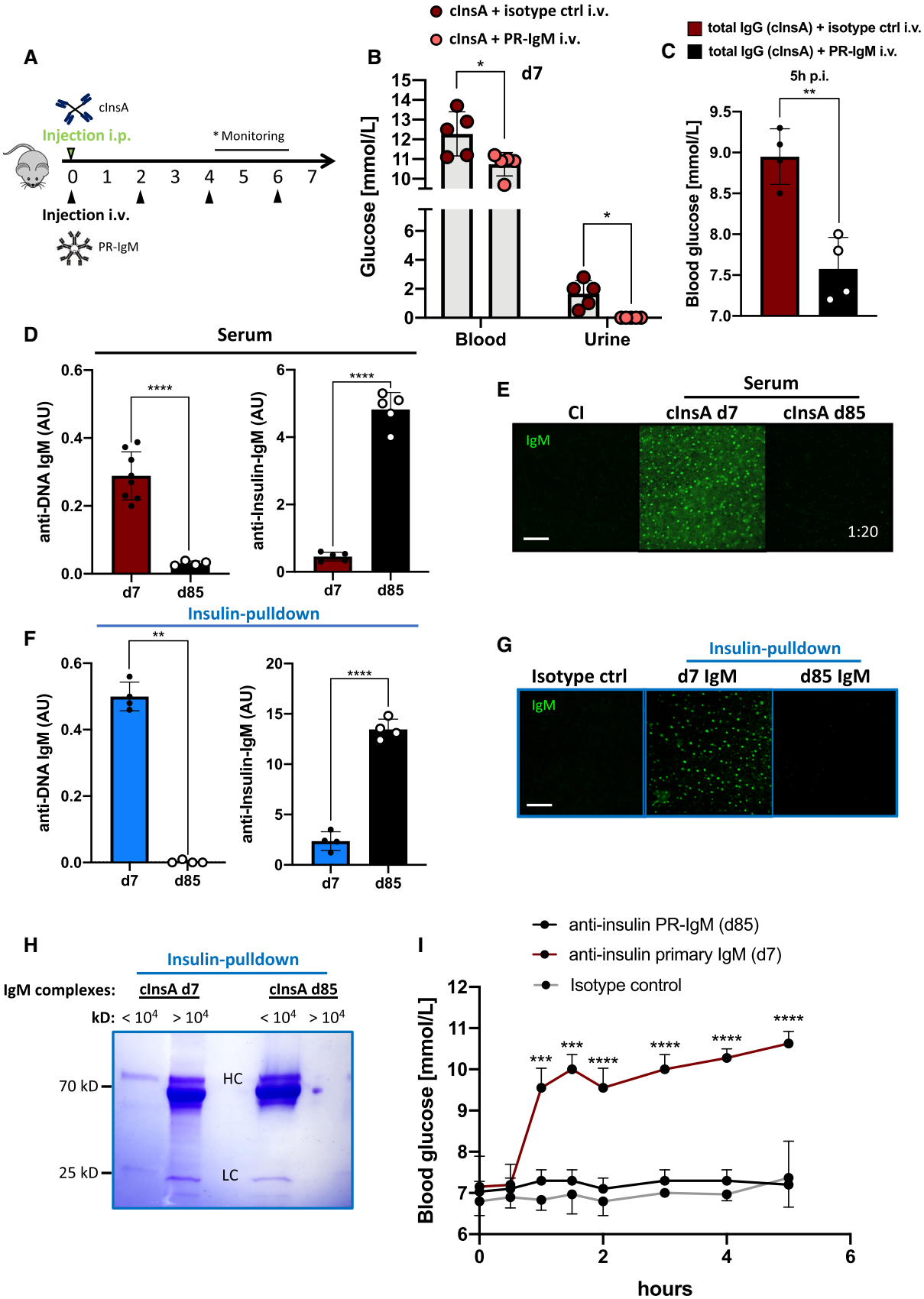

A
cInsA
Injection i.p.
* Monitoring
0 1 2 3 4 5 6 7
Injection i.v.
PR-IgM
B
cInsA + isotype ctrl i.v.
cInsA + PR-IgM i.v.
d7
Glucose [mmol/L]
Blood
Urine
C
total IgG (cInsA) + isotype ctrl i.v.
total IgG (cInsA) + PR-IgM i.v.
5h p.i.
Blood glucose [mmol/L]
D
Serum
anti-DNA IgM (AU)
anti-Insulin-IgM (AU)
d7
d85
E
Serum
CI
cInsA d7
cInsA d85
IgM
1:20
F
Insulin-pulldown
anti-DNA IgM (AU)
anti-Insulin-IgM (AU)
G
Insulin-pulldown
Isotype ctrl
d7 IgM
d85 IgM
IgM
H
Insulin-pulldown
IgM complexes:
cInsA d7
cInsA d85
kD: < 10^4 > 10^4 < 10^4 > 10^4
70 kD
25 kD
HC
LC
I
anti-insulin PR-IgM (d85)
anti-insulin primary IgM (d7)
Isotype control
Blood glucose [mmol/L]
hours

Figure 7.

using sera from InsA-immunized mice. The pulldown resulted in pure insulin-specific IgM as revealed by Western blot analysis. We blotted insulin-specific purified IgM onto membranes and examined the presence of IgM and IgG heavy chains. As expected, we could only detect IgM heavy chains indicating an IgG-free pulldown (Appendix Fig S13A). We also performed anti-DNA ELISA (Fig 7F, Appendix Fig S13B) and indirect immune fluorescence on HEp-2 slides (Fig 7G) using purified primary anti-insulin IgM or memory anti-insulin PR-IgM. The results confirm the finding that in contrast to primary IgM, purified anti-insulin PR-IgM is not polyreactive and specifically binds to insulin (Fig 7F and G). In addition, we performed ELISA-based competition assays by using soluble dsDNA as competitor. The results show that dsDNA is able to heavily interfere with primary IgM binding to insulin, but has only a slight interfering effect on PR-IgM (Appendix Fig S14). These results support the notion that PR-IgM is monospecific to insulin, whereas primary IgM remains polyreactive.

To directly test the hypothesis that primary anti-insulin IgM forms large immune complexes whereas PR-IgM does not, we incubated anti-insulin primary IgM or PR-IgM with insulin and DNA and determined the formation of immune complexes using size exclusion spin columns. In contrast to PR-IgM, we found that primary anti-insulin IgM forms mainly large complexes of $> 10^4$ kD (Fig 7H). To show that the purified primary anti-insulin IgM is responsible for the dysregulation of glucose metabolism, we injected 5 μg of purified anti-insulin primary IgM or PR-IgM intravenously and monitored blood glucose. In contrast to PR-IgM, we observed a vigorous increase in blood glucose after injection of purified primary anti-insulin IgM (Fig 7I). Interestingly, the increase in blood glucose emerged faster after injection of purified anti-insulin primary IgM as compared to total primary IgM (compare Fig 6G with Fig 7I).

In summary, these data suggest that increased specificity to autoantigen is important for autoreactive memory PR-IgM to be protective during immune responses (graphical abstract). Moreover, the induced generation of autoreactive PR-IgM is most likely a critical step in B-cell tolerance.

Discussion

A critical aspect for understanding autoreactive immune responses is the design of experimental systems that resemble physiological situation. A key characteristic of the present study is the use of wild-type animals expressing a normal B-cell repertoire combined with insulin as a widely studied autoantigen which regulates glucose metabolism (Tokarz *et al*, 2018). Moreover, anti-insulin antibodies represent an essential part of the diabetes mellitus metabolic disorder characterized by high blood glucose and associated complications (Uchigata *et al*, 1994, 2010; Pavithran *et al*, 2016; Hu & Chen, 2018). Thus, in contrast to transgenic mouse models expressing monospecific transgenic BCRs and cognate antigen, our experimental system uses a physiological B-cell repertoire in wild-type mice and a disease-related autoantigen.

Notably, the diabetes symptoms used as readout for the generation of anti-insulin antibodies are similar to exogenous insulin antibody syndrome (EIAS), which is a clinical syndrome associated with insulin antibodies induced by exogenous insulin in diabetic patients (Hu & Chen, 2018). Indeed, about half of the patients receiving insulin during diabetes therapy acquire anti-insulin antibodies that are associated with unpredictable phases of glucose metabolism dysregulation referred to as dysglycemia (Berson *et al*, 1956; Uchigata *et al*, 1994; Lahtela *et al*, 1997; Hu & Chen, 2018). In agreement with our data, the most abundant class of anti-insulin antibodies in EIAS patients is IgG (Fineberg *et al*, 2005) and these autoantibodies are sufficient for induction of insulin resistance (Ganz *et al*, 1990; Asai *et al*, 2003; Koyama *et al*, 2005). On the other hand, it has also been observed that some anti-insulin antibodies seem to act as carrier that bind to insulin and prolong its action in a kind of "reservoir-like" effect (Hu & Chen, 2018). It is tempting to speculate that the protective anti-insulin IgM discovered in our experiments serves as carrier that releases endogenous insulin in controlled manner and at the same time prevents IgG binding and subsequent destruction. Thus, understanding the function of protective anti-insulin IgM may not only help to protect endogenous insulin but might also lead to optimized release of the substituted insulin via the reservoir function.

The current results reveal an unexpected regulatory role of soluble monovalent antigen. Although by itself unable to mount considerable antibody responses, monovalent antigen modulates immune responses induced by multivalent antigen toward the generation of IgM. This occurs at the expense of IgG, and since autoreactive IgG is a hallmark of autoimmune diseases, monovalent antigen might prevent the outbreak of autoimmune diseases by shifting the immune responses toward protective IgM. Together with previous findings suggesting that IgD-BCR controls the responsiveness of mature B cells by sensing the antigen valency, it is conceivable that monovalent antigen modulates B-cell responsiveness and IgG antibody generation via the IgD-class BCR (Übelhart *et al*, 2015). As a consequence, autoimmune diseases might develop when the ratio of autoantigen complexes exceeds a distinct threshold which then leads to increased autoreactive IgG as compared to IgM. In fact, our data show that an increased ratio of multivalent to monovalent antigen is associated with increased ratio of IgG to IgM in the immune responses. This relationship is independent of whether the antigen is self-derived or foreign. Therefore, anti-insulin autoantibodies of IgM and IgG type were easily generated in wild-type mice after injection of insulin complexes suggesting that autoreactive B cells recognizing insulin are present in the periphery. Similarly, B cells recognizing the C-peptide, as an example for low-abundance autoantigen, are also present and induce specific autoantibodies upon encountering multivalent C-peptide. This suggests that the peripheral repertoire of B cells of wild-type animals contains autoreactive specificities for most likely every autoantigen. These autoreactive B cells are regulated by the relative amounts of antigen forms as shown for insulin in this study. The resulting model has fundamental consequences for B-cell selection, antibody responses after vaccination, B-cell tolerance, and control of harmful autoimmune responses. By proposing a dynamic regulation of B-cell responses including the inducible production of autoantigen-specific protective IgM, this model questions the central B-cell tolerance concept, which suggests that the elimination of autoreactive B-cell specificities in early stages of development is crucial for avoiding harmful autoreactive responses (Goodnow *et al*, 1988, 1989; Nemazee & Buerki, 1989; Nemazee & Bürki, 1989; Hartley *et al*, 1991; Brink *et al*, 1992). Given the ample generation of autoreactive antibodies and the protective role of autoreactive IgM shown here,

 © 2021 The Authors

it is likely that a highly diverse autoreactive primary B-cell repertoire is essential for the unrestricted generation of protective IgM to control harmful autoimmune responses. This might explain why immune deficiencies are often associated with autoimmune diseases as deficiencies might interfere with the generation of a diverse B-cell repertoire (Gupta & Gupta, 2017). According to this scenario, the secondary rearrangements of the immunoglobulin genes including receptor editing represent mechanisms that expand the B-cell repertoire and thus the ability to manage the potential changes in foreign or self-antigen. The important role of autoreactive B-cell specificities for B-cell development is exemplified by the autoreactive behavior of the precursor-BCR, which is expressed on developing early B cells (Köhler *et al*, 2008; Herzog & Jumaa, 2012).

A diverse B-cell repertoire ensures the generation of protective IgM to the same degree of diversity as that of generating pathogen-specific antibodies. The main difference is that IgG isotypes are characteristic for effective, long-term, pathogen-specific antibody responses. Interestingly, our data demonstrate that protective IgM is induced by recall immunizations and shows affinity maturation typical for memory responses. Therefore, it is likely that the control of destructive autoimmune reactions involves the inducible generation of autoreactive IgM as part of an adaptive tolerance memory that prevents self-destructive responses. Consequently, it is reasonable to consider the generation of memory IgM as important sign of autoreactive processes as compared with memory IgG as a standard indication for efficient pathogen-specific immunizations. These characteristics might be of great importance for vaccination strategies as increased ratio of memory IgM may be indicative of autoimmune processes. Given the autoreactive potential of B cells shown here and the possibility that certain individuals under yet unknown conditions cannot produce protective IgM and can therefore not control the autoimmune processes, determining the ratio of memory IgM and IgG might be a crucial step for vaccine design and assessment of vaccination results.

Thus, our study has important consequences for vaccine design and application as the development of vaccines relies on the current model of B selection proposing that central tolerance mechanisms remove most autoreactive B-cell specificities resulting in a peripheral B-cell repertoire mostly devoid of autoreactive potential. Accordingly, the proposed absence of autoreactive specificities would prevent vaccines from inducing autoreactive responses. However, our finding that the normal peripheral B-cell repertoire is capable of inducing broad autoreactive responses suggests that caution is required when designing and applying new vaccines.

Similarly, the use of sulfhydryl group-containing drugs was reported to be associated with dysglycemia and the development of anti-insulin autoantibodies (Wintersteiner, 1933; Pavithran *et al*, 2016). According to our data, it is conceivable that sulfhydryl-groups cause complex formation, possibly by mediating disulfide bonds, of autoantigens including insulin thereby triggering autoreactive B cells to produce insulin-specific antibodies. Given the autoreactive potential of normal B cells, medications, nutrients, protein degradation or cell death might contribute to the formation of autoantigen complexes and thus induce autoreactive responses.

Notably, natural IgM produced by B1 cells has been proposed to play a protective role in other human diseases associated with immune cell activation (Shapiro-Shelef & Calame, 2005; Cantrell, 2015) by altered self-structures. In arthrosclerosis for instance, natural IgM is proposed to bind to oxidized self-structures thereby preventing the activation of innate immune cells and the subsequent inflammation (Benedict & Kearney, 1999; Amir *et al*, 2012; Tsiantoulas *et al*, 2012). However, in contrast to the protective memory IgM described here, natural antibodies are produced in the absence of previous exposure to antigen and do not undergo affinity maturation as they usually lack mutations in their Ig genes (Nakamura *et al*, 1988).

The anti-insulin protective IgM (PR-IgM), which is produced during secondary responses, is likely to be memory IgM for several reasons. First, serum titers of anti-insulin IgM were greatly increased after boost immunization, which is typical of a memory response (Weill & Reynaud, 2020). Second, antigen affinity of IgM was increased from primary (d7) to secondary (d28) immune responses after the first boost at d21 and was maintained for long time after immunization. Third, the number of IgM^+ insulin-reactive B cells was considerably increased compared at d85 as compared with d7. Fourth, IgM on d85 is not polyreactive, and therefore, it is unlikely that PR-IgM is produced by recall primary responses which are clearly polyreactive according to our data.

The primary IgM, which induces diabetes symptoms in our study, most likely belongs to natural antibodies suggesting that polyreactive IgM may also induce harmful autoimmune responses. Currently, it is unclear how the high-affinity anti-insulin memory IgM protects insulin from removal by IgG or primary low-affinity IgM. It is possible that low-affinity anti-insulin IgM, due to reduced specificity for insulin, binds other autoantigens leading to higher molecular weight immune complexes that are bound and digested by phagocytes. Anti-insulin IgM possessing high specificity might prevent this scenario. Thus, an important consequence of the present study is the opportunity of inducing or restoring immune tolerance by characterization of the involved autoantigen and the affinity of antibody binding. Using insulin as an example for a common autoantigen shows that the ratio between monovalent antigen and complex multivalent antigen is crucial for regulating immune responses. Shifting the balance of autoantigen toward multivalent forms leads to autoreactive IgG antibodies associated with autoimmune diseases (Kaneko *et al*, 2006).

The induction of protective autoreactive memory IgM (PR-IgM) by ratios of soluble and complex antigen prevents the development of autoreactive IgG causing harmful autoreactive responses. It is conceivable that this process protects soluble as well as membrane-bound autoantigens, thereby preventing autoimmune targeting and destruction of respective cells/autoantigens. Based on molecular characterization of the self-structures involved in autoimmune diseases, the regulated induction of protective IgM might provide a new concept for the treatment of already manifest autoimmune diseases or for preventing their development.

Taken together, this study is a paradigm shift from a static model of B-cell development, in which absolute selection mechanisms are proposed to prevent initial generation of autoreactive specificities, toward a dynamic model of development, in which immune responses are regulated by relative amounts of antigen forms and antibody isotypes allowing an unrestricted potential of adaptive immune responses that are regulated by adaptive tolerance memory.

© 2021 The Authors

Materials and Methods

Mice

Eight- to 12-week-old female C57BL/6 mice and female B-cell-deficient mice (Hobeika *et al*, 2006) were immunized intraperitoneally (i.p.) with a mixture of 13–50 μg antigen with 50 μg CpG-ODN1826 (Biomers) in 1× PBS for the first injection. Following injections (boosts) were done without CpG-ODN1826. Control immunization (CI) mice received PBS and CpG-ODN1826 (50 μg/mouse). Long-term immune responses of immunized mice were monitored up to an age of over 30 weeks. Native biotinylated murine insulin was purchased from BioEagle. Animal experiments were performed in compliance with license 1,484 for animal testing at the responsible regional board Tübingen, Germany. All mice used in this study were bred and housed within the animal facility of Ulm University under specific-pathogen-free conditions or obtained from Jackson at the age of 6 weeks.

Peptides

C-Peptide peptides (RoyoBiotech, Shanghai) and insulin peptides (Peptides & Elephants, Berlin) were dissolved according to their water solubility in pure water or 1% Dimethylformamide (DMF). For covalent coupling of peptides to key hole limpet hemocyanin (KLH), a N-terminal cysteine was added. Coupling of peptides to streptavidin (SAV, Thermo Scientific) was done by addition of biotin to the N-terminus. The C-terminus was left unmodified with an OH-group for better handling.

Flow cytometry

Cell suspension was Fc-receptor blocked with polyclonal rat IgG-UNLB (2,4G2; BD) and stained according to standard protocols. Biotin-conjugated peptides/antibodies were detected using streptavidin Qdot605 (Molecular Probes; Invitrogen). Viable cells were distinguished from dead cells by usage of Fixable Viability Dye eFluor780 (eBioscience). Cells were acquired at a Canto II Flow Cytometer (BD). If not stated otherwise numbers in the dot plots indicate percentages in the respective gates whereas numbers in histograms state the mean fluorescence intensity (MFI).

Antibody specificity, conjugate, clone, supplier catalog number, dilution: anti-CD45R/B220 (PE-Cy7 RA3-6B2 Invitrogen, 25045282, 1:200); Anti-CD19, (PerCP-Cy5.5, 1D3, BD Biosciences, 551001, 1:200); Anti-CD11b (FITC, M1/70, BD Biosciences, 557396, 1:200); Anti-IgD (Biotin, southern Biotech, 1120-08, 1:300); Anti-IgG (APC, Poly4053, BioLegend, 405308, 1:400); Anti-IgM (eFluor 450, eB121-15F9, Invitrogen, 48-5890-82, 1:300); streptavidin (Qdot 605, Invitrogen, Q10001MP, 1:400); Anti-CD138 (PE, 281-2, BD Biosciences, 553714, 1:300); Anti-CD23 (PE, B384, BD Biosciences, 553139, 1:300); Anti-Ly6G (PE-Cy7, 1A8, BD Biosciences, 560601, 1:200); Anti-CD16/CD32 (Unlabeled, 2.4G2, BD Pharmingen, 553142, 1:100); Anti-GL-7 FITC (09054D, BD Biosciences, 553666, 1:100).

Enzyme-linked immunosorbent assay (ELISA)

A 96-Well plates (Nunc, MaxiSorp) were coated either with, native insulin (Sigma-Aldrich, Cat. 91077C), streptavidin (Thermo Scientific, Cat. 21125), or calf thymus DNA (Thermo Scientific, Cat.15633019), with 10 μg/ml, or anti-IgM, anti-IgG-antibodies (SouthernBiotech). Loading with a biotinylated peptide (2.5 μg/ml) of SAV-plates and blocking was done in 1% BSA blocking buffer (Thermo Fisher). Serial dilutions of 1:3 IgM or IgG antibodies (SouthernBiotech) were used as standard. The relative concentrations stated as arbitrary unit (AU), were determined via detection by Alkaline Phosphatase (AP)-labeled anti-IgM/anti-IgG (SouthernBiotech), respectively. The p-nitrophenylphosphate (pNPP; Genaxxon) in diethanolamine buffer was added and data were acquired at 405 nm using a Multiskan FC ELISA plate reader (Thermo Scientific). All samples were measured in duplicates.

For analysis of affinity maturation, results from plates coated with either peptide (1) or peptide (4) were calculated by dividing peptide (1) by peptide (4). Thus, results were stated as relative units [RU] within the figures.

For determination of serum levels of pancreatic lipase (PL), we used a mouse PL kit (MyBioSource, MBS733780) according to the manufacturer's protocol.

Antibody specificity, host/isotype, conjugate clone, class, supplier catalog number, dilution: anti-mouse IgM (Goat, IgG, Unlabeled, polyclonal, SouthernBiotech, 1020-01); anti-mouse IgG (Goat, IgG, Unlabeled, polyclonal, SouthernBiotech, 1030-01); Mouse IgM (Unlabeled, polyclonal, SouthernBiotech, 0101-01); Mouse IgG (Unlabeled, polyclonal, SouthernBiotech, 0107-01); anti-mouse IgM (Goat, AP, polyclonal, SouthernBiotech, 0120-04); anti-mouse IgG (Goat, AP, polyclonal, SouthernBiotech, 0130-04).

Enzyme-linked immuno-spot assay (ELISpot)

Total splenocytes were measured in triplicates with 300,000 cells/well. ELISpot plates were pre-coated with either native insulin (Sigma-Aldrich, Cat. 91077C), or C-peptide (RoyoBiotech). After 12–24 h incubation of the cells at 37°C, antigen-specific IgM or IgG was detected via anti-IgM-bio:SAV-AP or anti-IgG-bio:SAV-AP (Mabtech). Handling of the plates and antibody concentrations was done according to the manufacturer's recommendations.

HEp-2 slides and fluorescence microscopy

HEp-2 slides (EUROIMMUN, F191108VA) were used to asses reactivity of serum IgM or insulin-specific IgM to nuclear antigens (ANA). Sera of insulin-A-peptide-immunized mice on days 7 and 85 post-immunization were diluted to an equal concentration of IgM (approx. 500 ng/ml anti-Insulin-IgM in each sample) and applied onto the HEp-2 slides. Anti-IgM-FITC (eBioscience, Cat. 11-5790-81) was used for detection of ANA-IgM. Stained HEp-2 slides were analyzed using fluorescence microscope Axioskop 2 (Zeiss) and DMi8 software (Leica).

Monitoring of blood and urine glucose levels

Assessment of urine glucose levels was done using Combur 10 M Test stripes (Roche Diagnostics, Mannheim). Sterile stripes were used during daily mouse handling and the displayed color change after testing was compared to the manufacturer's standard of glucose levels in mmol/l. AccuCheck (Roche Diagnostics, Mannheim) blood glucose monitor was used to measure blood

 © 2021 The Authors

glucose levels of mice. Blood was taken from the tail vein from *ad libitum* fed mice and transferred onto sterile test stripes. Glucose levels were measured in mmol/l at days stated in the figures for each mouse per group. Control mice were tested with immunized littermates and measured at similar times of the day.

SDS–PAGE, Coomassie, and Western blot

Organs were taken immediately after sacrifice and lysed in RIPA buffer containing protease and phosphatase inhibitors (50 mM Tris–HCl, pH 7.4, 1% NP-40, 0.25% sodium deoxycholate, 150 mM NaCl, 1 mM EDTA (pH 8)), 1 mM sodium orthovanadate, 1 mM NaF, protease inhibitor cocktail (Sigma-Aldrich). Samples were separated on 10–20% SDS–polyacrylamide gels and either blotted onto PVDF membranes (Millipore) or incubated with Coomassie (Coomassie brilliant blue R-250, Thermo Fisher) for 45 min and subsequently de-stained. Membranes were blocked for 1 h at room temperature in 5% BSA PBS with constant agitation. Primary antibodies were diluted in 5% BSA PBS (BIOMOL Research Laboratories). Secondary antibodies were diluted in 5% BSA PBS. Development of the membrane and recording of the data were done with an optical system Fusion SL (Vilber).

Antibody specificity, host/isotype, conjugate, clone, class, supplier catalog number, dilution: anti-mouse-IgG (IgG1, HRP, Human, cell signaling, 7076 1: 10,000); anti-beta-actin (IgG, Rabbit, D6A8, cell signaling, 8457, 1:500); anti-rabbit-IgG (IgG, Goat, cell signaling, 7074, 1:10,000).

Pulldown of total serum immunoglobulins

Sera of immunized mice were taken immediately after euthanasia and either IgM or IgG were purified. Removal of antigen bound to antibodies was achieved by repeated freeze-thaw cycles of the serum and pH-shift during elution (Reverberi & Reverberi, 2007). For IgG protein G sepharose beads (Thermo Fisher) were used according to the manufacturer's protocol and dialyzed overnight in 10 times sample volume in 1× PBS. For IgM, HiTrap IgM columns (GE Healthcare, Sigma-Aldrich) were used according to the manufacturer's protocol and dialyzed overnight in 10 times sample volume 1× PBS. Quality control of the isolated immunoglobulins was addressed via SDS–PAGE and Coomassie and the amount of insulin-specific immunoglobulins determined via ELISA. Finally, 20–50 μg (1–10 μg insulin-specific-Ig) were injected intravenously.

Isolation of insulin-specific serum immunoglobulins

Sera of cInsA (complex insulin-A peptide) and control-immunized mice were taken immediately after euthanasia and prepared for insulin-specific immunoglobulin isolation. Streptavidin bead columns (Thermo Scientific, Cat. 21115) were loaded with 10 μg bio-insulin (BioEagle). The sera were incubated for 90 min at room temperature to ensure binding of insulin-specific antibodies to the beads. Isolation of the insulin antibodies was done by pH-shift using the manufacturer's elution and neutralization solutions. Quality of the isolated immunoglobulins was examined via Coomassie and Western blot analysis using anti-IgM heavy chain (Thermo Scientific, Cat. 62-6820) and anti-IgG heavy chain (Cell Signaling Technologies, Cat. 7076) antibodies. For further *in vivo* experiments, the isolated antibodies were dialyzed overnight (see above).

Bio-layer interferometry (BLI)

Bio-Layer Interferometric assays (BLItz device, ForteBio) were used to determine the affinity of antigen-antibody interactions (Kumaraswamy & Tobias, 2015). Here, we used insulin-specific IgM (see isolation of insulin-specific immunoglobulins) and insulin-bio (Thermo Fisher) as target. Targets were loaded onto streptavidin biosensors (ForteBio). Binding affinities of IgM to insulin were acquired in nm. Subsequently, the calculated affinity value (Ka) was used to determine the dissociation constant (K_d): $K_d = 1/K_a$. Following protocol was used: 30-s baseline, 30-s loading, 30-s baseline, 240-s association, 120-s dissociation. For buffering of samples, targets, and probes, the manufacturer's sample buffer (ForteBio) was used.

Flow Cytometric Bead Array for mouse inflammatory cytokines

To determine pancreas supernatant inflammatory cytokine levels of mice immunized with cInsulin or control immunization, we performed a BD Cytometric Bead Array (Mouse Inflammation, BD Biosciences, Cat.: 552364, Lot.: 005197). Samples were diluted according to the manufacturer's protocol. IL-12p70, TNF-α, IFN-γ, MCP-1, IL-10, and IL-6 APC-labeled beads were used together with PE-labeled detector reagent. The assay was measured at a FACS Canto II and analyzed via FlowJo10 software. Relative cytokine levels correlate to the mean fluorescence intensity of each cytokine bead within the PE channel.

Statistical analysis

Graphs were created and statistically analyzed by using GraphPad Prism (version 6.0h) software. The numbers of individual replicates or mice (n) are stated within the figure or figure legends. Data sets were analyzed by D'Agostino & Pearson omnibus normality test and/or Shapiro–Wilk normality test in GraphPad Prism software to determine whether they are normally distributed. If one of the data sets was not normally distributed or the sample number n was too small to perform the normality tests, non-parametric tests were used to calculate P-values. Statistical tests used to calculate P-values are stated within the figure legends. P-values > 0.05 were considered to be statistically significant ($^*P < 0.05$; $^{**}P < 0.01$; $^{***}P < 0.001$, $^{****}P < 0.0001$).

Data availability

This study includes no data deposited in external repositories.

Expanded View for this article is available online.

Acknowledgements

We thank C. Setz and M. Young for assistance in performing experiments, O. El Ayoubi for serum immunoglobulin pulldown, G. Allies for injections of mice and SDS–PAGE We thank M. Reth for critical reading of the manuscript. This work was supported by the DFG through TRR130 (B cells and beyond) project

© 2021 The Authors

01, SFB1074 (Experimental Models and Clinical Translation in Leukemia), SFB 1279 (Exploration of the Human Peptidome). Open Access funding enabled and organized by Projekt DEAL.

Author contributions

TA performed all experiments, analyzed and interpreted data, prepared the figures together with HJ and contributed to the writing of the manuscript. HJ designed the study, proposed experiments, supervised the work, and wrote the manuscript. Both authors read and discussed the manuscript.

Conflict of interest

HJ has applied for a patent for the use of PR-IgM to protect autoantigens.

References

Amir S, Hartvigsen K, Gonen A, Leibundgut G, Que X, Jensen-Jarolim E, Wagner O, Tsimikas S, Witztum JL, Binder CJ (2012) Peptide mimotopes of malondialdehyde epitopes for clinical applications in cardiovascular disease. *J Lipid Res* 53: 1316 – 1326

Asai M, Kodera T, Ishizeki K, Uebori S, Kashiwaya T, Itoh H, Makino I (2003) Insulin lispro reduces insulin antibodies in a patient with type 2 diabetes with immunological insulin resistance. *Diabetes Res Clin Pract* 61: 89 – 92

Benedict CL, Kearney JF (1999) Increased junctional diversity in fetal B cells results in a loss of protective anti-phosphorylcholine antibodies in adult mice. *Immunity* 10: 607 – 617

Benschop RJ, Brandl E, Chan AC, Cambier JC (2001) Unique signaling properties of B Cell antigen receptor in mature and immature B Cells: implications for tolerance and activation. *J Immunol* 167: 4172 – 4179

Berson SA, Yalow RS, Bauman A, Rothschild MA, Newerly K (1956) Insulin-I131 metabolism in human subjects: demonstration of insulin binding globulin in the circulation of insulin treated subjects. *J Clin Invest* 35: 170 – 190

Brink R, Goodnow CC, Crosbie J, Adams E, Eris J, Mason DY, Hartley SB, Basten A (1992) Immunoglobulin M and D antigen receptors are both capable of mediating B lymphocyte activation, deletion, or anergy after interaction with specific antigen. *J Exp Med* 176: 991 – 1005

Cantrell D (2015) Signaling in lymphocyte activation. *Cold Spring Harb Perspect Biol* 7: 1 – 14

Cooper GS, Stroehla BC (2003) The epidemiology of autoimmune diseases. *Autoimmun Rev* 2: 119 – 125

Cyster JG, Hartley SB, Goodnow CC (1994) Competition for follicular niches excludes self-reactive cells from the recirculating B-cell repertoire. *Nature* 371: 389 – 395

Fineberg SE, Kawabata T, Finco-Kent D, Liu C, Krasner A (2005) Antibody response to inhaled insulin in patients with type 1 or type 2 diabetes. An analysis of initial phase II and III inhaled insulin (Exubera) trials and a two-year extension trial. *J Clin Endocrinol Metab* 90: 3287 – 3294

Ganz MA, Unterman T, Roberts M, Uy R, Sahgal S, Samter M, Grammer LC (1990) Resistance and allergy to recombinant human insulin. *J Allergy Clin Immunol* 86: 45 – 51

Gay D, Saunders T, Camper S, Weigert M (1993) Receptor editing: An approach by autoreactive B cells to escape tolerance. *J Exp Med* 177: 999 – 1008

Gomez D, Addison A, De Rosa A, Brooks A, Cameron IC (2012) Retrospective study of patients with acute pancreatitis: Is serum amylase still required? *BMJ Open* 2: e001471

Goodnow CC, Crosbie J, Adelstein S, Lavoie TB, Smith-Gill SJ, Brink RA, Pritchard-Briscoe H, Wotherspoon JS, Loblay RH, Raphael K *et al* (1988) Altered immunoglobulin expression and functional silencing of self-reactive B lymphocytes in transgenic mice. *Nature* 334: 676 – 682

Goodnow CC, Crosbie J, Jorgensen H, Brink RA, Basten A (1989) Induction of self-tolerance in mature peripheral B lymphocytes. *Nature* 342: 385 – 391

Grönwall C, Vas J, Silverman GJ (2012) Protective roles of natural IgM antibodies. *Front Immunol* 3, 66

Gupta S, Gupta A (2017) Selective IgM deficiency-An underestimated primary immunodeficiency. *Front Immunol* 8: 1056

Hartley SB, Crosbie J, Brink R, Kantor AB, Basten A, Goodnow CC (1991) Elimination from peripheral lymphoid tissues of self-reactive B lymphocytes recognizing membrane-bound antigens. *Nature* 353: 765 – 769

Herzog S, Jumaa H (2012) Self-recognition and clonal selection: Autoreactivity drives the generation of B cells. *Curr Opin Immunol* 24: 166 – 172

Hobeika E, Thiemann S, Storch B, Jumaa H, Nielsen PJ, Pelanda R, Reth M (2006) Testing gene function early in the B cell lineage in mb1-cre mice. *Proc Natl Acad Sci U S A* 103: 13789 – 13794

Hu X, Chen F (2018) Exogenous insulin antibody syndrome (EIAS): A clinical syndrome associated with insulin antibodies induced by exogenous insulin in diabetic patients. *Endocr Connect* 7: R47 – R55

Kaneko Y, Nimmerjahn F, Ravetch JV (2006) Anti-inflammatory activity of immunoglobulin G resulting from Fc sialylation. *Science* 313: 670 – 673

Köhler F, Hug E, Eschbach C, Meixlsperger S, Hobeika E, Kofer J, Wardemann H, Jumaa H (2008) Autoreactive B Cell receptors mimic autonomous pre-B cell receptor signaling and induce proliferation of early B cells. *Immunity* 29: 912 – 921

Koyama R, Nakanishi K, Kato M, Yamashita S, Kuwahara H, Katori H (2005) Hypoglycemia and hyperglycemia due to insulin antibodies against therapeutic human insulin: treatment with double filtration plasmapheresis and prednisolone. *Am J Med Sci* 329: 259 – 264

Kreslavsky T, Wong JB, Fischer M, Skok JA, Busslinger M (2018) Control of B-1a cell development by instructive BCR signaling. *Curr Opin Immunol* 51: 24 – 31

Kumaraswamy S, Tobias R (2015) Label-free kinetic analysis of an antibody-antigen interaction using biolayer interferometry. In *Protein-protein interactions: methods and applications*, Meyerkord CL, Fu H (eds), 2nd edn, pp 165 – 182. New York: Springer

Lahtela JT, Knip M, Paul R, Antonen J, Salmi J (1997) Severe antibody-mediated human insulin resistance: Successful treatment with the insulin analog lispro: a case report. *Diabetes Care* 20: 71 – 73

Lobo PI (2016) Role of natural autoantibodies and natural IgM anti-leucocyte autoantibodies in health and disease. *Front Immunol* 7, 198

McHeyzer-Williams MG (2003) B cells as effectors. *Curr Opin Immunol* 15: 354 – 361

Nakamura M, Burastero SE, Ueki Y, Larrick JW, Notkins ALCP (1988) Probing the normal and autoimmune B cell repertoire with Epstein-Barr virus. Frequency of B cells producing monoreactive high affinity autoantibodies in patients with Hashimoto's disease and systemic lupus erythematosus. *J Immunol* 141, 4165 – 4172

Nemazee D, Buerki K (1989) Clonal deletion of autoreactive B lymphocytes in bone marrow chimeras. *Proc Natl Acad Sci U S A* 86: 8039 – 8043

Nemazee DA, Bürki K (1989) Clonal deletion of B lymphocytes in a transgenic mouse bearing anti-MHC class I antibody genes. *Nature* 337: 562 – 566

Nossal GJV, Pike BL (1978) Mechanisms of clonal abortion tolerogenesis: I. Response of immature hapten-specific B lymphocytes. *J Exp Med* 148: 1161 – 1170

Nossal GJV, Pike BL (1980) Clonal anergy: Persistence in tolerant mice of antigen-binding B lymphocytes incapable of responding to antigen or mitogen. *Proc Natl Acad Sci U S A* 77: 1602 – 1606

 © 2021 The Authors

O'Neill SK, Getahun A, Gauld SB, Merrell KT, Tamir I, Smith MJ, Dal Porto JM, Li QZ, Cambier JC (2011) Monophosphorylation of CD79a and CD79b ITAM motifs initiates a SHIP-1 phosphatase-mediated inhibitory signaling cascade required for B cell anergy. *Immunity* 35: 746 – 756

Padoa CJ, Crowther NJ, Thomas JW, Hall TR, Bekris LM, Torn C, Landin-Olsson M, Ortqvist E, Palmer JP, Lernmark A *et al* (2005) Epitope analysis of insulin autoantibodies using recombinant Fab. *Clin Exp Immunol* 140: 564 – 571

Pavithran PV, Bhavani N, Jayakumar RV, Menon AS, Kumar H, Menon VU, Nair V, Abraham N (2016) Autoantibodies to insulin and dysglycemia in people with and without diabetes: an underdiagnosed association. *Clin Diabetes* 34: 164 – 167

Reverberi R, Reverberi L (2007) Factors affecting the antigen-antibody reaction. *Blood Transfus* 5: 227 – 240

Setz CS, Khadour A, Renna V, Iype J, Gentner E, He X, Datta M, Young M, Nitschke L, Wienands J *et al* (2019) Pten controls B-cell responsiveness and germinal center reaction by regulating the expression of IgD BCR. *EMBO J* 38, e100249

Shapiro-Shelef M, Calame KC (2005) Regulation of plasma-cell development. *Nat Rev Immunol* 5: 230 – 242

Shimizu T, Kozono Y, Kozono H, Oda M, Azuma T (2004) Affinity maturation of secreted IgM pentamers on B cells. *Int Immunol* 16: 675 – 684

Smith RC, Southwell-Keely J, Chesher D (2005) Should serum pancreatic lipase replace serum amylase as a biomarker of acute pancreatitis? *ANZ J Surg* 75: 399 – 404

Suurmond J, Diamond B (2015) Autoantibodies in systemic autoimmune diseases: Specificity and pathogenicity. *J Clin Invest* 125: 2194 – 2202

Tiegs SL, Russell DM, Nemazee D (1993) Receptor editing in self-reactive bone marrow B cells. *J Exp Med* 177: 1009 – 1020

Tokarz VL, MacDonald PE, Klip A (2018) The cell biology of systemic insulin function. *J Cell Biol* 217: 2273 – 2289

Tsiantoulas D, Gruber S, Binder CJ (2012) B-1 cell immunoglobulin directed against oxidation-specific epitopes. *Front Immunol* 3: 1 – 6

Übelhart R, Hug E, Bach MP, Wossning T, Dühren-von Minden M, Horn AHC, Tsiantoulas D, Kometani K, Kurosaki T, Binder CJ *et al* (2015) Responsiveness of B cells is regulated by the hinge region of IgD. *Nat Immunol* 16: 534 – 543

Uchigata Y, Eguchi Y, Takayama-Hasumi S, Omori Y (1994) Insulin autoimmune syndrome (Hirata Disease): clinical features and epidemiology in Japan. *Diabetes Res Clin Pract* 22: 89 – 94

Uchigata Y, Hirata Y, Iwamoto Y (2010) Insulin autoimmune syndrome (Hirata disease): epidemiology in Asia, including Japan. *Diabetol Int* 1: 21 – 25

Wardemann H, Yurasov S, Schaefer A, Young JW, Meffre E, Nussenzweig MC (2003) Predominant autoantibody production by early human B cell precursors. *Science* 301: 1374 – 1377

Weill JC, Reynaud CA (2020) IgM memory B cells: specific effectors of innate-like and adaptive responses. *Curr Opin Immunol* 63: 1 – 6

Wintersteiner O, Abramson HA (1933) The isoelectric point of insulin. *J Biol Chem* 99: 741 – 753

Yang Z-W, Meng X-X, Xu P (2015) Central role of neutrophil in the pathogenesis of severe acute pancreatitis. *J Cell Mol Med* 19: 2513 – 2520

Zhang Z, Zemlin M, Wang YH, Munfus D, Huye LE, Findley HW, Bridges SL, Roth DB, Burrows PD, Cooper MD (2003) Contribution of VH gene replacement to the primary B cell repertoire. *Immunity* 19: 21 – 31

Zhu S, Larkin D, Lu S, Inouye C, Haataja L, Anjum A, Kennedy R, Castle D, Arvan P (2016) Monitoring C-peptide storage and secretion in islet b-cells *in vitro* and *in vivo*. *Diabetes* 65: 699 – 709

License: This is an open access article under the terms of the Creative Commons Attribution-NonCommercial-NoDerivs License, which permits use and distribution in any medium, provided the original work is properly cited, the use is non-commercial and no modifications or adaptations are made.

frontiers in Immunology

ORIGINAL RESEARCH
published: 03 August 2021
doi: 10.3389/fimmu.2021.709240

Primary Immune Responses and Affinity Maturation Are Controlled by IgD

Timm Amendt[†], *Omar El Ayoubi*[†], *Alexandra T. Linder*, *Gabriele Allies*, *Marc Young*, *Corinna S. Setz and Hassan Jumaa*[*]

Institute of Immunology, Ulm University Medical Center, Ulm, Germany

Mature B cells co-express IgM and IgD B cell antigen receptors (BCR) on their surface. While IgM BCR expression is already essential at early stages of development, the role of the IgD-class BCR remains unclear as most B cell functions appeared unchanged in IgD-deficient mice. Here, we show that IgD-deficient mice have an accelerated rate of B cell responsiveness as they activate antibody production within 24h after immunization, whereas wildtype (WT) animals required 3 days to activate primary antibody responses. Strikingly, soluble monovalent antigen suppresses IgG antibody production induced by multivalent antigen in WT mice. In contrast, IgD-deficient mice were not able to modulate IgG responses suggesting that IgD controls the activation rate of B cells and subsequent antibody production by sensing and distinguishing antigen-valences. Using an insulin-derived peptide we tested the role of IgD in autoimmunity. We show that primary autoreactive antibody responses are generated in WT and in IgD-deficient mice. However, insulin-specific autoantibodies were detected earlier and caused more severe symptoms of autoimmune diabetes in IgD-deficient mice as compared to WT mice. The rapid control of autoimmune diabetes in WT animals was associated with the generation of high-affinity IgM that protects insulin from autoimmune degradation. In IgD-deficient mice, however, the generation of high-affinity protective IgM is delayed resulting in prolonged autoimmune diabetes. Our data suggest that IgD is required for the transition from primary, highly autoreactive, to secondary antigen-specific antibody responses generated by affinity maturation.

Keywords: B cell selection, IgD, antigen-valency, autoimmunity, IgM, tolerance

OPEN ACCESS

Edited by:
Hermann Eibel, University of Freiburg Medical Center, Germany

Reviewed by:
Michel Cogne, University of Limoges, France
Arthur L. Shaffer, III, National Cancer Institute (NCI), United States

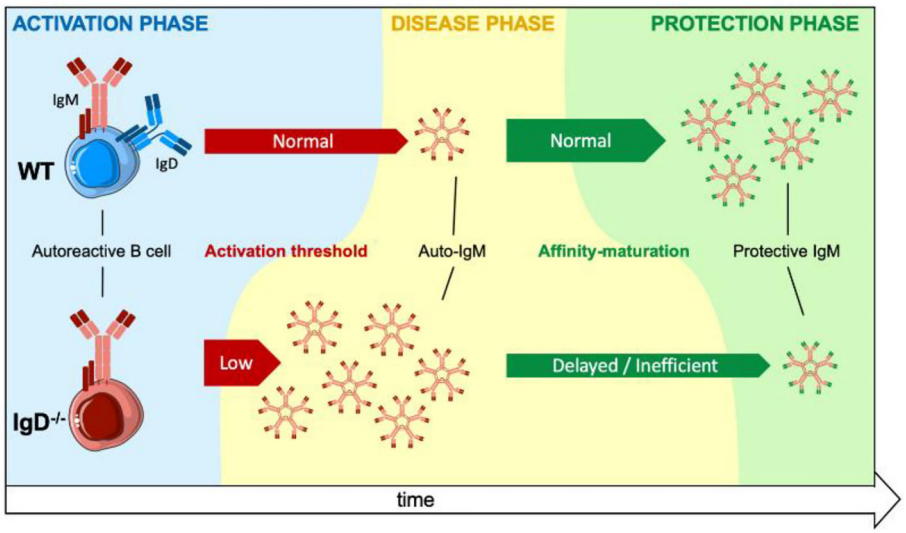
***Correspondence:**
Hassan Jumaa
hassan.jumaa@uni-ulm.de

[†]*These authors have contributed equally to this work*

Specialty section:
This article was submitted to B Cell Biology, a section of the journal Frontiers in Immunology

Received: *13 May 2021*
Accepted: *15 July 2021*
Published: *03 August 2021*

Citation:
Amendt T, Ayoubi OE, Linder AT, Allies G, Young M, Setz CS and Jumaa H (2021) Primary Immune Responses and Affinity Maturation Are Controlled by IgD. Front. Immunol. 12:709240. doi: 10.3389/fimmu.2021.709240



GRAPHICAL ABSTRACT |

INTRODUCTION

Maintaining physiological integrity by avoiding autoimmune reactions is achieved by self-tolerance. Currently, self-tolerance is believed to be divided into two programs. First, central tolerance that occurs in the bone marrow by deleting early self-reactive B cells or initiating receptor editing (1–4). Second, autoreactive B cells circumventing central tolerance are thought to undergo clonal anergy characterized by functional unresponsiveness and downmodulation of the IgM-class BCR (5, 6). However, these concepts can neither explain the variety of autoantibody-borne autoimmune diseases (7–9) nor provide therapeutic concepts. Importantly, the use of transgenic mouse models expressing highly affine monoclonal BCRs (1, 6) differ considerably from physiological conditions. In addition, recent studies reporting that anergic B cells from transgenic models behave like mature cells that are regulated by the antigen form and the BCR-class expressed on their membrane suggest that understanding the role of BCR-isotypes in mature B cell responsiveness is crucial for understanding B cell activation and tolerance (10, 11).

During early developmental stages, immature B cells exclusively express IgM-class BCR. Cells passing through the immature B cell stage leave the bone marrow and co-express IgM- and IgD-class BCRs sharing the same antigen-specificity but differ in the use of the heavy chain (HC) μ compared to δ. In mature B cells the IgD-class BCR becomes the predominant antigen receptor.

In the past decades, the IgD-class BCR was believed to be redundant with IgM and not involved in autoimmune processes (12–15). However, since IgD is barely detectable in human serum (16, 17) and shows structural and functional differences compared to IgM (15, 18, 19), a specialized role in B cell physiology is conceivable. Recent studies showed that IgM and IgD are associated in distinct membrane nanoclusters pairing with specific coreceptors (20, 21) and that IgD-deficient mice (12) also show delayed germinal center formation (11, 14).

Using cellular reconstitution systems or transgenic mice for hen-egg lysozyme (HEL) as model antigen, we recently reported that IgM- and IgD-class BCRs differ in their responsiveness to distinct antigen-valences. In contrast to the IgD-class BCR, IgM induces calcium flux after treatment with monovalent antigen (soluble HEL), whereas treatment with polyvalent antigen (complex HEL) activated both receptor classes. Interestingly, the presence of monovalent HEL blocked the activation of the IgD-class BCR by complex HEL due to the flexible hinge region of IgD (10, 11). Together, these data suggest a novel concept, termed adaptive tolerance and responsiveness, for the development, selection and activation of mature B-lymphocytes.

Here, we show that IgD controls the responsiveness and antibody secretion by B cells *in vivo* and that "self-tolerance" is achieved mainly by unique characteristics of immunoglobulin isotypes and by antigen-valence. Upon antigen encounter, IgD determines how fast an immune response is triggered and how long it lasts as a primary low-specific IgM response. This happens independent of whether the antigen belongs to self or non-self, which makes this IgD-mediated regulation key for the maturation of antibody responses and tolerance to self-structures.

METHODS

Mice

8 – 15-week-old female C57BL/6 mice and IgD-deficient (12) mice were immunized intraperitoneally (i.p.) with a mixture of 50 μg antigen with 50 μg CpG-ODN1826 (Biomers) in 1x PBS. For control immunization (CI) mice received PBS and CpG-ODN1826 (50 μg/mouse). Animal experiments were performed

in compliance with license 1484 for animal testing at the responsible regional board Tübingen, Germany. All mice used in this study were bred and housed within the animal facility of Ulm University under specific-pathogen-free conditions, or obtained from Charles River at 6 weeks of age. All animal experiments were done in compliance with the guidelines of the German law and were approved by the Animal Care and Committees of Ulm University and the local government.

Peptides and Immunogens

Insulin-A-chain derived peptides (InsA) (Peptides&Elephants, Berlin) were dissolved according to their water solubility. For covalent coupling of peptides to key hole limpet hemocyanin (KLH) the N-terminal cysteine was used. The amino acid sequence used (mouse Insulin-A-chain: CSLYQLENYCN) is fully homologue to human insulin. A detailed description of the InsA autoimmunity model is provided in Amendt and Jumaa, 2021 (EMBOJ). Coupling of peptides to Streptavidin (SAV, ThermoScientific) was done by addition of biotin to the N-terminus. The C-terminus was left with an OH-group for better handling. 4-hydroxy-3-nitrophenylacetyl coupled to KLH (NP(30)KLH) or BSA (NP(15)BSA) were purchased from Biosearch Technologies.

Flow Cytometry

Cell suspensions were Fc-receptor blocked with polyclonal rat IgG-UNLB (2,4G2; BD) and stained according to standard protocols. Detection of Biotin-conjugated peptides/antibodies were achieved by using Streptavidin Qdot605 (Molecular Probes; Invitrogen). Viable cells were distinguished from dead cells by using Fixable Viability Dye eFluor780 (eBioscience). Cells were acquired at a Canto II Flow Cytometer (BD). Plots indicate percentages in the respective gates whereas numbers in histogram plots show the mean fluorescence intensity (MFI).

Enzyme-Linked Immunosorbent Assay (ELISA)

96-Well plates (Nunc, Maxisorp) were coated with, native Insulin (Sigma-Aldrich, Cat. 91077C), Streptavidin (ThermoScientific, Cat. 21125), calf thymus DNA (ThermoScientific, Cat.15633019), or NP-BSA (Biosearch Technologies, N-5050H-100) with 10 µg/mL, or anti-IgM, anti-IgG-antibodies (SouthernBiotech). Biotinylated peptides (2,5 µg/mL) were loaded onto SAV-coated plates in 1% BSA blocking buffer (ThermoFisher). Sera were initially diluted 1:50. Serial dilutions of 1:3 IgM or IgG antibodies (SouthernBiotech) were used as standard. The relative concentrations, stated as arbitrary unit (AU), were determined *via* detection by Alkaline Phosphatase (AP)-labeled anti-IgM/anti-IgG (SouthernBiotech), respectively. The p-nitrophenylphosphate (pNPP; Genaxxon) in Diethanolamine buffer was added for starting of the reaction. Data were acquired at 405 nm using a Multiskan FC ELISA plate reader (Thermo Scientific). Samples were measured at least in duplicates.

For analysis of affinity-maturation (22), results from plates coated with InsA(1) or InsA(4) were calculated by dividing InsA(1) by InsA (4). Here, we used streptavidin with tetra- (ThermoScientific) or monovalent binding capacity. Subsequently, results were stated as relative units [RU].

Enzyme-Linked Immuno-Spot Assay (ELISpot)

Total splenocytes were measured in triplicates with cell numbers stated in the figure. Particular cell populations were sorted by using a FACS Aria flow cytometer. ELISpot plates were coated with native Insulin (Sigma-Aldrich, Cat. 91077C), NP-BSA (BiosearchTechnologies) anti-IgM (Mabtech). Seeded cells were incubated for 12 – 24 h at 37°C, antigen-specific IgM or IgG was detected *via* anti-IgM-bio and SAV-AP or anti-IgG-bio and SAV-AP (Mabtech). Experiments were done according to the manufacturer's instructions.

HEp-2 Slides and Fluorescence Microscopy

HEp-2 slides (EUROIMMUN, F191108VA) were used to asses anti-nuclear-reactivity (ANA) of immunoglobulins from murine sera. Sera of immunized mice on days indicated in the figures or figure legends were diluted to an equal concentration of IgM (approx. 300 ng/mL anti-Insulin-IgM in both immunized samples) and applied onto the HEp-2 slides. Anti-IgM-FITC (eBioscience, Cat. 11-5790-81) was used for visualization of ANA-IgM. A fluorescence microscope Axioskop 2 (Zeiss) and DMi8 software (Leica) were used to analyze stained HEp-2 slides.

Glucose Level Monitoring

Urine glucose levels were assessed using Combur 10 M Test stripes (Roche Diagnostics, Mannheim). Sterile stripes were used during daily mouse handling and the displayed color after testing was compared to the manufacturer's standard of glucose levels in mmol/L. An AccuCheck (Roche Diagnostics, Mannheim) blood glucose monitor was used to measure blood glucose levels of mice. Blood was taken freshly from the tail vein from *ad libitum* fed mice and transferred onto sterile test stripes. Glucose levels were measured in mmol/L at days stated in the figures for each mouse per group. Control-immunizations were done with littermates and measured together with experimental mice.

SDS-PAGE and Coomassie

Samples were separated on 10 – 20% SDS-polyacrylamide gels and incubated with Coomassie (Coomassie brilliant blue R-250, ThermoFisher) for 45 min and subsequently de-stained.

Pulldown of Total Serum Immunoglobulins

Serum of immunized mice was collected immediately after euthanization. Removal of antigen bound to antibodies was achieved by repeated freeze-thaw cycles of the serum and pH-shift during elution (23). Protein G sepharose beads (ThermoFisher) were used according to the manufacturers protocol and dialyzed overnight in 10 times sample volume in 1x PBS to isolate IgG. For IgM, HiTrap IgM columns (GE Healthcare, Sigma-Aldrich) were used according to the manufacturers protocol and dialyzed overnight in 10 times sample volume 1 x PBS. Quality-control of the isolated immunoglobulins was done *via* SDS-PAGE and Coomassie-staining and the concentration of insulin-specific immunoglobulins determined *via* ELISA.

Isolation of Insulin-Specific Serum Immunoglobulins

Serum of immunized mice was taken immediately after euthanization and transferred into serum collection tubes. Streptavidin bead columns (Thermo-Scientific, Cat. 21115) were loaded with 10 µg bio-Insulin (BioEagle) to pull down insulin-specific immunoglobulins. The sera were incubated for 90 min at room temperature to ensure sufficient binding of antibodies to the insulin-loaded beads. Purification of the insulin-antibodies was achieved by a pH-shift (pH 2.8) using the manufacturers elution and neutralization solutions. Quality of the isolated immunoglobulins was examined *via* Coomassie-staining and ELISA. For further *in vivo* experiments, the isolated antibodies were dialyzed as described above.

Bio-Layer Interferometry

Interferometric assays (BLItz device, ForteBio) were used to determine the affinity of protein-protein interactions. Here, we used insulin-specific IgM (see *Isolation of Insulin-Specific Serum Immunoglobulins*) and insulin-bio (ThermoFisher) as a target. The targets were loaded onto Streptavidin biosensors (ForteBio). Binding affinities of IgM to Insulin were acquired in nm. Therefore, the following protocol was used: 30 sec baseline, 30 sec loading, 30 sec baseline, 240 sec association, 60 sec dissociation. For buffering of samples, targets and probes, the manufacturer's sample buffer (ForteBio) was used.

Statistical Analysis

Graphs were created and statistical analysis was performed by using GraphPad Prism (version 6.0h) software. The numbers of individual replicates or mice (n) are stated within the figure or figure legends. Data sets were analyzed by D'Agostino & Pearson omnibus normality test and/or Shapiro-Wilk normality test in GraphPad Prism software to determine whether they are normally distributed. If one of the data sets was not normally distributed or the sample number n was too small to perform the normality tests, non-parametric tests were used to calculate p-values. In this study, p-values were calculated by tests stated in the respective figure legends. Students t-tests with Welch's correction were used to compare two groups within one experiment. P values > 0.05 were considered to be statistically significant (n.s.=not significant; *$p < 0.05$; **$p < 0.01$; ***$p < 0.001$, ****$p < 0.0001$).

RESULTS

The Presence of Soluble Antigen Suppresses IgG Production

A main conclusion of the adaptive tolerance and responsiveness model is that the ratio of IgM to IgD on mature B cells together with the ratio of soluble (monovalent) to complex (polyvalent) antigen in the microenvironment determine the threshold for B cell activation and antibody secretion. This proposes a dynamic model, in which the activation of mature B cells is not an unavoidable step after antigen-binding, as activation is regulated by the class of BCR expressed and the ratio of antigen-valences. Consequently, autoreactive mature B cells can exist without inducing destructive autoantibody responses as long as the cognate autoantigen is monovalent.

To test the concept of adaptive tolerance and responsiveness of B cells *in vivo*, we performed immunization experiments using the hapten NP (4-hydroxy-3-nitrophenylacetyl) coupled to KLH (Keyhole Limpet Hemocyanin) as a carrier (**Supplementary Figure 1A**). To this end, groups of wild-type (WT) mice were injected with either NP as soluble compound (sNP) or NP-KLH, referred to as polyvalent complex antigen (cNP), at similar molarity for NP (NP(30)KLH). NP-specific antibody responses were determined at day 7 (IgM) and day 14 (IgG) post immunization (**Figures 1A, B**). Similar to control immunization (CI) containing only CpG but no antigen, injection of only soluble hapten (sNP: cNP, 1:0) failed to induce clear IgM or IgG antibody responses, while injection of cNP (sNP:cNP, 0:1) was able to induce both. Adding sNP to cNP at 100:1 ratio did not alter anti-NP-IgM antibody responses. However, the anti-NP-IgG response was significantly impeded at 100:1 ratio for sNP to cNP (**Figure 1B** and **Supplementary Figure 1D**). Importantly, the IgG response to the carrier (KLH) was comparable regardless of the amount of soluble hapten added (**Supplementary Figure 1B**).

To further confirm these findings, we performed ELISpot assays for assessing the number of NP-specific antibody secreting cells. In agreement with the serum immunoglobulin data, the ELISpot results showed that adding sNP to cNP at 100:1 ratio reduces the number of IgG secreting cells whereas IgM secreting cells were unaffected (**Supplementary Figure 1C**). These data support the concept of soluble monovalent antigen interfering in immune responses to complex forms of the same antigen.

A crucial pillar of the concept proposes that the presence of IgD-class BCR is important for the observed regulation (**Figures 1A–C**). Thus, we tested the role of IgD by conducting the NP immunization experiments in IgD knockout mice lacking IgD-class BCR (**Figure 1A**). Notably, expression levels of surface IgM on marginal zone and follicular B cells of IgD-deficient (IgD-/-) mice were comparable to WT mice (**Supplementary Figure 2**).

IgD-deficient mice showed slightly elevated IgM responses as compared to WT mice. However, the IgG response was weaker and no inhibitory effect on IgG was observed when sNP was added to cNP prior to immunizing IgD-deficient mice (**Figure 1C** and **Supplementary Figure 1D**).

Together, these data suggest that mature B cells are able to fine-tune their immune response according to the antigen-valency, thereby leading to distinct IgM and IgG responses to different epitopes of the same antigen.

Accelerated Primary Immune Response in IgD-Deficient Mice

To further investigate the dynamics of immune responses in IgD-deficient mice, we monitored early antibody production. Compared to WT mice, IgD-deficient mice showed a NP-reactive IgM response already at day 1 after immunization (**Figure 2A**). This response was further amplified at day 3 and peaked at

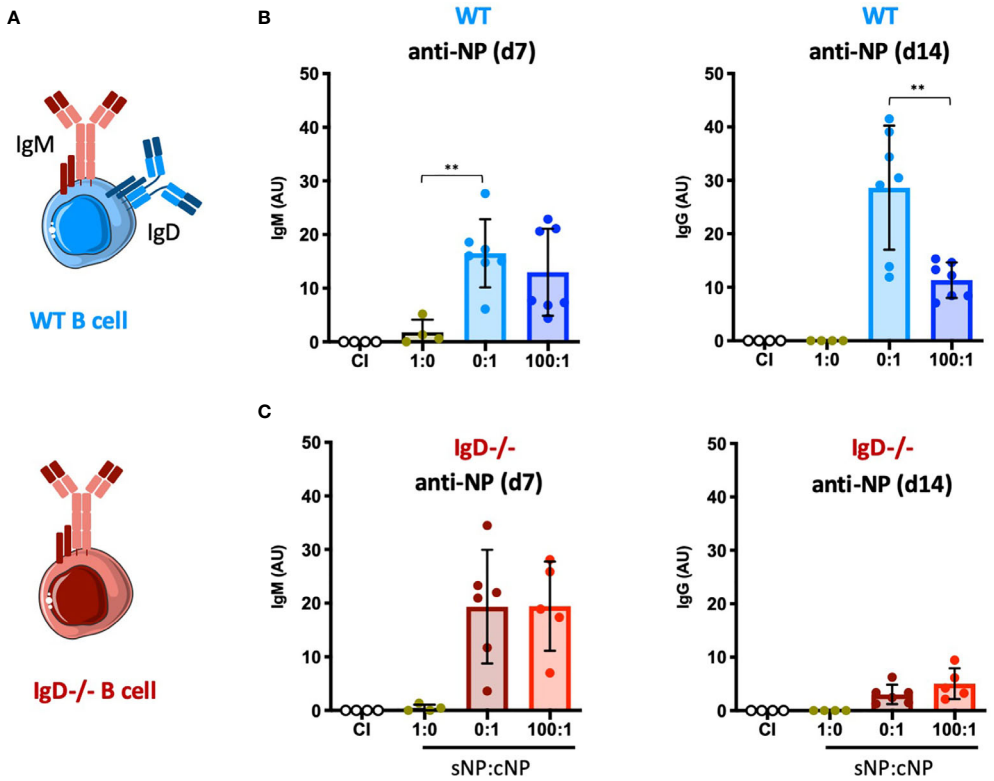


FIGURE 1 | Modulation of immune responses by monovalent antigen requires expression of the IgD-class BCR. **(A)** Schematic illustrations of a WT and IgD-deficient B cell. **(B, C)** NP-reactive serum immunoglobulins of WT mice **(B)** and IgD-deficient mice **(C)** injected with PBS (control immunization (CI), n=4/group), 4-hydroxy-3-nitrophenylacetyl only (sNP: 1:0; WT n=4, IgD-deficient n=4), complex NP (cNP: 0:1; WT n=7, IgD-deficient n=6) and soluble:complex NP (100:1; WT n=7, IgD-deficient n=5). Left panel showing anti-NP IgM on day 7, right panel shows anti-NP-IgG on day 14. Mean ± SD, students t-tests with Welch's correction were used to compare two groups within one experiment. **P < 0.01.

day 7 (**Figure 2B**). In contrast, no antibody response was observed at day 1 in WT mice. By day 3, WT mice showed a slight NP-reactive IgM response which peaked at day 7, however, remained slightly weaker than the day 7 NP-reactive IgM response in IgD-deficient mice (**Figures 1A, B**). To further characterize the specificity of the induced antibody response we performed classical autoreactivity assays including indirect immunofluorescence (IF) on HEp-2 slides and ELISA for anti-double stranded DNA (dsDNA). These experiments show that primary IgM antibodies, detected at day 1 throughout day 7 of IgD-deficient mice or by day 7 of WT mice, are autoreactive determined by recognition of nuclear structures (**Figures 2C, D**). Importantly, the control immunizations using only the adjuvant CpG showed no induction of anti-dsDNA antibodies as compared with unimmunized mice (data not shown). Further, to exclude a role of CpG in the production of autoreactive IgM, we stained HEp-2 slides with sera of control immunizations. Neither IgD-deficient mice nor WT mice showed elevated levels of autoreactive IgM in control immunizations with PBS or CpG alone (**Supplementary Figure 3**).

In summary, these results show that primary IgM responses are autoreactive and that IgD-deficiency allows rapid primary immune responses.

Sustained Primary Immune Response to Autoantigen in IgD-Deficient Mice

After testing hapten-specific antibody responses, we investigated whether the production of autoreactive primary antibodies in IgD-deficient mice differ when using autoantigens. To avoid the usage of transgenic mice that artificially harbor mono-specific B cells expressing a defined BCR that recognizes either a transgene product or endogenous structure, we selected insulin-related autoantigens as a physiologically relevant system for autoimmune diseases (Amendt and Jumaa 2021, *in press*).

To this end, we performed immunization experiments using an Insulin-A chain-derived peptide, referred to as InsA which is the most abundant epitope in autoantibody responses against insulin (24). The selected peptide was covalently coupled to the carrier KLH to generate a complex polyvalent antigen (InsA-KLH) which was then used in immunization experiments (**Figure 3A**). Subsequently, we monitored the antibody responses against the InsA peptide and native insulin to confirm the induction of harmful autoantibody responses. We found that InsA-KLH induced IgM antibody responses recognizing native insulin already at day 1 after immunization (**Figure 3B**). WT mice showed no insulin-reactive IgM at day 1.

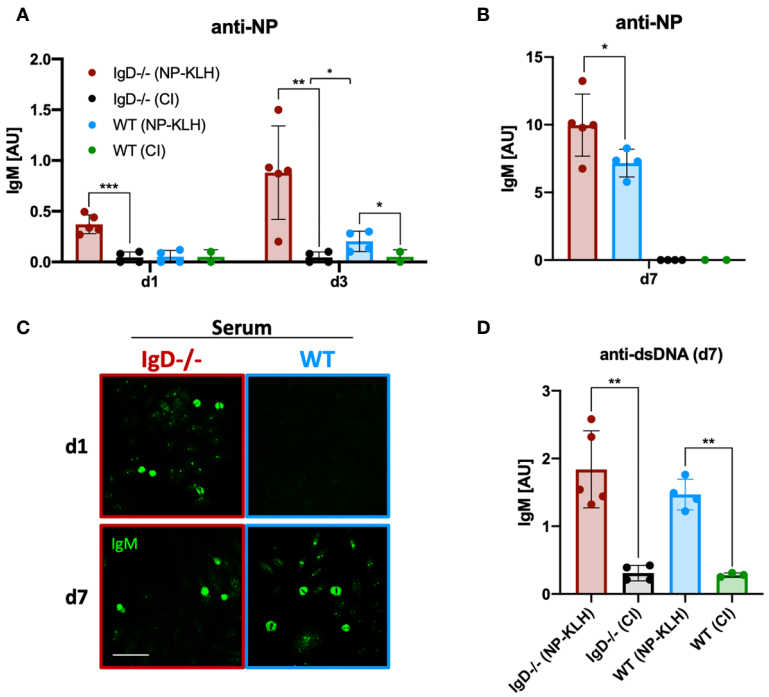


FIGURE 2 | IgD-deficient mice mount robust polyreactive IgM responses one day after immunization. **(A, B)** Serum immunoglobulin titers of NP-KLH (IgD-deficient n=5, WT n=4) and CpG ODN1826 (control immunization: CI, IgD-deficient n=4, WT n=2) injected mice measured by ELISA. NP-reactive IgM of day 1 and 3 **(A)** and day 7 **(B)**. Mean, ± SD, statistical significance was calculated by using Kruskal-Wallis-test. **(C)** Serum immunoglobulins reactive to self-molecules (DNA/RNA) of NP-KLH and CI injected IgD-deficient and WT mice tested *via* HEp2 slides. Fluorescence microscopy images are representative for three independent experiments. Scale bar: 10 µm. **(D)** Serum immunoglobulin titers of NP-KLH (IgD-deficient n=5, WT n=4) and CI injected (IgD-deficient n=4, WT n=2) mice measured by ELISA. dsDNA-reactive IgM of day 7 post immunization. Students t-tests with Welch's correction were used to compare two groups within one experiment. Mean, ± SD. *P < 0.05, **P < 0.01.

By day 7, WT mice showed anti-insulin IgM which, however, was reduced as compared to IgD-deficient mice (**Figure 3B**). By day 28 comparable amounts of insulin-reactive IgM were detected in both IgD-deficient and WT mice. However, only WT mice showed a considerable increase of insulin-specific IgG (**Figure 3B**, right panel). This IgG is responsible for the elevated blood glucose levels detected in these mice (see below).

Importantly, ELISpot analysis confirmed the increased number of anti-insulin antibody secreting cells in IgD-deficient mice at day 1 after immunization (**Supplementary Figure 4**).

To evaluate the polyreactive potential of the elicited anti-insulin IgM, we performed HEp-2 slides. The data show that anti-insulin IgM remained polyreactive throughout day 28 (boost on day 21), whereas the anti-insulin IgM of WT mice was no longer polyreactive (**Figure 3C**). Importantly, immunization with mixtures of InsA-KLH and soluble InsA peptide at 1:100, respectively, resulted in highly elevated blood glucose concentrations at day 1 and were therefore discontinued (see below, data not shown).

Together, our data suggest that IgD-deficient B cells elicit a rapid and strong primary immune response that persists for longer periods compared to WT mice. Thus, the shift into secondary, mature immune responses is delayed in IgD-deficient mice. Interestingly, IgD, which is a marker for mature B cells, is required for the transition of the immune response from primary to secondary phases.

Delayed Affinity Maturation Is Associated With Sustained Autoimmunity in IgD-Deficient Mice

Affinity maturation of antibody responses was reported to be delayed in IgD-deficient mice (14). To test this for self-molecules, we performed ELISA to determine the binding efficiency of the insulin-specific antibodies to high-valence or low-valence antigen. To this end, we used monovalent and polyvalent streptavidin and biotinylated InsA peptides to generate monovalent InsA(1) and polyvalent InsA(4) streptavidin complexes. Similar to previous reports (14, 22) an increased ratio of InsA(1)/InsA(4) indicates increased affinity. Our experiments revealed no significant increase of the affinity of insulin-reactive IgM antibodies between primary (d7) and secondary (d28) immunization for IgD-deficient mice. However, insulin-reactive IgM of WT mice showed a clear increase in InsA(1)/InsA(4) ratio which is characteristic for affinity maturation (**Figure 4A**). We confirmed these results by examining the direct binding affinity of insulin-specific IgM of different days from WT and IgD-deficient mice. Interferometric assays revealed that WT mice already reach high affinity insulin-IgM at day 52, whereas IgD-deficient mice do not reach a comparable level of affinity before day 72 (**Figure 4G**). Interestingly, both IgD-deficient mice and WT mice showed

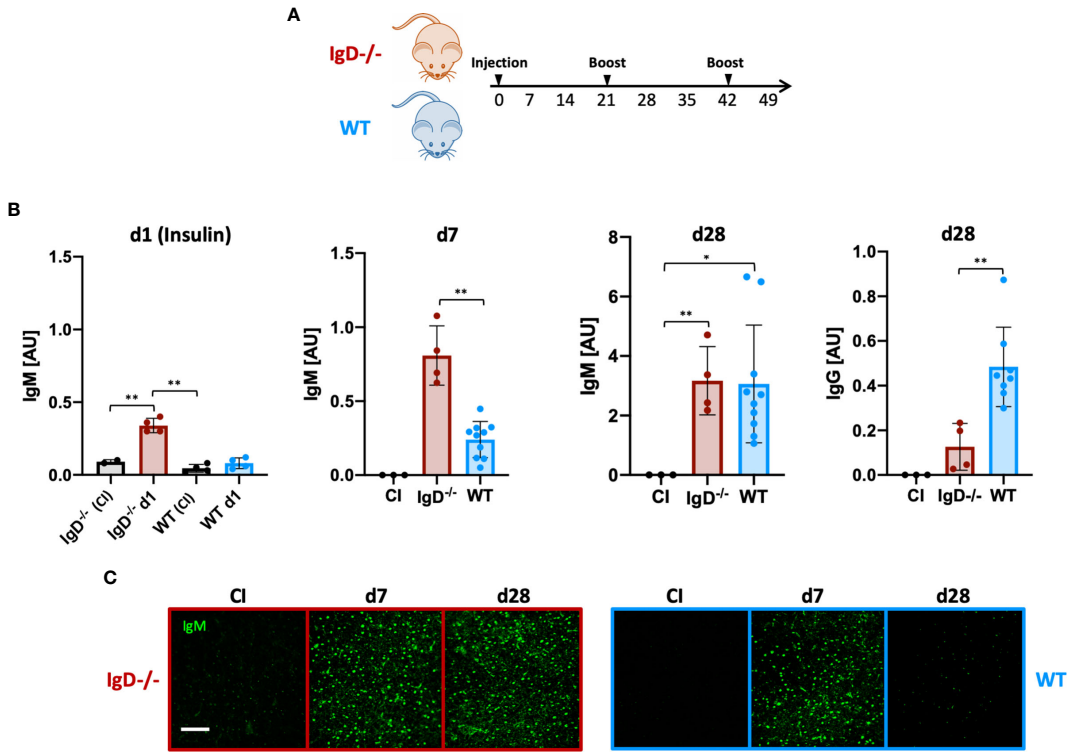


FIGURE 3 | The IgD-class BCR is required to prevent rapid immune response to autoantigens and induces affinity maturation. **(A)** Schematic immunization schedule of IgD-deficient and WT mice injected with InsA-KLH + CpG ODN1826 on day 0 and InsA-KLH on days 21 and 42. **(B)** Serum immunoglobulin titers reactive to native insulin of IgD-deficient (n=4) and WT (n=10) mice immunized with InsA-KLH or CI (n=3) measured by ELISA. Days are indicated in the figure. Mean, ± SD. Students t-tests with Welch's correction were used to compare two groups within one experiment. **(C)** Serum immunoglobulins reactive to self-molecules (DNA/RNA) of InsA-KLH and CI injected IgD-deficient (n=5/day) and WT (n=5/day) mice tested *via* HEp2 slides. Fluorescence microscopy images are representative of three independent experiments. Scale bar: 10 µm *P < 0.05, **P < 0.01.

clear signs of diabetes as detected by glucose amount in the urine and increased blood glucose levels. However, the symptoms of diabetes were more severe and evident already at day 1 in IgD-deficient mice as compared to WT mice (**Figures 4B, C**). Importantly, the increase in blood glucose concentrations in WT mice gradually declined after repeated boost immunizations and shortly after the second boost at day 42 the WT mice became resistant to InsA-induced diabetes (**Figure 4C**). IgD-deficient mice in contrast showed sustained diabetes symptoms throughout day 60 after immunization (**Figure 4C**). In fact, IgD-deficient mice required a third boost by day 70 to develop resistance to InsA-induced diabetes (**Supplementary Figures 5A, B**).

To show that high-affinity IgM generated during secondary booster immunizations is responsible for the control of diabetes induced by InsA immunization, we isolated insulin-specific IgM from WT mice after secondary immunization and injected it into IgD-deficient mice shortly after immunization with InsA-KLH. The results show that the isolated high-affinity IgM protected the IgD-deficient mice from developing diabetes at day 1 and therefore we refer to this IgM as protective IgM (PR-IgM) (**Figures 4D, E**). The underlying mechanism of PR-IgM generation and characterization is part of Amendt and Jumaa 2021 (*in press*). Similar to the above-mentioned results (**Figure 3D**) we performed indirect IF to confirm that affinity maturation resulted in PR-IgM which is highly specific for insulin without binding other autoantigens (**Figure 4F**).

These data show that defective affinity maturation in IgD-deficient mice (**Supplementary Figure 6**) leads to insufficient production of protective highly specific IgM thereby resulting in sustained autoimmune disorder.

Rapid Activation of IgD-Deficient B Cells After Immunization

To examine early changes on B cells after immunization, we performed FACS experiments to analyze lymphoid organs after immunization with InsA-KLH. This analysis revealed that immunization induced a substantial expansion of splenic B cells in IgD-deficient mice as compared to WT mice at day 1 (**Figure 5A**). Notably, the expansion of splenic B cells in IgD-deficient mice was associated with increased cell size, as shown by forward-scatter (FSC), in the IgD-deficient mice (**Figure 5A**). In full agreement, a considerable fraction (>21%) of B cells expressed the activation marker CD69 after immunization of IgD-deficient mice with InsA-KLH. Similar to control immunization of IgD-deficient mice with CpG alone, WT mice immunized with InsA-KLH or CpG alone showed a limited fraction (about 2-5%) of CD69 expressing cells (**Figure 5B**).

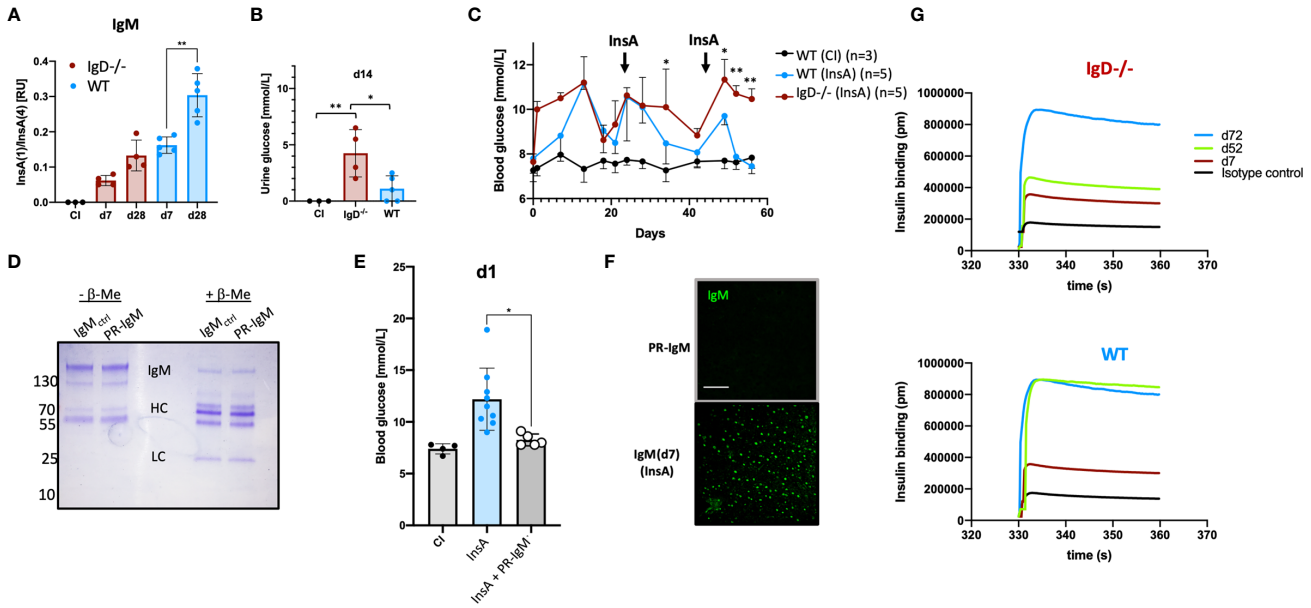


FIGURE 4 | The IgD-class BCR is required for affinity maturation of insulin-IgM to be protective and prevent autoimmune pathology. **(A)** Affinity of IgM to InsA peptides of InsA (InsA-KLH + CpG ODN1826) immunized IgD-deficient (n=4), WT (n=5) and Cl (n=3) mice measured by peptide-ratio ELISA (22).Plates were coated with Streptavidin bearing one [InsA(1)] or four [InsA(4)] biotin binding sites. Mean, ± SD, statistical significance was calculated by using repeated measure ANOVA-test. **(B)** Urine glucose values (mmol/L) measured by commercial urine stripes (Roche) of IgD-deficient (n=4) and WT (n=5) mice immunized with InsA-KLH or Cl (n=3). Mean, ± SD, statistical significance was calculated by using Kruskal-Wallis-test. **(C)** Blood glucose values (mmol/L) of IgD-deficient (n=4) and WT (n=5) mice immunized with InsA. Injections were done on day 0 (InsA-KLH + CpG ODN1826), day 21 (InsA-KLH), day 42 (InsA-KLH). Mean, ± SD, statistical significance was calculated by using repeated measure ANOVA-test comparing red and blue graphs. **(D)** Coomassie-stained SDS-PAGE showing reduced (+ β-ME) and non-reduced (- β-ME) IgM of clnsA and control immunized mice. Total serum IgM was isolated *via* HiTrap IgM columns (InsA d85 refers to PR-IgM). IgM monomer: 150 kD, IgM HC: 70 kD, IgM LC: 25 kD. **(E)** Blood glucose values (mmol/L) of IgD-deficient immunized with InsA-KLH (n=9), WT control immunized mice (n=4) and IgD-deficient mice immunized with InsA-KLH and injected with PR-IgM i.v. (n=5). Mean, ± SD, statistical significance was calculated by using Kruskal-Wallis-test. **(F)** Serum immunoglobulins reactive to self-molecules (DNA/RNA) of IgM (PR-IgM and day 7 primary IgM) isolated from InsA-KLH immunized mice tested *via* HEp2 slides. Fluorescence microscopy images are representative for three independent experiments. Scale bar: 10 µm. **(G)** Interferometric assay to determine the affinity of IgM to insulin. Insulin-specific isolated IgM of IgD-deficient (top panel) or WT (bottom panel) mice immunized with InsA. Affinity of IgM of different days is shown in pm. Graphs are representative of three independent experiments *P < 0.05, **P < 0.01.

Further characterization revealed that a population of CD23-/CD21- cells was increased in IgD-deficient mice immunized with InsA-KLH compared to immunized WT counterpart or IgD-deficient mice from control immunization (**Figure 5C**). The CD23-/CD21-cells correspond to activated B cells (**Supplementary Figures 7A–C**) which predominantly express IgM-class BCR and intermediate amounts of IgD in WT mice (**Figure 5D**). In particular, CD23 expression on B cells is greatly down-regulated in InsA-KLH immunized IgD-deficient mice on day 1 as compared to controls (**Figure 5E**). This is consistent with available data showing that CD23 is downregulated upon B cell activation (25).

Thus, our results suggest that IgD-deficient B cells are rapidly activated after immunization and that the responsive cells are CD23-/CD21- with elevated levels of IgM BCR expression.

Antibody Secretion by CD23-/CD21- Cells

Our recent data showed that CD23-/CD21- cells are antibody-secreting cells. Therefore, we investigated antibody secretion by splenocytes at day 1 after immunization. ELISpot analysis showed that the proportion of antibody-secreting cells is slightly increased in IgD-deficient mice when total splenic cells were used (**Figure 6A**). However, when ELISpot analysis was performed after FACS sorting for CD23-/CD21- cells or CD23+ follicular B cells, we found that antibody secretion was predominantly associated with CD23-/CD21- cells (**Figure 6B**). The increased proportion of the CD23-/CD21- in InsA-KLH immunized IgD-deficient mice was associated with increased proportion of antibody-secreting cells (**Figure 6B**). Interestingly, only a small fraction of follicular CD23+ B cells from WT mice developed into antibody-secreting cells and no effect of the immunization was observed at day 1 while IgD-deficient follicular CD23+ B cells showed an increase in antibody-secreting cells (**Figures 6C, D**). In order to further characterize the CD23-/CD21- B cell population, we performed FACS experiments. We found that these cells lack the typical markers for plasma cells (CD138) or B-1 B cells (CD43, CD11b). Interestingly, however, these cells showed highly increased MHC-class II expression suggesting that they are activated B cells (**Supplementary Figure 8**).

Interestingly, IgD-deficient B cells in peritoneal cavity further showed an increase of $CD138^{+}$ cells at day 1 after immunization, whereas WT counterparts remained unchanged (**Supplementary Figure 9**).

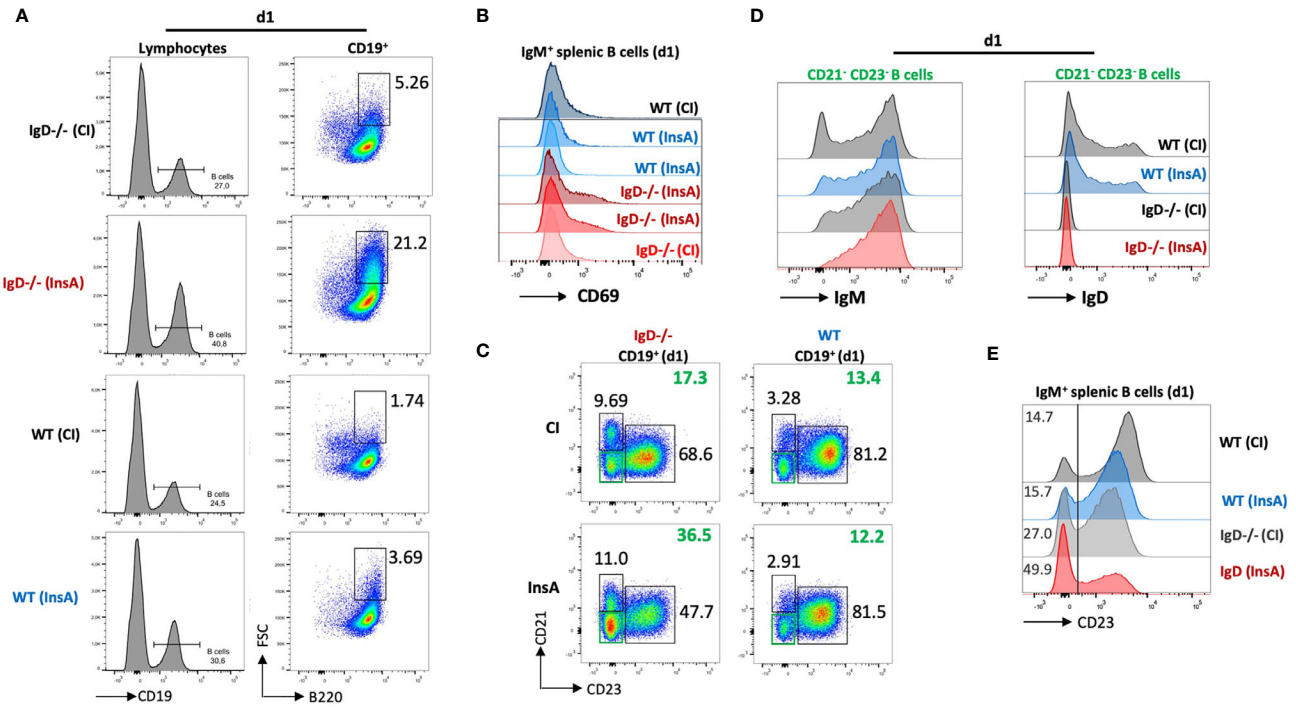


FIGURE 5 | The IgD-class BCR controls a rapidly responding CD21$^-$CD23$^-$ B cell population that is able to secrete autoantibodies 24 hours after immunization. **(A – E)** Flow cytometric analysis of IgD-deficient (n=4/group) and WT (n=4/group) mice immunized with InsA-KLH + CpG ODN1826 or CpG ODN1826 (Cl). All panels show representative plots pre-gated on lymphocytes (FSC/SSC), single cells (SSC-H/SSC-W) and viable cells (fixable viability dye, FVD$^-$). **(A)** Histogram of CD19 expression used to gate B cells (CD19$^+$) within lymphocyte gate (left). Enlarged (activated) IgM$^+$ B cells (FSC^{hi} B220$^+$) within B cell gate (right). **(B)** Histogram showing activated B cells by CD69 expression pre-gated on IgM$^+$ B cells. **(C)** Representative plot showing marginal zone B cells (CD21^{hi} CD23^{lo}), follicular B cells (CD21^{lo} CD23^{hi}) and CD21$^-$ CD23$^-$ (double negative) B cell population in InsA and Cl immunized IgD-deficient or WT mice. **(D)** Histograms of CD21$^-$CD23$^-$ B cells IgM expression (left) and IgD expression (right). **(E)** Histogram showing CD23 expression in IgM$^+$ splenic B cells.

In summary, these data suggest that immunization results in increased CD23-/CD21- antibody-secreting cells that develop within one day in IgD-deficient mice.

Primary Immune Responses Have Restricted Polyreactivity

The results presented above indicate that primary immune responses are autoreactive regardless of the utilized antigen. In fact, primary anti-NP- as well as primary anti-insulin-IgM showed nuclear staining in HEp-2 slides indicative of polyreactive behavior. In full agreement, the primary anti-NP-IgM also showed anti-dsDNA binding in ELISA experiments (**Figure 2D**). Subsequently, we tested the hypothesis whether primary IgM immune responses might always induce the same class of autoreactive B cells that might be omnipotent with regard to autoantigen binding. To this end, we tested whether the anti-NP primary immune response induces diabetes symptoms due to binding to insulin. However, despite the increased polyreactivity, neither IgD-deficient nor WT mice showed any changes in blood glucose levels in the course of NP immunization (**Figures 7A, C**). Further, InsA-KLH immunized WT and IgD-deficient mice showed an expected increase in blood glucose levels (**Figure 7C**). The primary IgM of these mice also showed significant polyreactivity, as determined by anti-dsDNA ELISA (**Figures 7B, D**). Nevertheless, no increased anti-insulin binding was observed in the sera of IgD-deficient or WT mice after NP immunization (**Figures 7E, G**, top). Vice versa, InsA-KLH immunized mice did not show increased NP binding (**Figures 7F, H**, bottom).

Together, these data suggest that, despite their increased autoreactivity to nuclear structures and dsDNA, primary IgM immune responses in IgD-deficient as well as in WT mice have no infinite polyreactivity. In conclusion, primary IgM responses appear to be broadly poly- and self-reactive, but still remain somehow specific for their cognate antigen.

DISCUSSION

In this study we investigated the importance of the IgD-class BCR expression for mature B cell function *in vivo*. Notably, the flexible hinge region in the HC enables IgD expressing B cells to distinguish between polyvalent complex form and monovalent soluble form of the same antigen (10, 11). This ability of IgD results in an unique control mechanism for B cell activation, in which the ratio of polyvalent to monovalent antigen determines B cell responsiveness. In fact, as monitored by calcium mobilization *in vitro*, polyvalent

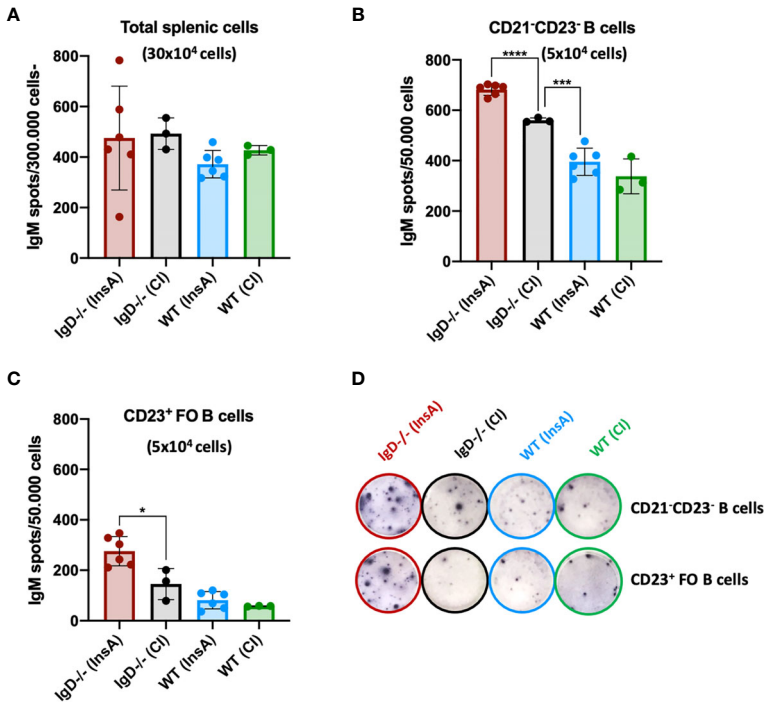


FIGURE 6 | The CD21⁻ CD23⁻ B cell population is the major source of IgM-secreting cells under the control of the IgD-class BCR. **(A–D)** ELISpot analyses showing IgM secreting splenic cells of InsA-KLH + CpG ODN1826 or control (CpG ODN1826) immunized (CI) mice 24 hours after injection. IgM secretion by **(A)** total splenic cells, **(B)** CD21⁻CD23⁻ sorted B cells, **(C)** CD23⁺ follicular B cells, **(D)** representative images of ELISpot wells of indicated cell numbers, genotypes and immunizations. Two independent experiments with n=3/group for CI and n=6/group for InsA-KLH were performed. Mean, ± SD, students t-tests with Welch's correction was used to compare two groups within one experiment. *P < 0.05, ***P < 0.001, ****P < 0.0001.

antigen activates signaling in IgD expressing cells while monovalent antigen interferes with this responsiveness (10, 11, 14, 19, 26).

To investigate the importance of the unique IgD function *in vivo*, we determined the antibody immune response to monovalent or polyvalent forms of an hapten or a disease-relevant antigen (insulin) in wildtype as compared to IgD-deficient mice (10, 12, 27).

The results show that monovalent antigen suppresses IgG antibody production triggered by cognate polyvalent antigen in IgD expressing cells regardless of whether the antigen belongs to self or non-self. In the absence of IgD, soluble antigen cannot alter the IgG antibody response while an immediate production of primary antigen-reactive IgM antibody response is triggered and maintained for extended times as compared with IgD expressing cells in WT mice. This phenomenon might have crucial consequences for IgG antibody responses against autoantigens which could be present in complexes as a result of cell death, protein turnover or interaction with foreign structures. Since autoreactive IgG is a hallmark of autoimmune diseases, our data suggest the presence of IgD together with an excess of soluble monovalent form of the same antigen interferes with the activation of autoreactive IgG antibody secretion. Because the antibody secreting cells described in this study lack typical B1-B cell markers, the contribution of B1-B cells to the deregulation of primary responses in IgD-deficient mice is unclear. However, the reduced IgD-class BCR expression detected on B1-B cells suggests that these cells are prone to the induction of rapid primary immune responses targeting self and non-self which is in agreement with available data (28–30).

Interestingly, IgD expression is also required for efficient activation of memory responses as indicated by the decreased IgG responses to NP and InsA in IgD-deficient mice compared to wildtype controls. Thus, IgD is required for both triggering an efficient memory immune response and at the same time for avoiding such immune responses if the activating antigen is self, which is distinguished as mainly monovalent non-complex antigen. Given that the generation of long-lasting antibody memory responses, which are not self-destructive, is essential for effective immune protection and that IgD is required for these processes, it can be concluded that IgD is a key regulator for balanced antibody responses. This is in full agreement with previous results suggesting that IgD is required for acceleration of affinity maturation in early phases of the immune response (14). Moreover, the suggested role of IgD in affinity maturation corresponds to the prolonged phase of primary IgM antibody response in IgD-deficient mice. Remarkably, this primary IgM is autoreactive and might lead to prolonged autoimmune damage as in the case of insulin-derived peptides. Thus, another important characteristic of IgD function is limiting the duration of autoreactive primary IgM responses by accelerating the generation of highly specific IgM that protects autoantigen

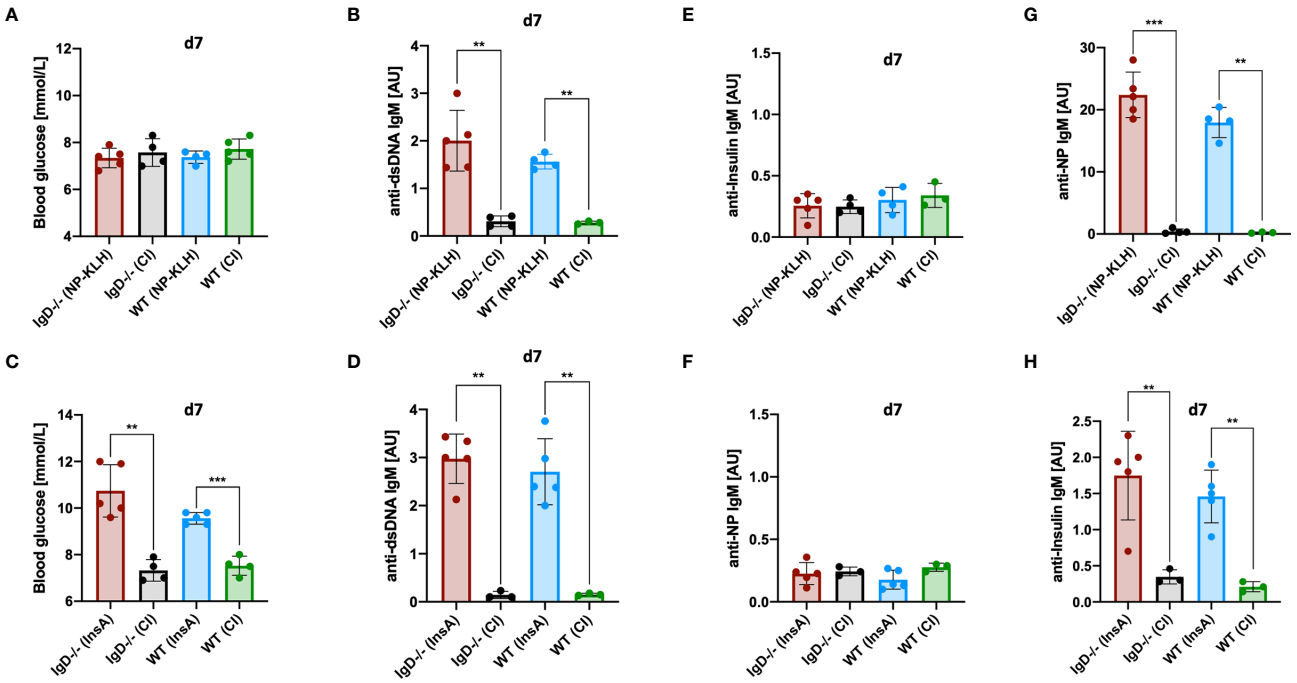


FIGURE 7 | Primary IgM is antigen-specific and polyreactive but not cross-reactive. **(A, C)** Blood glucose levels (mmol/L) of IgD-deficient and WT mice immunized with NP-KLH + CpG and controls (CpG-ODN1826) **(A)**, or immunized with InsA-KLH + CpG and controls **(C)**. Mean, ± SD, statistical analysis was done by using Kruskal-Wallis-test. **(B, D)** Serum immunoglobulin titers of IgD-deficient and WT mice immunized with either NP-KLH + CpG and controls **(B)** or InsA-KLH + CpG and controls **(D)** reactive to dsDNA measured by ELISA. Mean, ± SD, statistical analysis was done by using Kruskal-Wallis-test. **(E–H)** Serum immunoglobulin titers of IgD-deficient and WT mice immunized with either NP-KLH + CpG or InsA-KLH + CpG and controls reactive to Insulin (top panel) or InsA-KLH + CpG and controls immunized mice reactive to NP (bottom) **(E, F)** and reactive to NP or Insulin **(G, H)** measured by ELISA. Mean, ± SD, statistical analysis was done by using Kruskal-Wallis-test $^{**}P < 0.01$, $^{***}P < 0.001$.

from autoimmune destruction. In fact, the generation of protective memory IgM is delayed in the IgD-deficient mice.

Interestingly, IgD has been associated with the control of autoimmunity and quiescence of autoreactive B cells, as IgD BCR was suggested to be less sensitive than IgM BCR to endogenous antigen (31, 32). However, the underlying mechanism for this control of autoreactive B cells remained unclear.

Our results suggest that IgD BCR regulates the responsiveness and antibody secretion *in vivo* by sensing antigen-valency regardless of whether the antigen belongs to self or non-self. An excess of monovalent antigen relative to polyvalent antigen interferes with IgG production and activates the generation of high affinity IgM antibodies by triggering IgD expressing mature B cells. An excess of polyvalent antigen leads to efficient IgG memory responses by activated mature B cells. The result is fine-tuned sensing of antigen forms and consequent regulation of the dynamics of B cell activation and antibody responses. This is defective in IgD-deficient B cells which are immediately activated already at day 1 after immunization suggesting that the presence of IgD prevents deregulated activation of B cells. This is in agreement with recent data showing that the IgD-class BCR is required for maintaining the organization of signaling complexes in distinct nanoclusters at the cell surface (21, 33). This organization keeps naïve B cells in a resting state, in which stimulatory co-receptors are confined in the IgD BCR nanoclusters and thus away from IgM BCR, which seems to trigger robust cell activation when associated with the stimulatory molecules. If this organization is disrupted, which usually occurs upon antigen binding, the stimulatory co-receptors traffic into the IgM nanoclusters resulting in B cell activation (21, 33). It is likely that IgD-deficient B cells have disrupted organization of nanoclusters as stimulatory co-receptors cannot be confined to IgD nanoclusters and may thus easily associate with IgM resulting in accelerated activation of IgD-deficient B cells. It was recently reported that IgM and IgD-class BCR play opposing roles in B cell survival and that the IgD-class BCR negatively affects B cell activation and differentiation (34). Here, we show that the IgD-class BCR prevents rapid B cell activation and IgM antibody secretion, which is in agreement with the notion that IgD is likely a negative regulator of B cell activation. Furthermore, available data suggest an important role of IgD for CXCR4 function, a chemokine receptor required for germinal center function and thus affinity maturation (35). These data support the uniqueness of the IgD-class BCR and underline the importance of nanocluster organization for the negative regulatory role of IgD (35). In fact, IgD-deficient B cells might have a lower threshold for activation as the confinement in the regulatory IgD clusters is

blocked. This is in agreement with available data suggesting that IgM BCR, but not IgD, is required for the survival of transformed B cells (36).

Other studies proposed that the IgM-class BCR induces functional unresponsiveness (so-called anergy), while the IgD-class BCR attenuates this anergy reaction (37). This anergy reaction was associated with the induction of transcription factors such as EGR1/EGR2 (37). However, the induction of EGR1/EGR2 was assigned to anergy and not to IgD expression. Moreover, the IgD-deficient B cells expressing only IgM were proposed to be prone to rapid anergy when encountering self-antigen, as the lack of IgD-class BCR prevents the proposed attenuation of anergy and leads to irreversible unresponsiveness. Consequently, IgD-deficient mice should not be able to mount any autoantibody responses. In contrast, our study shows that the absence of the IgD-class BCR leads to rapid and uncontrolled autoantibody responses when encountering autoantigen complexes suggesting a repressive role for IgD.

Importantly, we have recently shown that the responsiveness of B cells is regulated by unique features of the IgD-class BCR being responsive to polyvalent antigen while being regulated by monovalent antigen (10, 11).

In addition to the role of IgD in controlling B cell activation and proliferation, cells lacking IgD can produce primary IgM but are defective in the generation of protective high affinity IgM. This defect might lead to the production of autoreactive IgG and autoimmune diseases such as systemic lupus erythematosus (SLE) (38–41), Sjögren syndrome (39, 42–44) or inflammatory myopathy (45, 46) which are characterized by autoreactive IgG antibodies recognizing DNA or nuclear structures. The defective generation of high affinity protective IgM by IgD-deficient cells is in agreement with previous data showing that mice deficient for secreted IgM (sIgM) are prone to autoimmunity (47–50). Notably, sIgM-deficient mice developed high titers of anti-dsDNA-IgG in young age (47–50).

In contrast to IgG, IgM expressing B cells recognizing DNA or nuclear structures seem to be abundant in the naïve B cell repertoire resulting in primary responses that are polyreactive. Remarkably, this polyreactivity is partial as both antigens used in this study, NP-KLH and InsA-KLH, led to primary IgM reactive to dsDNA and nuclear structures but lacked reactivity to the respective other antigen. It is conceivable that the partial polyreactivity of primary IgM antibodies is not random and is rather required as part of an efficient primary immune response, in which reactivity with common autoantigens facilitates the generation of immune complexes that are required for the activation of efficient secondary antibody responses. However, a defect in the production of protective IgM or a deregulated switch to IgG can convert the important property of complex formation into an autoimmune disease. Prior studies using pentameric IgM Fc-receptor (FCMR) deficient mice (51, 52) further underline the importance of IgM in initiating powerful secondary responses. In particular, these mice show increased formation of germinal centers, increased plasma cell differentiation and increased autoantibody production, which is in line with the proposed role for primary IgM in our study (51–53).

In summary, our findings suggest that IgD is required for controlling the duration of primary autoreactive IgM production and to control the maturation of secondary antibody responses. For foreign antigens, this maturation results in efficient generation of IgG memory responses. For autoantigens, IgD-mediated maturation of antibody responses leads to efficient generation of high affinity IgM autoantibodies that protect autoantigens. Thus, defective IgD function results in deregulated activation of B cells and may well lead to defective immune responses, autoimmune diseases or uncontrolled proliferation.

DATA AVAILABILITY STATEMENT

The original contributions presented in the study are included in the article/**Supplementary Material**. Further inquiries can be directed to the corresponding author.

ETHICS STATEMENT

The animal study was reviewed and approved by Regierungspräsidium Tübingen (license 1484), Baden-Württemberg, Germany.

AUTHOR CONTRIBUTIONS

TA and OA planned, performed and analyzed experiments, interpreted data, and contributed to writing of the manuscript. AL performed and analyzed FACS experiments. GA, MY, and CS performed ELISA experiments. HJ designed the experiments, wrote the manuscript, and supervised the study. All authors contributed to the article and approved the submitted version.

FUNDING

This work was supported by the DFG through TRR130 (B cells and beyond) project 01, SFB1074 (Experimental Models and Clinical Translation in Leukemia), SFB 1279 (Exploration of the Human Peptidome), and ERC advanced grant (694992), DFG single grant, JU 463/5-1.

SUPPLEMENTARY MATERIAL

The Supplementary Material for this article can be found online at: https://www.frontiersin.org/articles/10.3389/fimmu.2021.709240/full#supplementary-material

REFERENCES

1. Nemazee DA, Bürki K. Clonal Deletion of B Lymphocytes in a Transgenic Mouse Bearing Anti-MHC Class I Antibody Genes. *Nature* (1989) 337:562–6. doi: 10.1038/337562a0
2. Nemazee D, Buerki K. Clonal Deletion of Autoreactive B Lymphocytes in Bone Marrow Chimeras. *Proc Natl Acad Sci USA* (1989) 86:8039–43. doi: 10.1073/pnas.86.20.8039
3. Nossal GJV, Pike BL. Clonal Anergy: Persistence in Tolerant Mice of Antigen-Binding B Lymphocytes Incapable of Responding to Antigen or Mitogen. *Proc Natl Acad Sci USA* (1980) 77:1602–6. doi: 10.1073/pnas.77.3.1602
4. Wardemann H, Yurasov S, Schaefer A, Young JW, Meffre E, Nussenzweig MC. Predominant Autoantibody Production by Early Human B Cell Precursors. *Sci (80-.)* (2003) 301:1374–7. doi: 10.1126/science.1086907
5. Goodnow CC, Crosbie J, Adelstein S, Lavoie TB, Smith-Gill SJ, Brink RA, et al. Altered Immunoglobulin Expression and Functional Silencing of Self-Reactive B Lymphocytes in Transgenic Mice. *Nature* (1988) 334:676–82. doi: 10.1038/334676a0
6. Goodnow CC, Crosbie J, Jorgensen H, Brink RA, Basten A. Induction of Self-Tolerance in Mature Peripheral B Lymphocytes. *Nature* (1989) 342:385–91. doi: 10.1038/342385a0
7. du Pré MF, Blazevski J, Dewan AE, Stamnaes J, Kanduri C, Sandve GK, et al. B Cell Tolerance and Antibody Production to the Celiac Disease Autoantigen Transglutaminase 2. *J Exp Med* (2020) 217(2):e20190860. doi: 10.1084/jem.20190860
8. Suurmond J, Diamond B. Autoantibodies in Systemic Autoimmune Diseases: Specificity and Pathogenicity. *J Clin Invest* (2015) 125:2194–202. doi: 10.1172/JCI78084
9. Ludwig RJ, Vanhoorelbeke K, Leypoldt F, Kaya Z, Bieber K, McLachlan SM, et al. Mechanisms of Autoantibody-Induced Pathology. *Front Immunol* (2017) 8:603. doi: 10.3389/fimmu.2017.00603
10. Übelhart R, Hug E, Bach MP, Wossning T, Dühren-von Minden M, Horn AH, et al. Responsiveness of B Cells is Regulated by the Hinge Region of IgD. *Nat Immunol* (2015) 16:534–43. doi: 10.1038/ni.3141
11. Setz CS, Khadour A, Renna V, Iype J, Gentner E, He X, et al. Pten Controls B-Cell Responsiveness and Germinal Center Reaction by Regulating the Expression of IgD BCR. *EMBO J* (2019) 38(11):e100249. doi: 10.15252/embj.2018100249
12. Nitschke L, Kosco MH, Kohler G, Lamers MC. Immunoglobulin D-Deficient Mice can Mount Normal Immune Responses to Thymus-Independent and -Dependent Antigens. *Proc Natl Acad Sci USA* (1993) 90:1887–91. doi: 10.1073/pnas.90.5.1887
13. Brink R, Goodnow CC, Crosbie J, Adams E, Eris J, Mason DY, et al. Immunoglobulin M and D Antigen Receptors are Both Capable of Mediating B Lymphocyte Activation, Deletion, or Anergy After Interaction With Specific Antigen. *J Exp Med* (1992) 176:991–1005. doi: 10.1084/jem.176.4.991
14. Roes J, Rajewsky K, Immunoglobulin D. (IgD)-Deficient Mice Reveal an Auxiliary Receptor Function for IgD in Antigen-Mediated Recruitment of B Cells. *J Exp Med* (1993) 177:45–55. doi: 10.1084/jem.177.1.45
15. Geisberger R, Lamers M, Achatz G. The Riddle of the Dual Expression of IgM and IgD. *Immunology* (2006) 118:429–37. doi: 10.1111/j.1365-2567.2006.02386.x
16. Josephs SH, Buckley RH. Serum IgD Concentrations in Normal Infants, Children, and Adults and in Patients With Elevated IgE. *J Pediatr* (1980) 96:417–20. doi: 10.1016/S0022-3476(80)80684-6
17. Shan M, Carrillo J, Yeste A, Gutzeit C, Segura-Garzón D, Walland AC, et al. Secreted IgD Amplifies Humoral T Helper 2 Cell Responses by Binding Basophils *via* Galectin-9 and CD44. *Immunity* (2018) 49:709–724.e8. doi: 10.1016/j.immuni.2018.08.013
18. Hobeika E, Maity PC, Jumaa H. Control of B Cell Responsiveness by Isotype and Structural Elements of the Antigen Receptor. *Trends Immunol* (2016) 37:310–20. doi: 10.1016/j.it.2016.03.004
19. Gutzeit C, Chen K, Cerutti A. The Enigmatic Function of IgD: Some Answers at Last. *Eur J Immunol* (2018) 48:1101–13. doi: 10.1002/eji.201646547
20. Yang J, Reth M. Oligomeric Organization of the B-Cell Antigen Receptor on Resting Cells. *Nature* (2010) 467:465–9. doi: 10.1038/nature09357
21. Maity PC, Blount A, Jumaa H, Ronneberger O, Lillemeier BF, Reth M, et al. B Cell Antigen Receptors of the IgM and IgD Classes are Clustered in Different Protein Islands That are Altered During B Cell Activation. *Sci Signal* (2015) 8 (394):ra93. doi: 10.1126/scisignal.2005887
22. Shimizu T, Kozono Y, Kozono H, Oda M, Azuma T. Affinity Maturation of Secreted IgM Pentamers on B Cells. *Int Immunol* (2004) 16:675–84. doi: 10.1093/intimm/dxh069
23. Reverberi R, Reverberi L. Factors Affecting the Antigen-Antibody Reaction. *Blood Transfus* (2007) 5:227–40. doi: 10.2450/2007.0047-07
24. Padoa CJ, Crowther NJ, Thomas JW, Hall TR, Bekris LM, Torn C, et al. Epitope Analysis of Insulin Autoantibodies Using Recombinant Fab. *Clin Exp Immunol* (2005) 140:564–71. doi: 10.1111/j.1365-2249.2005.02802.x
25. Liu C, Richard K, Wiggins M, Zhu X, Conrad DH, Song W, et al. CD23 can Negatively Regulate B-Cell Receptor Signaling. *Sci Rep* (2016) 6:1–8. doi: 10.1038/srep25629
26. Thi Cuc B, Pohar J, Fillatreau S. Understanding Regulatory B Cells in Autoimmune Diseases: The Case of Multiple Sclerosis. *Curr Opin Immunol* (2019) 61:26–32. doi: 10.1016/j.coi.2019.07.007
27. Kim YM, Pan JY, Korbel GA, Peperzak V, Boes M, Ploegh HL, et al. Monovalent Ligation of the B Cell Receptor Induces Receptor Activation But Fails to Promote Antigen Presentation. *Proc Natl Acad Sci USA* (2006) 103:3327–32. doi: 10.1073/pnas.0511315103
28. Baumgarth N. A Hard(y) Look at B-1 Cell Development and Function. *J Immunol* (2017) 199:3387–94. doi: 10.4049/jimmunol.1700943
29. Holodick NE, Vizconde T, Hopkins TJ, Rothstein TL. Age-Related Decline in Natural IgM Function: Diversification and Selection of the B-1a Cell Pool With Age. *J Immunol* (2016) 196:4348–57. doi: 10.4049/jimmunol.1600073
30. Lobo PI. Role of Natural Autoantibodies and Natural IgM Anti-Leucocyte Autoantibodies in Health and Disease. *Front Immunol* (2016) 7:198. doi: 10.3389/fimmu.2016.00198
31. Zikherman J, Parameswaran R, Weiss A. Endogenous Antigen Tunes the Responsiveness of Naive B Cells But Not T Cells. *Nature* (2012) 489:160–4. doi: 10.1038/nature11311
32. IgM and IgD B Cell Receptors Differentially Respond to Endogenous Antigens and Control B Cell Fate. *eLife*. doi: 10.7554/eLife.35074
33. Kläsener K, Jellusova J, Andrieux G, Salzer U, Böhler C, Steiner SN, et al. CD20 as a Gatekeeper of the Resting Stage of Human B Cells. *bioRxiv* (2020) 118:2020.07.31. doi: 10.1073/pnas.2021342118
34. Yasuda S, Sun J, Zhou Y, Wang Y, Lu Q, Yamamura M, et al. Opposing Roles of IgM and IgD in BCR-Induced B-Cell Survival. *Genes to Cells* (2018) 23:868–79. doi: 10.1111/gtc.12635
35. Becker M, Hobeika E, Jumaa H, Reth M, Maity PC. CXCR4 Signaling and Function Require the Expression of the IgD-Class B-Cell Antigen Receptor. *Proc Natl Acad Sci USA* (2017) 114:5231–6. doi: 10.1073/pnas.1621512114
36. ten Hacken E, Sivina M, Kim E, O'Brien S, Wierda WG, Ferrajoli A, et al. Functional Differences Between IgM and IgD Signaling in Chronic Lymphocytic Leukemia. *J Immunol* (2016) 197:2522–31. doi: 10.4049/jimmunol.1600915
37. Sabouri Z, Perotti S, Spierings E, Humburg P, Yabas M, Bergmann H, et al. IgD Attenuates the IgM-Induced Anergy Response in Transitional and Mature B Cells. *Nat Commun* (2016) 7:1–11. doi: 10.1038/ncomms13381
38. Eisenberg RA, Tan EM, Dixon FJ. Presence of Anti-Sm Reactivity in Autoimmune Mouse Strains*. *J Exp Med* (1978) 147:582–7. doi: 10.1084/jem.147.2.582
39. Tan EM. Antinuclear Antibodies: Diagnostic Markers for Autoimmune Diseases and Probes for Cell Biology. *Adv Immunol* (1989) 44:93–151. doi: 10.1016/S0065-2776(08)60641-0
40. Kaul A, Gordon C, Crow MK, Touma Z, Urowitz MB, van Vollenhoven R, et al. Systemic Lupus Erythematosus. *Nat Rev Dis Prim* (2016) 2:16039. doi: 10.1038/nrdp.2016.39
41. Pathak S, Mohan C. Cellular and Molecular Pathogenesis of Systemic Lupus Erythematosus: Lessons From Animal Models. *Arthritis Res Ther* (2011) 13(5):241. doi: 10.1186/ar3465
42. Jonsson R, Gordon TP, Konttinen YT. Recent Advances in Understanding Molecular Mechanisms in the Pathogenesis and Antibody Profile of Sjögren's Syndrome. *Curr Rheumatol Rep* (2003) 5:311–6. doi: 10.1007/s11926-003-0010-z
43. Nikolov NP, Illei GG. Pathogenesis of Sjögren's Syndrome. *Curr Opin Rheumatol* (2009) 21:465–70. doi: 10.1097/BOR.0b013e32832eba21
44. Cooper GS, Stroehla BC. The Epidemiology of Autoimmune Diseases. *Autoimmun Rev* (2003) 2:119–25. doi: 10.1016/S1568-9972(03)00006-5

45. Stuhlmüller B, Schneider U, González-González JB, Feist E. Disease Specific Autoantibodies in Idiopathic Inflammatory Myopathies. *Front Neurol* (2019) 10:438. doi: 10.3389/fneur.2019.00438
46. Mimori T, Imura Y, Nakashima R, Yoshifuji H. Autoantibodies in Idiopathic Inflammatory Myopathy: An Update on Clinical and Pathophysiological Significance. *Curr Opin Rheumatol* (2007) 19:523–9. doi: 10.1097/BOR.0b013e3282f01a8c
47. Boes M. Role of Natural and Immune IgM Antibodies in Immune Responses. *Mol Immunol* (2000) 37:1141–9. doi: 10.1016/S0161-5890(01)00025-6
48. Boes M, Esau C, Fischer MB, Schmidt T, Carroll M, Chen J. Enhanced B-1 Cell Development, But Impaired IgG Antibody Responses in Mice Deficient in Secreted IgM. *J Immunol* (1998) 160:4776–87.
49. Boes M, Schmidt T, Linkemann K, Beaudette BC, Marshak-Rothstein A, Chen J. Accelerated Development of IgG Autoantibodies and Autoimmune Disease in the Absence of Secreted IgM. *Proc Natl Acad Sci USA* (2000) 97:1184–9. doi: 10.1073/pnas.97.3.1184
50. Ehrenstein MR, Cook HT, Neuberger MS. Deficiency in Serum Immunoglobulin (Ig)M Predisposes to Development of IgG Autoantibodies. *J Exp Med* (2000) 191:1253–7. doi: 10.1084/jem.191.7.1253
51. Choi S-C, Wang H, Tian L, Murakami Y, Shin DM, Borrego F, et al. Mouse IgM Fc Receptor, FCMR, Promotes B Cell Development and Modulates Antigen-Driven Immune Responses. *J Immunol* (2013) 190:987–96. doi: 10.4049/jimmunol.1202227
52. Nguyen TTT, et al. The IgM Receptor Fcμr Limits Tonic BCR Signaling by Regulating Expression of the IgM BCR. *Nat Immunol* (2017) 18:321–33. doi: 10.1038/ni.3677
53. Wang H, Coligan JE, Morse HC. Emerging Functions of Natural IgM and its Fc Receptor FCMR in Immune Homeostasis. *Front Immunol* (2016) 7:1–7. doi: 10.3389/fimmu.2016.00099

Conflict of Interest: The authors declare that the research was conducted in the absence of any commercial or financial relationships that could be construed as a potential conflict of interest.

Publisher's Note: All claims expressed in this article are solely those of the authors and do not necessarily represent those of their affiliated organizations, or those of the publisher, the editors and the reviewers. Any product that may be evaluated in this article, or claim that may be made by its manufacturer, is not guaranteed or endorsed by the publisher.

Copyright © 2021 Amendt, Ayoubi, Linder, Allies, Young, Setz and Jumaa. This is an open-access article distributed under the terms of the Creative Commons Attribution License (CC BY). The use, distribution or reproduction in other forums is permitted, provided the original author(s) and the copyright owner(s) are credited and that the original publication in this journal is cited, in accordance with accepted academic practice. No use, distribution or reproduction is permitted which does not comply with these terms.

Autoreactive antibodies control blood glucose by regulating insulin homeostasis

Timm Amendt[a], Gabriele Allies[a], Antonella Nicolò[a], Omar El Ayoubi[a], Marc Young[a], Tamás Röszer[b], Corinna S. Setz[a], Klaus Warnatz[c], and Hassan Jumaa[a,1]

[a]Institute of Immunology, Ulm University Medical Center, 89081 Ulm, Germany; [b]Institute of Neurobiology, Ulm University, 89081 Ulm, Germany; and [c]Center for Chronic Immunodeficiency, University Hospital Freiburg, Albert-Ludwigs-Universität Freiburg, 79104 Freiburg, Germany

Edited by Michael Reth, Institute of Biology III, Faculty of Biology, Albert-Ludwigs-Universitat Freiburg, Freiburg, Germany; received August 25, 2021; accepted December 23, 2021

Homeostasis of metabolism by hormone production is crucial for maintaining physiological integrity, as disbalance can cause severe metabolic disorders such as diabetes mellitus. Here, we show that antibody-deficient mice and immunodeficiency patients have subphysiological blood glucose concentrations. Restoring blood glucose physiology required total IgG injections and insulin-specific IgG antibodies detected in total IgG preparations and in the serum of healthy individuals. In addition to the insulin-neutralizing anti-insulin IgG, we identified two fractions of anti-insulin IgM in the serum of healthy individuals. These autoreactive IgM fractions differ in their affinity to insulin. Interestingly, the low-affinity IgM fraction (anti-insulin IgM^{low}) neutralizes insulin and leads to increased blood glucose, whereas the high-affinity IgM fraction (anti-insulin IgM^{high}) protects insulin from neutralization by anti-insulin IgG, thereby preventing blood glucose dysregulation. To demonstrate that anti-insulin IgM^{high} acts as a protector of insulin and counteracts insulin neutralization by anti-insulin IgG, we expressed the variable regions of a high-affinity anti-insulin antibody as IgG and IgM. Remarkably, the recombinant anti-insulin IgM^{high} normalized insulin function and prevented IgG-mediated insulin neutralization. These results suggest that autoreactive antibodies recognizing insulin are key regulators of blood glucose and metabolism, as they control the concentration of insulin in the blood. Moreover, our data suggest that preventing autoimmune damage and maintaining physiological homeostasis requires adaptive tolerance mechanisms generating high-affinity autoreactive IgM antibodies during memory responses.

B cells | autoimmunity | IgM | IgG | aging

Maintaining homeostasis is a complex interplay of the hormone system, immune system, and metabolism (1, 2). B cells and antibody-secreting plasma cells are fundamentally involved in immunity, as they are able to recognize an enormous number of epitopes due to random rearrangement of variable (V), diversity (D), and joining (J) gene segments (3, 4). B cells originate from hematopoietic stem cells in the bone marrow, where, in early stages, two IgM-heavy chains and two surrogate light chains form the pre–B cell receptor (pre-BCR) (5). Autoreactive specificities are believed to be subjected to removal by clonal deletion or receptor editing (6–8). Immature B cells expressing an IgM-class B cell antigen receptor (IgM–BCR) leave the bone marrow and home to the spleen, where they mature further (9). The maturation of B cells in the periphery includes downmodulation of IgM and up-regulation of the IgD-class BCR (10–13). Recently, our group has shown that the IgD-class BCR is exclusively responsive to polyvalent antigen (10) and that the modulation of IgG responses via soluble (auto)-antigens in vivo also occurs in an IgD-dependent manner (14). Furthermore, mice as well as humans harbor a large number of autoreactive IgD^{+} B cells (15, 16) of which the function remains unclear.

Autoreactive B cells and plasma cells that secrete autoantibodies of the IgG isotype might cause autoimmune diseases such as systemic lupus erythematosus (17), type 1 diabetes (T1D) (18), or rheumatoid arthritis (19–21). Here, autoreactive IgG is capable of neutralizing its autoantigen or opsonizing it for further degradation or destruction by the innate immune system (22). Furthermore, autoantibody-containing immune complexes are able to induce inflammation (23, 24). Another class of autoreactive antibodies is represented by polyreactive natural IgM (nIgM) that has been extensively studied (25, 26). nIgM is secreted by B1-B cells and known to clear oxidized lipids and other potentially harmful self-molecules (27). Thus, nIgM is able to suppress sterile inflammation and therefore required to be secreted in an antigen-encounter–independent fashion (25, 26). In sum, autoreactive IgG and IgM are known to remove self-targets, and disease outbreak is dependent on the isotype present.

In mice, we recently identified an autoreactive IgM class that is able to bind and stabilize its cognate antigen. We refer to this class of autoreactive IgM as protective regulatory IgM (PR-IgM) (28). A key characteristic of PR-IgM is high affinity and monospecificity to its antigen. PR-IgM is induced in the course of autoreactive immune responses and results in the protection of cognate autoantigen from degradation or uptake by macrophages. We refer to this phenomenon as adaptive tolerance. However, the presence of PR-IgM in humans is yet unclear.

Significance

The random nature of antibody repertoire generation includes the potential of producing autoantibodies recognizing self-structures. It is believed that establishing immunological tolerance and prevention of autoimmune diseases require the removal of antibody specificities recognizing self. Using insulin as a common and physiologically important autoantigen, we show that anti-insulin antibodies associated with autoimmune diabetes can readily be detected in mice and humans and are involved in the physiological regulation of blood glucose levels. Importantly, human high-affinity, anti-insulin IgM antibodies protect insulin from autoimmune degradation by anti-insulin IgG antibodies. Thus, in contrast to the proposed negative selection, self-recognition and the production of highly autoreactive IgM antibodies are important for tolerance induction.

Author contributions: H.J. designed research; T.A., G.A., A.N., O.E.A., M.Y., T.R., C.S.S., and K.W. performed research; K.W. contributed new reagents/analytic tools; T.A. analyzed data; and T.A. and H.J. wrote the paper.

Competing interest statement: T.A., M.Y., and H.J. have filed patent applications for the use of protective-regulatory insulin antibodies.

This article is a PNAS Direct Submission.

This open access article is distributed under Creative Commons Attribution-NonCommercial-NoDerivatives License 4.0 (CC BY-NC-ND).

[1]To whom correspondence may be addressed. Email: hassan.jumaa@uni-ulm.de.

This article contains supporting information online at http://www.pnas.org/lookup/suppl/doi:10.1073/pnas.2115695119/-/DCSupplemental.

Published February 7, 2022.

Downloaded by guest on February 7, 2022

Here, we show that PR-IgM specific for insulin accumulates with age in humans and is able to stabilize insulin in vivo. Furthermore, we show that autoreactive IgG in humans and mice is involved in the fine-tuning of metabolic homeostasis by regulating physiological insulin concentrations. In fact, antibody deficiency is associated with dysglycemia, which is restored after the transfer of total IgG from healthy donors.

Results

Anti-insulin IgG Regulates Blood Glucose Concentration. Using insulin as a common and important autoantigen, we recently developed a simple animal model for testing the induction of autoreactive antibody responses (28). The heterodimeric hormone insulin consists of an alpha and beta chain that are covalently linked via disulfide bonds. In addition, the alpha chain also contains an internal disulfide bond (29). Importantly, we were able to show that the presence of polyvalent insulin was sufficient to induce an autoimmune response which can easily be monitored by deregulated glucose concentration in blood and urine similar to diabetes (30, 31). During these experiments, we noticed that a considerable amount of total IgG isolated from naıve wildtype (WT) mice was reactive to insulin (Fig. 1 *A* and *B*). To confirm these data, we performed ELISpot assays and found that anti-insulin IgG-secreting plasma cells are present in the spleen of WT mice (Fig. 1*C*). When we measured the blood glucose concentrations in WT and B cell–deficient mice [mb1-deficient mice (32)], which cannot produce antibodies (*SI Appendix*, Fig. S1), we detected a surprising difference. Unexpectedly, the mb1-deficient mice showed abnormally reduced blood glucose levels as compared to WT controls (Fig. 1*D*). In full agreement, enzyme-linked immunosorbent assay (ELISA) experiments revealed significantly increased serum insulin concentrations in mb1-deficient mice compared to WT mice (*SI Appendix*, Fig. S2). Notably, the mb1-deficient mice show comparable body weight to that of WT mice as determined in previous investigations.

To test whether this abnormal decrease is caused by antibody deficiency, we injected total IgG from WT mice, or an anti-insulin IgG-depleted control of the same total IgG, intravenously (i.v.) into mb1-deficient mice. We found that blood glucose concentration increased with the total murine IgG but not with the anti-insulin IgG-depleted control (Fig. 1*E*). In order to test the consequence of reduced steady-state blood glucose on the fitness, we performed wire hanging tests to assess motor function and found that mb1-deficient mice show significantly reduced wire hanging times as compared to WT controls. Importantly, this deficit in wire hanging times was restored after the intravenous injection of total murine IgG (Fig. 1*F*). In addition, mb1-deficient mice also showed dysregulated blood glucose levels after rotarod exercise (*SI Appendix*, Fig. S3).

Since total IgG preparations from healthy donors are often used as intravenous immunoglobulin (IVIg) infusions in the treatment of immunodeficiency (33), we tested the presence of anti-insulin IgG in these preparations. All preparations contained substantial amounts of anti-insulin IgG. However, the anti-insulin IgG concentration seemed to be increased if the United States was the country of origin (*SI Appendix*, Fig. S4). Since insulin is highly conserved between man and mouse, we injected human IVIg into the mb1-deficient mice and detected a decrease in insulin concentration (Fig. 1*G*). Notably, the IVIg preparations used for in vivo studies did not contain sugars as stabilizers and thus cannot affect blood glucose levels directly (33). Moreover, injecting 50 μg human IVIg into WT mice led to increased blood glucose, and this effect required anti-insulin IgG since the depletion of the anti-insulin IgG from human IVIg prevented the IVIg-induced increase in blood glucose (Fig. 1*H* and *SI Appendix*, Fig. S5).

To test whether the IVIg injection shows similar results in human CVID (common variable immunodeficiency) patients suffering from antibody deficiency (*SI Appendix*, Table S1), we monitored blood glucose before and after IVIg injection. Similar to mb1-deficient mice, antibody-deficient patients showed reduced blood glucose concentrations as compared to healthy donors. Importantly, the concentration of serum glucose increased and reached normal levels briefly after the following IVIg infusion (Fig. 1*I*). Furthermore, immunodeficiency patients that received IVIg showed decreased serum insulin levels immediately after the infusion (*SI Appendix*, Fig. S6).

To show that the anti-insulin IgG present in IVIg is specific for insulin, we determined the affinity via biolayer interferometry (BLI). A dissociation constant of 10^{-11} suggests that the anti-insulin IgG is highly specific for insulin (Fig. 1*J*).

These data suggest that anti-insulin IgG is present in healthy individuals and might be required for the regulation of blood glucose concentration.

Blood Glucose Is Regulated by Antibody Class and Affinity. To further confirm our finding regarding the presence of anti-insulin antibodies in healthy individuals, we monitored the level of anti-insulin IgG and IgM in the blood of different age groups. We found that anti-insulin IgG was similar in young and aged humans (Fig. 2*A*), while anti-insulin IgM seemed to decline with age in males and females (Fig. 2*B*). Interestingly, the human anti-insulin IgM recognizes multiple epitopes of insulin (*SI Appendix*, Fig. S7).

In agreement with the high specificity, the anti-insulin IgG showed no binding to any cellular structure in indirect immunofluorescence assay (IIFA) on HEp-2 cells, which is a commonly used method for the detection of antinuclear antibodies (ANA) (34) (*SI Appendix*, Fig. S8). The anti-insulin IgM, however, consisted of two fractions that can be biochemically separated according to their affinity to insulin (35). Low-affinity anti-insulin IgM (IgM^{low}) is eluted from the insulin column at a higher pH (5) as compared to high-affinity anti-insulin IgM (IgM^{high}), which requires acidic conditions (pH = 2.8) for elution (Fig. 2*C*). The IgM^{low} fraction shows polyreactivity as detected by binding to nuclear structures in IIFA and double-stranded DNA (dsDNA) binding in ELISA, whereas the IgM^{high} fraction is virtually negative in these assays (Fig. 2 *D* and *E*). Furthermore, we confirmed the difference in affinity by performing BLI assays and found that IgM^{low} and IgM^{high} possess a dissociation constant of 10^{-7} and 10^{-10}, respectively (Fig. 2*F*). To test the effect of the different IgM fractions on glucose metabolism, we injected identical amounts of insulin-reactive IgM^{low} and IgM^{high} into WT mice. Increased blood glucose was observed within 2 h after injection in the mice that received IgM^{low}, whereas IgM^{high} did not significantly alter blood glucose levels (Fig. 2*G*). Moreover, we tested whether IgM^{high} plays a regulatory role under conditions of abnormally increased insulin concentrations that may cause hypoglycemia. To this end, we injected 0.5 μg insulin in combination with IgM^{high} or unspecific IgM isotype control. Strikingly, the presence of anti-insulin IgM^{high}, but not the IgM isotype control, prevented the drastic decrease in blood glucose that occurred immediately after insulin injection (Fig. 2*H*). To further test the regulatory role of IgM^{high} in protecting insulin from IgG-mediated degradation, we combined the anti-insulin IgM^{high} with anti-insulin IgG purified from IVIg preparations. The data show that the anti-insulin IgM^{high} acts as PR-IgM preventing the IgG-mediated neutralization of insulin, which results in increased blood glucose levels (Fig. 2*I* and *SI Appendix*, Fig. S9). These data suggest that anti-insulin IgM^{high} is important for regulating glucose metabolism by protecting insulin from IgG-mediated neutralization and by binding excessive insulin, thereby preventing drastic declines in insulin concentrations. The decrease in insulin-reactive IgM with age

Downloaded by guest on February 7, 2022

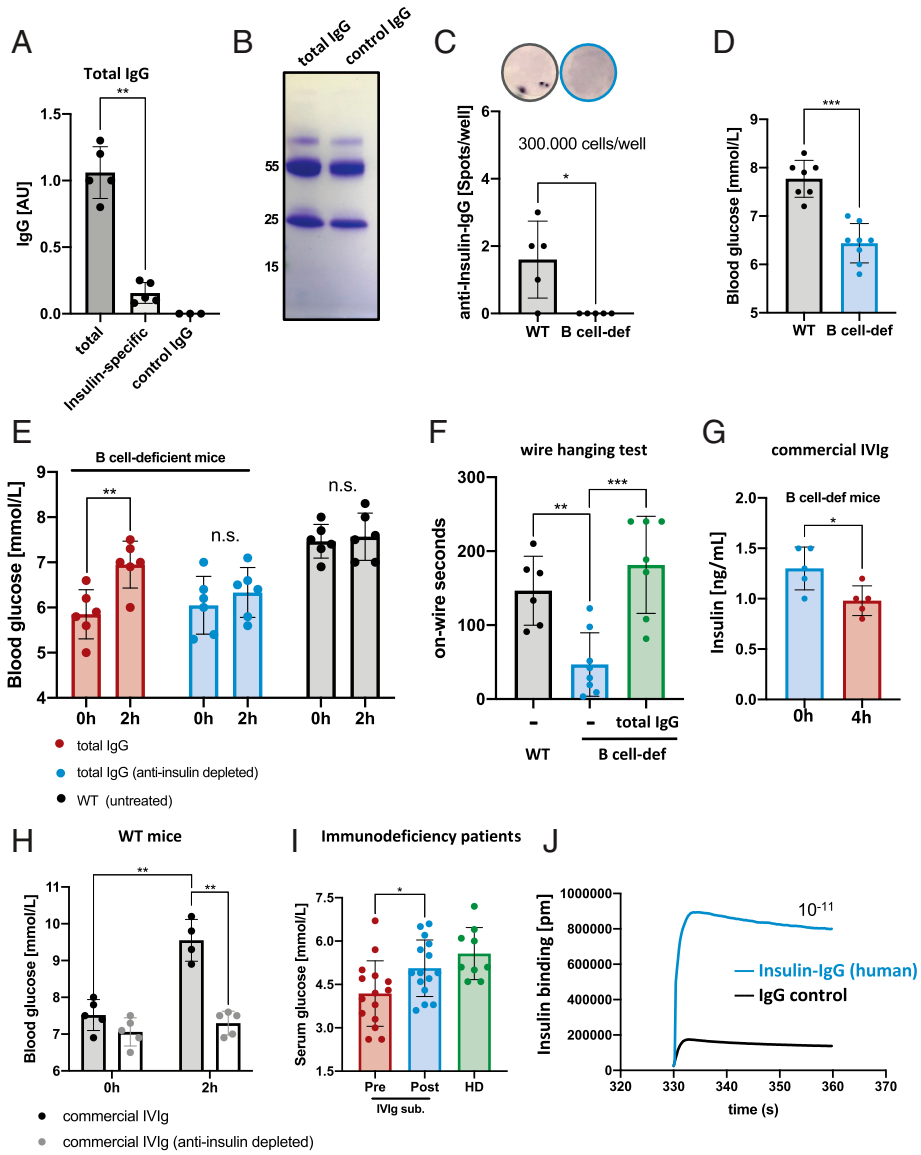


Fig. 1. Autoantibodies are required to balance homeostasis in mice. (*A*) Insulin-specific IgG concentrations of different IgG pulldowns measured by ELISA (coating: native insulin). Total: total IgG pulldown via protein G ($n = 5$), Insulin-specific: IgG pulldown via insulin bait column ($n = 5$), control IgG ($n = 3$). Mean ± SD, statistical significance was calculated using Kruskal–Wallis test. Arbitrary unit (AU) = μg/mL, $^{**}P < 0.01$. (*B*) Coomassie-stained SDS-PAGE showing total IgG (pulldown from serum) and IgG control (total IgG depleted for anti-insulin IgG) under reducing conditions (β-mercaptoethanol). The image is representative of three independent experiments. The marker on the left is shown in kilodaltons (kDa). (*C*) Anti-insulin IgG–secreting splenocytes of naïve WT and mb1-deficient mice measured by ELISpot (coating: native insulin). The cells were seeded at 300,000 cells/well and incubated for 48 h ($n = 5$/group), mean ± SD, statistical significance was calculated using Mann–Whitney *U* test. Top images of wells are representative of three independent experiments. $^{*}P < 0.05$. (*D*) Blood glucose levels of naïve WT and mb1-deficient mice measured with a commercial blood glucose monitor (mmol/L). Mean ± SD, statistical significance was calculated using Mann–Whitney *U* test. $^{***}P < 0.001$. (*E*) Blood glucose levels of WT and mb1-deficient mice (red: $n = 6$, blue: $n = 6$) i.v. injected with 200 μg total IgG, IgG depleted for anti-insulin IgG measured at indicated hours. Mean ± SD, statistical significance was calculated using repeated measure ANOVA test. $^{**}P < 0.01$, n.s. = not significant. (*F*) Motor function of WT and mb1-deficient mice as measured by wire-hanging test (on-wire seconds). Gray: WT untreated ($n = 6$), blue: mb1-deficient untreated ($n = 8$), green: mb1-deficient injected with 200 μg total IgG ($n = 7$). Mean ± SD, statistical significance was calculated using Kruskal–Wallis test. $^{**}P < 0.01$, $^{***}P < 0.001$. (*G*) Serum insulin concentrations of mb1-deficient mice injected with 200 μg commercial human IVIg as measured by ELISA at indicated time points ($n = 5$). Mean ± SD, statistical significance was calculated using Mann–Whitney *U* test. $^{*}P < 0.05$. (*H*) Blood glucose levels of WT mice injected with 200 μg commercial human IVIg (black: $n = 5$ for 0 h, $n = 4$ for 2 h post-injection) and commercial human IVIg depleted for anti-insulin IgG (gray: $n = 5$) measured by a commercial blood glucose monitor (mmol/L) at indicated hours. Mean ± SD, statistical significance was calculated using repeated measure ANOVA test. $^{**}P < 0.01$. (*I*) Serum glucose levels of immunodeficiency patients (CVID) that received commercial IVIg before (pre, $n = 15$) and after (post, $n = 15$) infusion compared to healthy donors (HD, $n = 9$). Mean ± SD, statistical significance was calculated using Kruskal-Wallis test. $^{*}P < 0.05$. (*J*) Insulin-binding affinity of human anti-insulin IgG determined by BLI. The K_d (dissociation constant) was calculated by using the K_a (association constant): $1/K_a$. Data are representative of three independent experiments performed in three dilution steps per sample.

(Fig. 1*A*) prompted us to test whether the anti-insulin IgM^{high} or IgM^{low} is affected by this decrease. We determined the amount of anti-insulin IgM^{high} or IgM^{low} in young and old healthy donors and found that the ratio of anti-insulin IgM^{high} increases with age (Fig. 2*J*).

Together, these data suggest that glucose metabolism is regulated by different classes of antibodies and that anti-insulin IgM^{high} acts as PR-IgM that regulates glucose metabolism by regulating insulin homeostasis, which seems to be particularly important with age.

Downloaded by guest on February 7, 2022

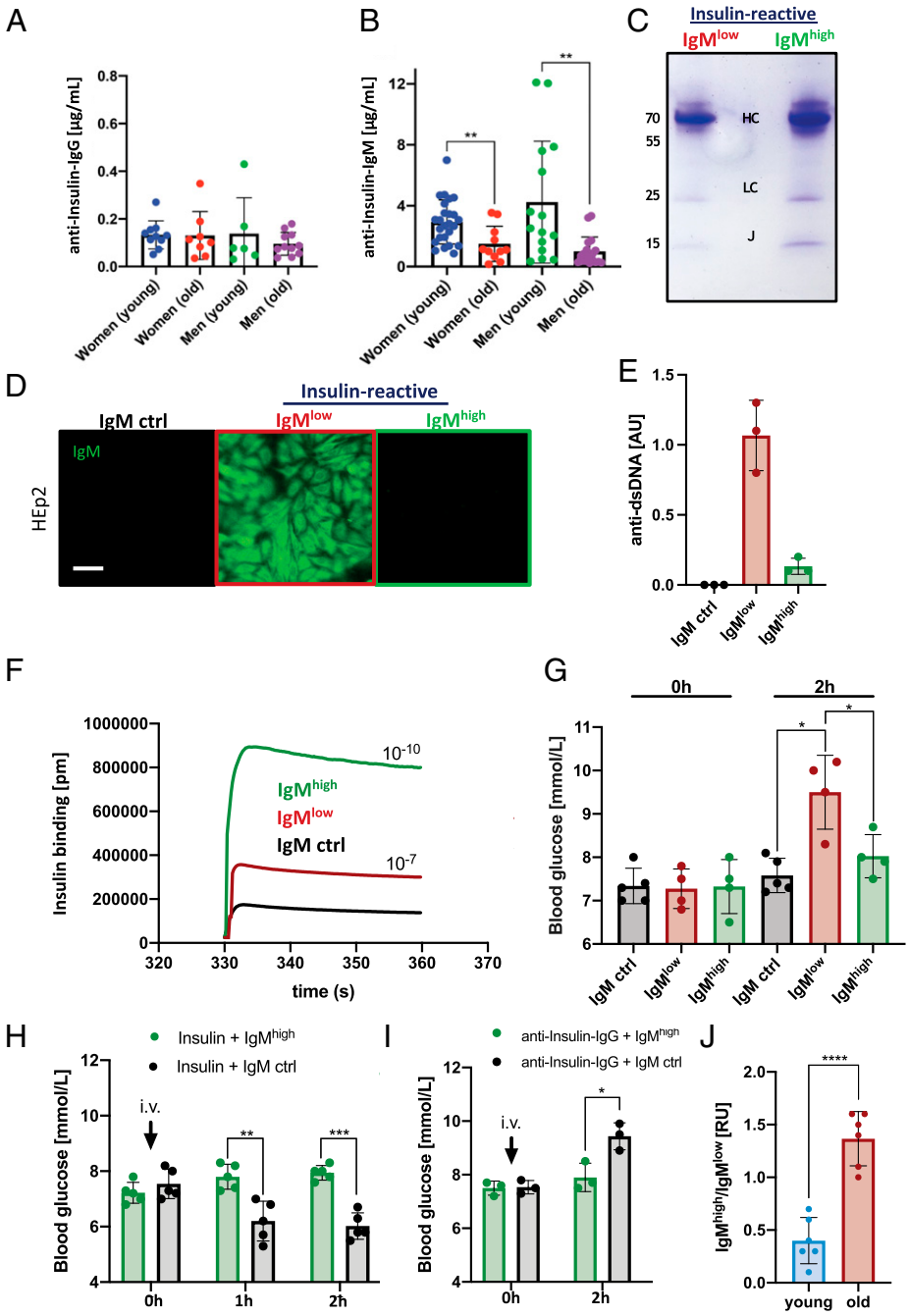


Fig. 2. Neutralizing and PR-IgM is present in humans. (*A* and *B*) Serum anti-insulin IgG (*A*) and IgM (*B*) concentrations of young (<30 y) and old (>65 y) human individuals measured by ELISA (coating: native Insulin). Women (young): $n = 25$, women (old): $n = 11$, men (young): $n = 15$, men (old): $n = 12$. Mean ± SD, statistical significance was calculated using Kruskal–Wallis test. $^{**}P < 0.01$. (*C*) Coomassie-stained SDS-PAGE showing low-affinity anti-insulin IgM (red) and high-affinity anti-insulin IgM (green) after purification under reducing conditions (β-mercaptoethanol). Image is representative of three independent experiments. Marker on the left is shown in kDa, HC (heavy chain): 70 kDa, LC (light chain): 25 kDa, J (J-chain): 15 kDa. (*D*) HEp2 slides showing nuclear structure–reactive IgM (ANA) of insulin-reactive IgM pulldowns. Black: monoclonal IgM control ($n = 6$), red: low-affinity anti-insulin IgM ($n = 6$), green: high-affinity anti-insulin IgM ($n = 6$). (Scale bar: 10 µm.) Green fluorescence indicates HEp2 cell binding. Images are representative of four independent experiments. (*E*) Anti-dsDNA IgM concentrations of insulin-specific IgM pulldowns as measured by ELISA (coating: calf-thymus dsDNA). IgM control (ctrl, $n = 3$), IgM^{low} ($n = 3$), IgM^{high} ($n = 3$). Mean ± SD, statistical significance was calculated using Kruskal–Wallis test (all comparisons were n.s.). (*F*) Insulin-binding affinity of human anti-insulin IgM pulldowns determined by BLI. The K_d (dissociation constant) was calculated by using the K_a (association constant): $1/K_a$. Data are representative for three independent experiments performed in three dilution steps. (*G*) Blood glucose levels of WT mice i.v. injected with 100 µg human insulin-specific IgM and human IgM control (black: $n = 5$, red: $n = 4$, green: $n = 4$). Mean ± SD, statistical significance was calculated using repeated measure ANOVA test. $^{*}P < 0.05$. (*H* and *I*) Blood glucose levels of WT mice intravenously injected with 100 µg human insulin-specific IgM (uppercase refers to affinity fraction) and human IgM control together with 500 ng native insulin (insulin + IgM^{high}, green: $n = 5$; insulin + IgM control: $n = 5$) (*H*) or together with 100 µg human anti-insulin IgG ($n = 3$/group) (*I*). Mean ± SD, statistical significance was calculated using repeated measure ANOVA test. $^{*}P < 0.05$, $^{**}P < 0.01$, $^{***}P < 0.001$. (*J*) Ratio of insulin-specific IgM of young (<30 y, $n = 6$) and old (>65 y, $n = 6$) individuals as determined by ELISA. Insulin-specific IgM was isolated via insulin bait columns prior to ELISA experiments. Mean ± SD, statistical significance was calculated using Kruskal–Wallis test. $^{****}P < 0.0001$.

Downloaded by guest on February 7, 2022

Induction of Anti-insulin Antibodies by Insulin Complexes. The presence of anti-insulin antibodies raises the question about the potential mechanisms of an adaptive generation of autoreactive antibodies. We have recently shown that autoreactive antibodies can easily be elicited by polyvalent antigen in classical immunization experiments involving adjuvants (28). To show that complexed autoantigen is capable of inducing autoreactive antibody responses independent of any adjuvants, we incubated insulin with a typical homobifunctional crosslinker, 1,2-phenylene-bis-maleimide (36), which covalently binds to free sulfhydryl (SH) groups of cysteine in proteins, thereby cross-linking the protein of interest (Fig. 3*A*). Importantly, SH group–containing drugs were reported to induce anti-insulin autoantibodies (37–39). Moreover, increased pancreas activity and elevated insulin production result in the abnormal formation of disulfide bonds between insulin peptides, which may generate abnormal insulin forms that are more susceptible for SH group–mediated cross-linking, and thus complex formation, under conditions of oxidative stress (40–43). The homobifunctional cross-linking of insulin with 1,2-phenylene-bis-maleimide was tested in sodium dodecyl sulfate–polyacrylamide gel electrophoresis (SDS-PAGE), and the cross-linked insulin was purified using size-exclusion spin columns excluding monomeric and dimeric insulin (Fig. 3*B*). The insulin complexes were dialyzed and injected into WT mice (20 μg per mouse) without any additional adjuvants. As control, we performed a typical immunization using CpG as the adjuvant and streptavidin as a foreign carrier. We found that the insulin complexes lead to increased blood glucose levels and anti-insulin IgM at day 7 (d7) of treatment similar to the immunization (Fig. 3 *C* and *D*). Notably, the insulin complex itself did not affect blood glucose levels shortly after injection, suggesting that the biological activity of insulin is abrogated by protein complex formation (*SI Appendix*, Fig. S10). In addition, insulin-reactive IgG was detectable by ELISA on d14 and d26 (*SI Appendix*, Fig. S11). The repeated injection of insulin complexes at d21 resulted in further deregulation of glucose metabolism (Fig. 3*E*). Thus, we injected anti-insulin IgM^{high} at d22, 1 d after the injection of the insulin complexes. We found that anti-insulin IgM^{high} was able to prevent the blood glucose deregulation induced by the injection of insulin complexes (Fig. 3*E*).

Our previous work suggests that anti-insulin IgG induces pancreas inflammation and infiltration by macrophages and granulocytes (28). Next, we tested whether anti-insulin IgM^{high} was also able to prevent IgG-mediated pancreas inflammation. We found that anti-insulin IgM^{high} prevents pancreas inflammation and damage as shown by the decrease of macrophage ($CD11b^+/Ly6G^+$) and neutrophil ($Ly6G^+$) infiltration in the pancreas and the decrease of serum pancreatic lipase (Fig. 3 *F* and *G* and *SI Appendix*, Fig. S12).

As a mechanism for the protective role of anti-insulin IgM^{high} as compared to anti-insulin IgM^{low}, we proposed that the polyreactivity of the latter, which also binds dsDNA, induces the formation of immune complexes that can be phagocytosed by macrophages. In contrast, anti-insulin IgM^{high} is highly specific for insulin and does not form large immune complexes. We hypothesized that the inability of IgM^{high} to form large immune complexes results in poor phagocytosis by macrophages and therefore leads to a prolonged half-life of bound antigen. To test this, we incubated anti-insulin IgM^{high} or anti-insulin IgM^{low} with insulin in the presence of genomic dsDNA. Macrophages can phagocytose IgM immune complexes (44–46), and it is proposed that IgM-mediated phagocytosis is mediated by CD11b/CD18 but is independent of the FcμR, which binds to IgM but is mainly expressed by lymphocytes and not by macrophages (47–49). We found an increased binding/phagocytosis of anti-insulin IgM^{low} as compared to anti-insulin IgM^{high} (Fig. 3*H* and *SI Appendix*, Fig. S13). In addition, IgM^{high} was able to protect insulin from degradation, as the decline of insulin was greater in the supernatants containing anti-insulin IgM^{low} as compared to anti-insulin IgM^{high} antibodies (*SI Appendix*, Fig. S14).

These data show that anti-insulin antibodies can be generated under conditions activating the formation of insulin complexes, which results in deregulated glucose metabolism that can be counteracted by anti-insulin IgM^{high} that acts as PR-IgM.

Recombinant Anti-insulin IgM Regulates Blood Glucose. The results in Fig. 2 suggest that insulin-specific PR-IgM might be of great therapeutic interest, as it regulates insulin homeostasis and might prevent pancreas malfunction, both of which are essential for normal physiology and the prevention of diabetes. According to our data, an anti-insulin IgM can act as PR-IgM if it possesses high binding affinity to insulin and is not reactive to other autoantigens such as dsDNA or nuclear structures in IIFA. We hypothesized that a human insulin-specific IgG antibody can be converted into insulin-specific PR-IgM by exchanging the constant region.

Thus, we cloned and expressed a published human insulin-specific monoclonal antibody (50) as IgG1 (IgG_{MY}) and IgM (IgM_{MY}). To test the quality of our in vitro–produced antibodies, we assessed their glycosylation by PNGaseF treatment, which resulted in reduced molecular weight as compared to untreated controls suggesting a functional glycosylation (*SI Appendix*, Fig. S15). We determined the affinity of both IgG and IgM to be 10^{-9} (K_D) (Fig. 4*A*). Almost no dsDNA binding was observed in ELISA, and no nuclear staining was observed in IIFA as compared to total human serum IgM (Fig. 4 *B* and *C*). Moreover, by injection into mice, we tested if the monomeric anti-insulin IgM is capable of protecting insulin from degradation. Anti-insulin IgG led to a blood glucose increase, which was abolished when monomeric IgM_{MY} was present (Fig. 4*D*).

To test whether the resulting recombinant human anti-insulin IgM_{MY} possesses protective regulatory functions, we coinjected it with insulin and found that anti-insulin IgM_{MY} prevents a drastic drop in glucose concentration induced by an excess of insulin (Fig. 4*E*). Moreover, anti-insulin IgM_{MY} protects insulin from anti-insulin IgG_{MY}–mediated neutralization, as it prevents the increase in blood glucose induced by anti-insulin IgG_{MY} (Fig. 4*F*). In addition, anti-insulin IgM_{MY} counteracts the leak of glucose into urine (Fig. 4*G*).

These data suggest that expressing a high-affinity insulin-specific antibody as IgM regulates insulin homeostasis, prevents a deregulation of blood glucose concentration, and might grant novel strategies for diabetes treatment.

Discussion

This study shows that autoreactive anti-insulin IgM and IgG antibodies are normally present in WT animals and in human subjects. Moreover, the presence of such autoantibodies is neither an accident nor a failure in negative selection, it is rather an important element in the regulation of insulin concentration and glucose metabolism. An even more surprising result is the finding that the affinity of autoreactive anti-insulin IgM determines the outcome of its interaction with insulin. A high-affinity anti-insulin IgM is protective, while low-affinity IgM is destructive. Since low-affinity IgM is positive in IIFA (HEp2) and recognizes additional autoantigens such as dsDNA, it is multispecific, while high-affinity IgM is monospecific, as it recognizes only insulin. The multispecific nature of the low-affinity IgM leads to the formation of larger immune complexes (28), which seems to accelerate insulin phagocytosis and, most likely, its degradation by macrophages, thereby leading to an increase in blood glucose levels. Obviously, the most unexpected finding is the protective role of the high-affinity IgM toward insulin, as

Downloaded by guest on February 7, 2022

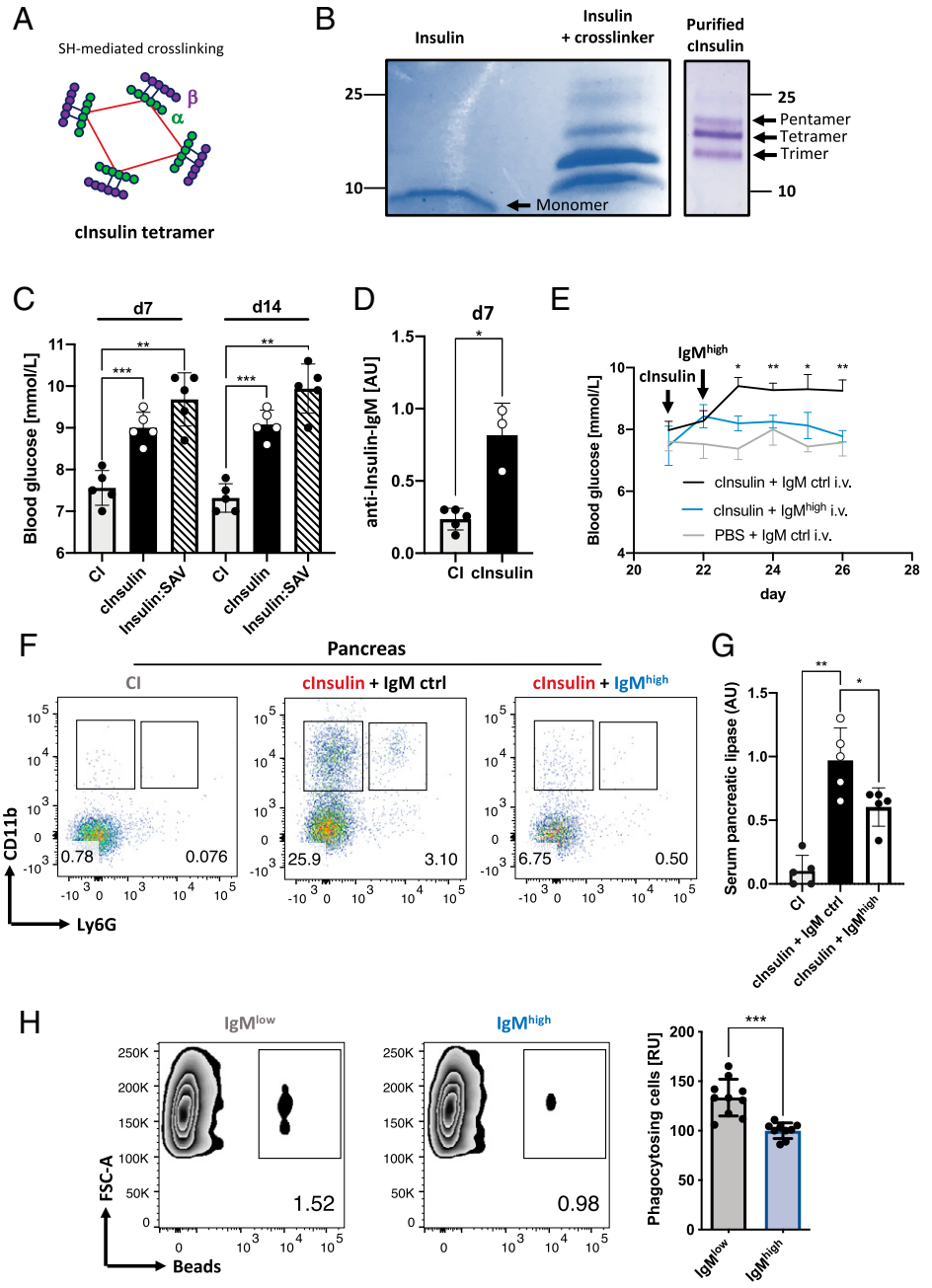


Fig. 3. Endogenous insulin complexes induce robust autoimmunity in mice. (*A*) Schematic illustration of insulin tetramers (cInsulin) generated by reactive SH group–mediated carbon–sulfur bond cross-linking via 1,2-phenylene-bis-maleimide. Black lines: endogenous disulfide bonds, red lines: cross-linking induced carbon–sulfur bonds. Alpha and beta chain of insulin are indicated by green and purple, respectively. (*B*) Coomassie-stained nonreducing BN-PAGE showing soluble insulin (6 kDa) and cross-linked insulin (>6 kDa). cInsulin complexes after purification with a 10-kDa size exclusion column are on *Right*. Images are representative of three independent experiments. Markers on the left/right site indicate band size in kDa. (*C*) Blood glucose levels of WT mice i.p. injected with PBS (CI: $n = 5$), cInsulin ($n = 5$), or Insulin:SAV (bio-Insulin:streptavidin, $n = 5$) on day 7 and day 14 post-injection (p.i.). Mean ± SD, statistical significance was calculated using repeated measures ANOVA test. $^{**}P < 0.01$, $^{***}P < 0.001$. (*D*) Serum anti-insulin IgM concentrations of WT mice i.p. injected with PBS (control injection; CI, $n = 5$) and cInsulin ($n = 3$) on day 7 p.i. measured by ELISA at indicated days (coating: native insulin). Mean ± SD, statistical significance was calculated using Mann–Whitney *U* test. $^{*}P < 0.05$. (*E*) Blood glucose levels of WT mice i.p. injected with PBS (CI, $n = 5$) or cInsulin ($n = 5$) on day 0 and day 21 followed by i.v. injections of 100 μg anti-insulin IgM^{high} or 100 μg IgM ctrl on days 22 through 26. Mean ± SD, statistical significance was calculated using repeated measure ANOVA test. $^{*}P < 0.05$, $^{**}P < 0.01$. (*F*) Flow cytometric analysis of mice i.p. injected with PBS (CI, $n = 5$) or cInsulin ($n = 5$/group) together with i.v. injections of 100 μg anti-insulin IgM^{high} or 100 μg IgM control. Panels show pancreatic macrophages (CD11b^{+}) and neutrophils (Ly6G^{+}) pregated on viable cells (fixable viability dye^{-}). Images are representative of three independent experiments. (*G*) Serum pancreatic lipase levels of WT mice i.p. injected with PBS (CI, $n = 5$) and cInsulin ($n = 5$/group) together with i.v. injections of 100 μg anti-insulin IgM^{high} or 100 μg IgM control. Mean ± SD, statistical significance was calculated using Kruskal–Wallis test. $^{*}P < 0.05$, $^{**}P < 0.01$. (*H*) Flow cytometric analysis of bead-based phagocytosis assay performed with high- and low-affinity human anti–Insulin-IgM (IgM^{low} $n = 10$, IgM^{high} $n = 10$) preincubated with dsDNA. Representative zebra plots are on *Left*, and quantitative analysis normalized to IgM^{high} is on *Right*. Mean ± SD, statistical significance was calculated using Mann–Whitney *U* test. $^{***}P < 0.001$.

Downloaded by guest on February 7, 2022

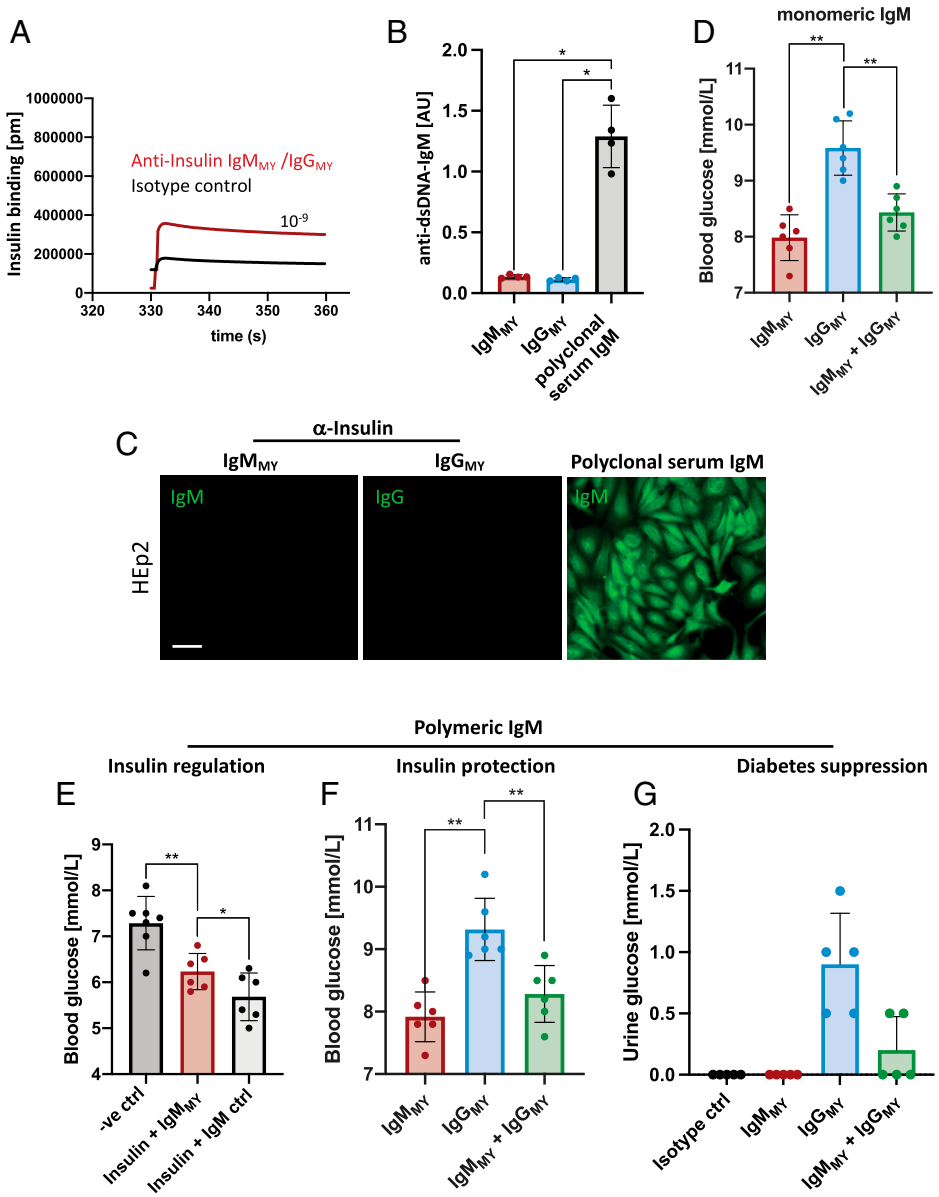


Fig. 4. Monoclonal human insulin-IgM is able to protect insulin in vivo. (*A*) Insulin-binding affinity of monoclonal human anti-insulin Ig determined by BLI. The K_d (dissociation constant) was calculated by using the K_a (association constant): $1/K_a$. Shown data are representative for three independent experiments performed in three dilution steps per sample. (*B*) Anti-dsDNA IgM concentration of insulin-specific IgM pulldowns as measured by ELISA (coating: calf-thymus DNA). IgM$_{MY}$ ($n = 4$), IgG$_{MY}$ ($n = 4$), and polyclonal serum IgM (positive control, $n = 4$). Mean ± SD, statistical significance was calculated using Kruskal–Wallis test. $^*P < 0.05$. (*C*) HEp-2 slides showing anti-nuclear structure-reactive (ANA) monoclonal IgM$_{MY}$ ($n = 6$), IgG$_{MY}$ ($n = 6$), and polyclonal serum IgM (positive control, $n = 6$). (Scale bar: 10 μm.) Green fluorescence indicates HEp-2 cell binding. Images are representative of three independent experiments. (*D*) Blood glucose levels of WT mice i.v. injected with 100 μg monomeric IgM$_{MY}$ ($n = 6$), IgG$_{MY}$ ($n = 6$), and both combined ($n = 6$) 2 h post-injection. Mean ± SD, statistical significance was calculated using Kruskal–Wallis test. $^{**}P < 0.01$. (*E*) Blood glucose levels of WT mice i.v. injected with PBS (−ve ctrl, $n = 7$), 500 ng insulin with 100 μg polymeric IgM$_{MY}$ ($n = 6$) and 500 ng insulin with IgM control ($n = 6$) 2 h post-injection. Mean ± SD, statistical significance was calculated using Kruskal–Wallis test. $^*P < 0.05$, $^{**}P < 0.01$. (*F*) Blood glucose levels of WT mice i.v. injected with 100 μg polymeric IgM$_{MY}$ ($n = 6$), IgG$_{MY}$ ($n = 6$), and both combined ($n = 6$) 2 h post-injection. Mean ± SD, statistical significance was calculated using Kruskal–Wallis test. $^{**}P < 0.01$. (*G*) Urine glucose levels of WT mice immunized with cInsulin and i.v. injected with 100 μg IgM control ($n = 6$), 100 μg polymeric IgM$_{MY}$ ($n = 5$), 100 μg IgG$_{MY}$ ($n = 5$), and both combined ($n = 5$) every 24 h. Measurement shows 8 d post-injection. Mean ± SD, statistical significance was calculated using Kruskal–Wallis test. All comparisons were not significant (n.s.).

antibody function is thought to result in the neutralization of the target antigen. We refer to the generation of a protective antibody as adaptive tolerance because, in contrast to the destructive primary IgM, PR-IgM is generated in the course of secondary immune responses and affinity maturation. We expect canonical B-2 B cells to be the origin of the primary autoreactive neutralizing IgM responses, which are usually short lived. After affinity maturation, long-lived PR-IgM is most likely produced by conventional IgM$^+$/CD27$^+$ memory B cell–derived plasma cells or circulating splenic marginal zone B cells (51, 52). Our data suggest that the ratio of soluble (monovalent) to complex (polyvalent) antigen dictates the outcome of antibody class and that increased monovalent antigen favors the generation of memory IgM over IgG. It remains to be investigated whether these IgM memory B cells in mice and humans are germinal center derived.

Downloaded by guest on February 7, 2022

In full agreement, our results show that anti-insulin antibody responses are induced by polyvalent insulin complexes generated by chemical cross-linking via carbon–sulfur bonds and independent of any additional adjuvants. SH group–containing drugs are used as immunosuppressive medication [Azathioprine (53)], antilymphoma treatment [Alethine (54)], or acute bronchitis treatment [Erdosteine (55)]. Strikingly, their use was reported to result in the development of anti-insulin autoantibodies (39, 41). Reactive SH groups mediate the generation of protein complexes by the formation of disulfide or carbon–sulfur bonds under oxidizing conditions (56). It is tempting to speculate that peptide hormones such as insulin or other proteins containing free SH groups are disposed to complex formation under oxidative stress when the concentration of oxidants in the body exceeds the capacity of physiologically present antioxidants that balance oxidative stress. Thus, the anti-insulin antibody response induced in this study by oxidative cross-linking of insulin might mimic the physiological conditions which lead to autoantibody production. The oxidative stress-mediated cross-linking of insulin together with the increased amount of misfolded or abnormally cross-linked insulin peptides under conditions of elevated insulin production might lead to recurrent antibody responses against insulin. An inability of the immune system to generate PR-IgM by adaptive tolerance might represent the first step in the development of metabolic disorders associated with blood glucose. According to this scenario, T1D develops when anti-insulin IgG production exceeds or replaces PR-IgM production, resulting in the failure to protect insulin and to prevent pancreas damage. On the other hand, in type 2 diabetes, the production of PR-IgM may decline because of the decreasing generation of new B cells with age (57, 58). In full agreement, the ratio of high-affinity anti-insulin IgM is highly increased in healthy aged humans as compared to young individuals. Thus, a broad B cell repertoire seems to be important for controlling autoimmunity since high-affinity protective IgM has to be produced against virtually every self-structure in order to protect it from self-destructive low-affinity IgM or IgG. This might explain the common relationship between immunodeficiency and autoimmunity (59).

Another important conclusion of our study is that antibodies are not only required for protection from pathogens. Antibodies can also regulate the amount of key physiological factors in the blood such as insulin and are thus important regulators of metabolism and physiology. In addition to the production rate and consumption by target cells, the insulin concentration seems to be regulated by the equilibrium of protective and destructive autoantibodies. In this scenario, protective IgM acts as reservoir that makes insulin quickly accessible while anti-insulin IgG or low-affinity IgM neutralizes the excess of insulin. Our data are supported by experiments showing that high-fat-diet mice (HFD) receiving a B cell–depleting therapy (anti–CD20-IgG) went from hyperglycemic to normoglycemic, suggesting that autoreactive antibodies represent an important part in the development of diabetes and the regulation of metabolism (60). Moreover, the study presented a unique panel of IgG autoantibodies involved in insulin resistance in patients, underlining the importance of glucose metabolism-regulating autoantibodies (60).

This view is further supported by studies reporting severe metabolic disorders in immunodeficiency patients (61). Indeed, CVID patients with drastic hypoglobulinemia showed signs of dysglycemia and defects in fatty acid metabolism (61, 62). In full agreement, our study shows that antibody-deficient mice suffer from dysglycemia and that injecting total IgG or insulin-reactive autoantibodies results in the normalization of blood glucose levels. It remains to be investigated if severe combined immunodeficiency patients, who completely lack B cells and show pan-hypogammaglobulinemia, show dysregulation of blood glucose homeostasis because of the absence of regulatory autoantibodies.

Most likely, other peptide hormones or self-structures are similar to insulin regulated by autoantibodies. Methods for the immortalization of memory B cells can be used for the characterization of protective IgM antibodies (63). Alternatively, converting an autoantigen-specific IgG into IgM-class antibodies might open new venues for the treatment of human autoimmune disorders by protecting the autoantigen. This might create an opportunity to turn ongoing autoimmune diseases into remission. In full agreement, we show that by converting a previously described anti-insulin IgG into IgM reversed its function from an insulin-neutralizing into a protecting agent.

A further conclusion of our findings is that the highly autoreactive primary IgM repertoire represents a high risk for autoreactive damage if high-affinity PR-IgM cannot be generated by secondary immune responses and somatic hypermutation. This suggests that the memory IgM repertoire consists mostly of PR-IgM generated in the course of adaptive tolerance. This also suggests that the defects in somatic hypermutation lead to failure in PR-IgM generation and autoimmune damage induced by the primary IgM. In full agreement, all forms of hyper IgM syndrome (HIGM) are associated with severe autoimmunity (59, 64–66). HIGM patients are particularly prone to developing IgM-mediated autoimmune diseases such as immune thrombocytopenia, hemolytic anemia, and nephritis (65, 67, 68). Notably, autoreactive IgM antibodies that cause autoimmune diseases in HIGM patients are always unmutated and therefore of low affinity to autoantigens (67). These studies report an excessive pathogenic potential of low-affinity autoreactive IgM leading to manifest and severe autoimmunity supporting our concept of neutralizing (low-affinity) and protective (high-affinity) autoreactive IgM.

Together, our findings demonstrate an important role for autoantibodies in physiological homeostasis and suggest that adaptive tolerance is a key mechanism for maintaining physiological integrity.

Materials and Methods

Mice. Female 8- to 15-wk-old C57BL/6 mice (WT) and mb1-deficient mice (69) were intraperitoneally (i.p.) or i.v. injected with samples containing antigens or antibodies in 1× phosphate-buffered saline (PBS). Control injection mice received PBS in a total volume of 100 μL/mouse. We used the following molecules and concentrations for i.v. and i.p. injections: total murine IgG (200 μg/mouse i.v.), commercial human IVIg (200 μg/mouse i.v.), human insulin-specific IgM isolated from serum (100 μg/mouse i.v.), cInsulin (20 μg/mouse i.p.), insulin-bio:streptavidin complexes (20 μg/mouse i.p.), native insulin (0.5 μg/mouse i.p.), monoclonal insulin-specific IgM (100 μg/mouse. i.v.), and monoclonal insulin-specific IgG (100 μg/mouse i.v.). The animal experiments were performed in compliance with the guidelines of German law and were approved by the Animal Care and Committees of Ulm University and the local government under the license number 1484. All mice used in this study were either bred and housed within the animal facility of Ulm University under specific pathogen-free conditions (mb1-deficient mice) or obtained from Charles River at 6 wk of age (WT mice).

Cross-linking of Native Insulin. Native human insulin (Merck) was prediluted in 1% dimethyl sulfoxide (in H_2O) to 1 mg/mL. Chemical carbon–sulfur-cross-linking of thiol groups was achieved by using 1,2-phenylen-bis-maleimide (13118–04-2) at 100 μg/mL for 48 h at room temperature in the dark. Afterward, excess 1,2-phenylen-bis-maleimide was removed by using a 10-kDa cut-off spin column (Abcam, ab93349). Purified insulin complexes (cInsulin) were used for i.p. injections. Quality control was done by using a nonreducing SDS-PAGE and Coomassie staining or blue native (BN)-PAGE.

Macrophage Phagocytosis Assay. The effect of IgM^{high} and IgM^{low} on the antibody-mediated clearance was assessed in mouse phagocytic J774A.1 cell line. Red fluorescent latex beads (2 μm in diameter, Sigma-Aldrich) were coated with purified IgM^{high} and IgM^{low} in a 1:7 ratio and incubated for 45 min at 37 °C. IgM promotes the clearance of small particles and apoptotic microparticles by macrophages (44). The IgM-coated latex beads were

Downloaded by guest on February 7, 2022

suspended in serum-free culture medium and added to J774A.1macrophages at a 5:1 ratio. After 180-min incubation, the cells were washed in PBS to remove nonengulfed beads. The cells were detached with trypsinization and fixed in 4% paraformaldehyde and subsequently analyzed with a BD LSR II flow cytometer. The macrophage population was identified as described before (70), and the proportion of macrophages containing ingested particles was determined based on the fluorescent signal of the ingested latex beads.

Flow Cytometry. The detailed description is available in ref. 11. Briefly, cell suspensions were Fc receptor blocked with polyclonal rat IgG-UNLB (2,4G2; BD) and stained according to standard protocols. Viable cells were distinguished from dead cells by using Fixable Viability Dye eFluor780 (eBioscience), and stained cells were acquired at a Canto II Flow Cytometer (BD).

ELISA. Antigen-specific ELISAs are described in ref. 28 in detail. Briefly, 96-well plates (Nunc, Maxisorp) were coated with 10 μg/mL native insulin (Sigma-Aldrich, catalog no. [cat.] 91077C) or 2.5 μg/mL calf thymus dsDNA (Thermo Scientific, cat.15633019). Standard coating was done by using anti-IgM, anti-IgG-antibodies (SouthernBiotech). The relative concentrations stated as an arbitrary unit or absolute concentration (μg/mL) were determined via detection by alkaline phosphatase (AP)-labeled anti-IgM/anti-IgG (SouthernBiotech) by using p-nitro-phenylphosphate (Genaxxon) in diethanolamine buffer, respectively.

Enzyme-Linked Immuno-Spot Assay (ELISpot). Total splenocytes were measured in triplicates with cell numbers stated in the figure. ELISpot plates were coated with native Insulin (Sigma-Aldrich, cat. 91077C), anti-IgM (Mabtech), or anti-IgG (Mabtech). Seeded cells were incubated for 12 to 24 h at 37 °C, and antigen-specific IgM or IgG was detected via anti-IgM-bio and SAV-AP or anti–IgG-bio and SAV-AP (Mabtech). The experiments were performed according to the manufacturer's instructions.

HEp-2 Slides and Fluorescence Microscopy. HEp-2 assays with corresponding autoantibodies are described in ref. 28 in detail. Briefly, serum samples indicated in the figures or figure legends were diluted to an equal concentration of IgM (approximately 300 ng/mL anti–Insulin-IgM in both immunized samples) and applied onto the HEp-2 slides (EUROIMMUN, F191108VA). Anti—IgM-APC (allophycocyanin) (eBioscience) and anti–IgG-APC (eBioscience) were used for the visualization of ANA-IgM/-IgG.

Glucose Level Monitoring and Insulin Concentration Determination. The assessment of blood and urine glucose levels is described in ref. 28 in detail. Briefly, we used an Accu Chek (Roche Diagnostics) blood glucose monitor (mmol/L) and took blood from the tail vein. Serum or blood insulin concentrations of human and mouse samples were determined by using commercial ELISA kits by Crystal Chem (mouse: no. 90080, human: no. 90095) according to the manufacturers protocol.

SDS-PAGE and BN-PAGE. The samples were separated on 10 to 20% SDS-polyacrylamide gels, which were incubated with Coomassie (Coomassie brilliant blue R-250, Thermo Fisher) for 45 min and subsequently de-stained. In order to visualize native protein complexes, we used BN-PAGES (SERVA) with BN buffer (1:1 sample to buffer).

Pulldown of Total Serum Immunoglobulins. The serum of injected mice was collected immediately after euthanasia at the indicated days. The antigen bound to antibodies was removed by repeated freeze–thaw cycles of the serum and pH shift during elution (71). Protein G Sepharose beads (Thermo Fisher) were used according to the manufacturer's protocol and obtained antibodies dialyzed overnight in 10 times sample volume of 1× PBS. For isolation of IgM, HiTrap IgM columns (GE Healthcare, Sigma-Aldrich) were used according to the manufacturer's protocol and dialyzed overnight in 10 times sample volume of 1× PBS. The quality of the isolated immunoglobulins was checked via SDS-PAGE and Coomassie staining, and the concentration of antigen-specific immunoglobulins was determined by ELISA.

Isolation of Antigen-Specific Immunoglobulins. Streptavidin bead columns (Thermo Scientific, cat. 21115) were loaded with 10 μg bio-insulin (BioEagle) in order to isolate insulin-specific immunoglobulins. The samples (sera or isolated antibodies) were incubated for 90 min at room temperature to ensure sufficient binding of antibodies to the insulin-loaded beads. The purification of the insulin antibodies was achieved by a pH shift (pH 2.8) using the manufacturer's elution and neutralization solutions. Note, the fractionation into low- and high-affinity fractions was done by eluting with pH 5 (low affinity) and subsequently with pH 2.8 (high affinity). The quality of the isolated immunoglobulins was determined via reduced and nonreduced Coomassie-stained SDS-PAGEs and the quantity determined by ELISA. For further in vivo experiments, the isolated antibodies were dialyzed as described in *Pulldown of Total Serum Immunoglobulins*).

BLI. Interferometric assays (BLItz device, ForteBio) were used to determine the affinity of protein–protein interactions (72) as described in ref. 28.

Wire-Hanging Test. The linear wire-hanging test was used to assess the motor strength and function of mice (73). Individual mice were put onto a 36-cm elevated horizontal wire above a cage; subsequently, the mice tried to stay on the wire by using their paws and muscle strength. The ability in time (seconds) of each mouse to stay on the wire was recorded. A maximum time duration of 240 s was set. Each mouse went through the test three times in a row. The mean value was calculated from the measured data. Blood glucose values were determined before and after the test.

Rotarod Test. To assess motor function and blood glucose levels after physical exercise, the rotarod test was performed (74). Before the start of the experiment, the blood glucose level of the mice was determined. Afterward, they were placed on the running drum of the Rotarod apparatus with a continuous rotation of 32 rpm. At 30 s, the experiment was stopped, and the blood glucose values were measured.

Statistical Analysis. Graphs were created and statistically analyzed by using GraphPad Prism (version 9.1.2) software. The numbers of individual replicates or mice (n) are stated within the figure legends. Datasets were preanalyzed by a D'Agostino and Pearson omnibus normality test and/or a Shapiro–Wilk normality test to determine if the values were normally distributed. If one of the datasets was not normally distributed or the sample number n was too small to perform the normality tests, nonparametric tests were used to calculate P values. In this study, P values were calculated by tests stated in the respective figure legends. Student's t tests with Welch's correction were used to compare two groups within one experiment. P values > 0.05 were considered to be statistically significant (n.s. = not significant; $*P < 0.05$; $**P < 0.01$; $***P < 0.001$, $****P < 0.0001$).

Data Availability. All study data are included in the article and/or supporting information.

ACKNOWLEDGMENTS. We thank the group of T. Böckers for the free use of the mouse behavior experimental room and M. Reth for critical reading and fruitful discussion. Furthermore, we thank Ina Harder for the serum sampling of immunodeficiency patients. This work was supported by the Deutsche Forschungsgemeinschaft (DFG) through TRR130 (B cells and beyond) project 01, SFB1074 (Experimental Models and Clinical Translation in Leukemia), SFB 1279 (Exploration of the Human Peptidome), and DFG Single Grant JU 463/5-1.

1. H. Modell *et al.*, A physiologist's view of homeostasis. *Adv. Physiol. Educ.* **39**, 259–266 (2015).
2. B. Crimeen-Irwin, K. Scalzo, S. Gloster, P. L. Mottram, M. Plebanski, Failure of immune homeostasis—The consequences of under and over reactivity. *Curr. Drug Targets Immune Endocr. Metabol. Disord.* **5**, 413–422 (2005).
3. N. Hozumi, S. Tonegawa, Evidence for somatic rearrangement of immunoglobulin genes coding for variable and constant regions (K-chain mRNA/restriction enzymes/RNA*DNA hybridization). *Proc. Natl. Acad. Sci. U.S.A.* 73, 3628–3632 (1976).
4. D. B. Roth, V(D)J recombination: Mechanism, errors, and fidelity. *Microbiol. Spectr.*, https://doi.org/10.1128/microbiolspec.MDNA3-0041-2014 (2014).
5. T. Tsubata, M. Reth, The products of pre-B cell-specific genes (λ 5 and VpreB) and the immunoglobulin mu chain form a complex that is transported onto the cell surface. *J. Exp. Med.* **172**, 973–976 (1990).
6. D. Gay, T. Saunders, S. Camper, M. Weigert, Receptor editing: An approach by autoreactive B cells to escape tolerance. *J. Exp. Med.* **177**, 999–1008 (1993).
7. D. Nemazee, K. Buerki, Clonal deletion of autoreactive B lymphocytes in bone marrow chimeras. *Proc. Natl. Acad. Sci. U.S.A.* **86**, 8039–8043 (1989).
8. C. C. Goodnow *et al.*, Altered immunoglobulin expression and functional silencing of self-reactive B lymphocytes in transgenic mice. *Nature* **334**, 676–682 (1988).
9. K. Pieper, B. Grimbacher, H. Eibel, B-cell biology and development. *J. Allergy Clin. Immunol.* **131**, 959–971 (2013).
10. R. Übelhart *et al.*, Responsiveness of B cells is regulated by the hinge region of IgD. *Nat. Immunol.* **16**, 534–543 (2015).
11. C. S. Setz *et al.*, Pten controls B-cell responsiveness and germinal center reaction by regulating the expression of IgD BCR. *EMBO J.* **38**, e100249 (2019).
12. S. B. Hartley *et al.*, Elimination from peripheral lymphoid tissues of self-reactive B lymphocytes recognizing membrane-bound antigens. *Nature* **353**, 765–769 (1991).
13. J. Roes, K. Rajewsky, D. Immunoglobulin, Immunoglobulin D (IgD)-deficient mice reveal an auxiliary receptor function for IgD in antigen-mediated recruitment of B cells. *J. Exp. Med.* **177**, 45–55 (1993).
14. T. Amendt *et al.*, Primary immune responses and affinity maturation are controlled by IgD. *Front. Immunol.* **12**, 709240 (2021).

Downloaded by guest on February 7, 2022

15. Y. Hao, P. O'Neill, M. S. Naradikian, J. L. Scholz, M. P. Cancro, A B-cell subset uniquely responsive to innate stimuli accumulates in aged mice. *Blood* **118**, 1294–1304 (2011).
16. M. P. Cancro, Age-associated B cells. *Annu. Rev. Immunol.* **38**, 315–340 (2020).
17. A. Kaul *et al.*, Systemic lupus erythematosus. *Nat. Rev. Dis. Primers* **2**, 16039 (2016).
18. C. E. Taplin, J. M. Barker, Autoantibodies in type 1 diabetes. *Autoimmunity* **41**, 11–18 (2008).
19. K. Itoh *et al.*, Clonal expansion is a characteristic feature of the B-cell repetoire of patients with rheumatoid arthritis. *Arthritis Res.* **2**, 50–58 (2000).
20. P. M. Johnson, W. P. Faulk, Rheumatoid factor: Its nature, specificity, and production in rheumatoid arthritis. *Clin. Immunol. Immunopathol.* **6**, 414–430 (1976).
21. J. S. Smolen *et al.*, Rheumatoid arthritis. *Nat. Rev. Dis. Primers* **4**, 18001 (2018).
22. H. Zhang *et al.*, Serum IgG subclasses in autoimmune diseases. *Medicine (Baltimore)* **94**, e387 (2015).
23. C. Franceschi, P. Garagnani, G. Vitale, M. Capri, S. Salvioli, Inflammaging and 'Garbaging'. *Trends Endocrinol. Metab.* **28**, 199–212 (2017).
24. J. Suurmond, B. Diamond, Autoantibodies in systemic autoimmune diseases: Specificity and pathogenicity. *J. Clin. Invest.* **125**, 2194–2202 (2015).
25. M. Boes, Role of natural and immune IgM antibodies in immune responses. *Mol. Immunol.* **37**, 1141–1149 (2000).
26. C. Grönwall, J. Vas, G. J. Silverman, Protective roles of natural IgM antibodies. *Front. Immunol.* **3**, 66 (2012).
27. D. Tsiantoulas, S. Gruber, C. J. Binder, B-1 cell immunoglobulin directed against oxidation-specific epitopes. *Front. Immunol.* **3**, 415 (2013).
28. T. Amendt, H. Jumaa, Memory IgM protects endogenous insulin from autoimmune destruction. *EMBO J.* **40**, e107621 (2021).
29. M. A. Weiss, The structure and function of insulin: Decoding the TR transition. *Vitam. Horm.* **80**, 33–49 (2009).
30. A. Katsarou *et al.*, Type 1 diabetes mellitus. *Nat. Rev. Dis. Primers* **3**, 17016 (2017).
31. R. A. DeFronzo *et al.*, Type 2 diabetes mellitus. *Nat. Rev. Dis. Primers* **1**, 15019 (2015).
32. E. Hobeika *et al.*, Testing gene function early in the B cell lineage in mb1-cre mice. *Proc. Natl. Acad. Sci. U.S.A.* **103**, 13789–13794 (2006).
33. S. Albin, C. Cunningham-Rundles, An update on the use of immunoglobulin for the treatment of immunodeficiency disorders. *Immunotherapy* **6**, 1113–1126 (2014).
34. C. Buchner, C. Bryant, A. Eslami, G. Lakos, Anti-nuclear antibody screening using HEp-2 cells. *J. Vis. Exp.* **88**, e51211 (2014).
35. H. J. Issaq, T. P. Conrads, G. M. Janini, T. D. Veenstra, Methods for fractionation, separation and profiling of proteins and peptides. *Electrophoresis* **23**, 3048–3061 (2002).
36. B. Arora, R. Tandon, P. Attri, R. Bhatia, Chemical crosslinking: Role in protein and peptide science. *Curr. Protein Pept. Sci.* **18**, 946–955 (2017).
37. X. Hu, F. Chen, Exogenous insulin antibody syndrome (EIAS): A clinical syndrome associated with insulin antibodies induced by exogenous insulin in diabetic patients. *Endocr. Connect.* **7**, R47–R55 (2018).
38. Y. Uchigata, Y. Hirata, Y. Iwamoto, Insulin autoimmune syndrome (Hirata disease): Epidemiology in Asia, including Japan. *Diabetol. Int.* **1**, 21–25 (2010).
39. Y. Uchigata, Y. Eguchi, S. Takayama-Hasumi, Y. Omori, Insulin autoimmune syndrome (Hirata disease): Clinical features and epidemiology in Japan. *Diabetes Res. Clin. Pract.* **22**, 89–94 (1994).
40. L. Haataja *et al.*, Disulfide mispairing during proinsulin folding in the endoplasmic reticulum. *Diabetes* **65**, 1050–1060 (2016).
41. M. Karimi *et al.*, Reactivity of disulfide bonds is markedly affected by structure and environment: Implications for protein modification and stability. *Sci. Rep.* **6**, 38572 (2016).
42. T. N. Vinther *et al.*, Additional disulfide bonds in insulin: Prediction, recombinant expression, receptor binding affinity, and stability. *Protein Sci.* **24**, 779–788 (2015).
43. B. van Lierop *et al.*, Insulin in motion: The A6-A11 disulfide bond allosterically modulates structural transitions required for insulin activity. *Sci. Rep.* **7**, 17239 (2017).
44. M. L. Litvack, M. Post, N. Palaniyar, IgM promotes the clearance of small particles and apoptotic microparticles by macrophages. *PLoS One* **6**, e17223 (2011).
45. F. Uher, I. Dobronyi, J. Gergely, Binding of different ligands to IgM-Fc receptors of rat leucocytes. *Immunology* **45**, 387–393 (1982).
46. Y. Zorina, J. Stricker, A. O. Caggiano, D. C. Button, Human IgM antibody rHIgM22 promotes phagocytic clearance of myelin debris by microglia. *Sci. Rep.* **8**, 9392 (2018).
47. C. A. Ogden, R. Kowalewski, Y. Peng, V. Montenegro, K. B. Elkon, IGM is required for efficient complement mediated phagocytosis of apoptotic cells in vivo. *Autoimmunity* **38**, 259–264 (2005).
48. J. R. Weinstein *et al.*, IgM-dependent phagocytosis in microglia is mediated by complement receptor 3, not Fcα/μ receptor. *J. Immunol.* **195**, 5309–5317 (2015).
49. W. Pan, O. Ogunremi, G. Wei, M. Shi, H. Tabel, CR3 (CD11b/CD18) is the major macrophage receptor for IgM antibody-mediated phagocytosis of African trypanosomes: Diverse effect on subsequent synthesis of tumor necrosis factor α and nitric oxide. *Microbes Infect.* **8**, 1209–1218 (2006).
50. H. Ikematsu, Y. Ichiyoshi, E. W. Schettino, M. Nakamura, P. Casali, VH and Vκ segment structure of anti-insulin IgG autoantibodies in patients with insulin-dependent diabetes mellitus. Evidence for somatic selection. *J. Immunol.* **152**, 1430–1441 (1994).
51. S. Weller *et al.*, Human blood IgM "memory" B cells are circulating splenic marginal zone B cells harboring a prediversified immunoglobulin repertoire. *Blood* **104**, 3647–3654 (2004).
52. M. Seifert, R. Küppers, Human memory B cells. *Leukemia* **30**, 2283–2292 (2016).
53. S. E. Baranzini, Autoimmune disorders. *Genomic Pers. Med.* **2**, 822–838 (2013).
54. L. Wang, L. Rong Li, K. H. Young, New agents and regimens for diffuse large B cell lymphoma. *J. Hematol. Oncol.* **13**, 1–23 (2020).
55. M. Cazzola, I. Floriani, C. P. Page, The therapeutic efficacy of erdosteine in the treatment of chronic obstructive bronchitis: A meta-analysis of individual patient data. *Pulm. Pharmacol. Ther.* **23**, 135–144 (2010).
56. J. M. J. M. Ravasco, H. Faustino, A. Trindade, P. M. P. Gois, Bioconjugation with Maleimides: A useful tool for chemical biology. *Chemistry* **25**, 43–59 (2019).
57. D. Frasca, B. B. Blomberg, Aging affects human B cell responses. *J. Clin. Immunol.* **31**, 430–435 (2011).
58. D. Frasca, A. Diaz, M. Romero, A. M. Landin, B. B. Blomberg, Age effects on B cells and humoral immunity in humans. *Ageing Res. Rev.* **10**, 330–335 (2010).
59. G. Bussone, L. Mouthon, Autoimmune manifestations in primary immune deficiencies. *Autoimmun. Rev.* **8**, 332–336 (2009).
60. D. A. Winer *et al.*, B cells promote insulin resistance through modulation of T cells and production of pathogenic IgG antibodies. *Nat. Med.* **17**, 610–617 (2011).
61. A. Fischer, Human primary immunodeficiency diseases: A perspective. *Nat. Immunol.* **5**, 23–30 (2004).
62. A. D. B. Webster, Metabolic defects in immunodeficiency diseases. *Clin. Exp. Immunol.* **49**, 1–10 (1982).
63. E. Traggiai *et al.*, An efficient method to make human monoclonal antibodies from memory B cells: Potent neutralization of SARS coronavirus. *Nat. Med.* **10**, 871–875 (2004).
64. A. Durandy, Hyper-IgM syndromes: A model for studying the regulation of class switch recombination and somatic hypermutation generation. *Biochem. Soc. Trans.* **30**, 815–818 (2002).
65. M. Hervé *et al.*, CD40 ligand and MHC class II expression are essential for human peripheral B cell tolerance. *J. Exp. Med.* **204**, 1583–1593 (2007).
66. G. J. Arason, G. H. Jorgensen, B. R. Ludviksson, Primary immunodeficiency and autoimmunity: Lessons from human diseases. *Scand. J. Immunol.* **71**, 317–328 (2010).
67. M. R. Barbouche *et al.*, Comprehensive review of autoantibodies in patients with hyper-IgM syndrome. *Cell. Mol. Immunol.* **15**, 610–617 (2018).
68. J. A. Winkelstein *et al.*, The X-linked hyper-IgM syndrome: Clinical and immunologic features of 79 patients. *Medicine (Baltimore)* **82**, 373–384 (2003).
69. R. Pelanda *et al.*, Cre recombinase-controlled expression of the mb-1 allele. *Genesis* **32**, 154–157 (2002).
70. H. Yu *et al.*, Breast milk alkylglycerols sustain beige adipocytes through adipose tissue macrophages. *J. Clin. Invest.* **129**, 2485–2499 (2019).
71. R. Reverberi, L. Reverberi, Factors affecting the antigen-antibody reaction. *Blood Transfus.* **5**, 227–240 (2007).
72. S. Kumaraswamy, R. Tobias, "Label-free kinetic analysis of an antibody-antigen interaction using biolayer interferometry" in *Protein-Protein Interactions: Methods and Applications: Second Edition* (Springer, New York, 2015), pp. 165–182.
73. E. Hoffman, S. J. Winder, A modified wire hanging apparatus for small animal muscle function testing. *PLoS Curr.* **8**, 1e2bec4e78697b7b0ff80ea25a1d38be (2016).
74. R. J. Hamm, B. R. Pike, D. M. O'Dell, B. G. Lyeth, L. W. Jenkins, The rotarod test: An evaluation of its effectiveness in assessing motor deficits following traumatic brain injury. *J. Neurotrauma* **11**, 187–196 (1994).

Downloaded by guest on February 7, 2022